Keynote Speech: Technological Paradigm Shift & Network Security

Prof. Dr. Parmanand

Dean

School of Computing and Engineering

Galgotias University

Greater Noida, UP, India

Abstract

We are living in the modern era of Sustaining versus Disruptive technology. Disruptive technology is market driven. It is completely new approach that has the potential to create a new industry or transform an existing one. It is dominantly network based technology. It requires quality Internet with sufficient bandwidth to sustain the apps based applications. These apps are easily accessible from smart phone, Tablet, Laptop etc. Network security is a major concern of these applications because of its accessibilities. Different types of network attacks are possible & needs to prevent appropriately by using different suitable techniques.

Part I: Industry and Community Contribution Type Papers

1. Knowledge Management: Machine for Human Civilization

Rajendra Man Banepali
Knowledge Management Associate
United Nations Information Centre, Kathmandu, Nepal

Abstract

Trust and Truth epistemologically construct knowledge. Netizen culture has driven knowledge management into a new direction enriching its qualities to contribute into performance of end-user. Capturing, Development and Sharing are basic three components of Knowledge Management which ultimately optimizes performance of target group or individuals through information ecology. Those three components, especially sharing component, make more exceptional than conventional perception of information management. Selecting best resources in acquisition, quality assurance of meta-data of resources in development and implementation of appropriate tools for sharing are prominent issues to explore in research of knowledge management. This article has explored how institutional knowledge management, like of United Nations Information Centre in Nepal, could be achieved implementing digital technology in association with organizational mechanism which ultimately reveals machine for human's purpose.

2. Emerging Framework for Regulation of Over-The-Top (OTT) Services in SATRC Countries

Er. Bijay Kumar Roy

Technical Department, Nepal Telecommunications Authority (NTA)

Kamaladi, Kathmandu, Nepal

rbijay@gmail.com

Abstract

The separation of application and network layers has enabled Over-The-Top (OTT) Service Providers to deliver their service directly to end users. OTT service refers application and services which are accessible over the internet e.g. Viber, Skype, WhatsApp, Google Talk, Facebook, Instagram, Netflix etc. OTT providers are said to be the "free riders" on the internet access network established by Mobile Network Operators (MNOs) or Telecommunications Service Providers (TSPs) or Internet Service Providers (ISPs) even though the TSPs or ISPs are paid for the transport of the data in the form of a flat rate or volume based charge by the users. OTT Service Providers are creating commercial as well as technical challenges to TSPs/MNOs/ISPs by providing services often free of charge and in direct competition to the TSPs/MNOs/ISPs services,

thus eroding some of their most important revenue sources e.g. International Telephony and SMS services etc. South Asian Telecommunications Regulators' Council (SATRC) member states, which comprise SAARC countries along with the Islamic Republic of Iran, are facing challenges of regulating OTT services. This exploratory research proposes three strategies or approaches viz. Hands-free, Opportunistic and Collaborative strategy to deal with the OTT challenges. The member states may decide and implement which is appropriate in particular telecom market protecting the national interest.

Keywords: *OTT Services, SATRC, Viber, OTT Impact, OTT Challenges, TSP, ISP, MNO*

3. Regulatory bodies, current telecom situational analysis and future strategies of Nepal

Manish Mallick
Electronics Engineer
Ministry of Information and Communication
Singhadarbar, Kathmandu, Nepal
manishmallick@moic.gov.np

Pankaj Chandra
Technical Officer
Ministry of Information and Communication
Singhadarbar, Kathmandu, Nepal
pankaj@moic.gov.np

Abstract

The fourth generation wireless communication systems have been deployed or are soon to be deployed in many countries. The Ministry of Information and Communication (MoIC) and the regulatory body of Nepal, the Nepal Telecommunication Authority(NTA)has been following the recommendations and standards set by International Telecommunication Union (ITU). The NTA recently permitted Nepal Telecom to operate 4G technology in the 1800 MHz band. Also there is a provision for other operators with necessary infrastructure to get permission for operation of 4G. Wireless system designers have been facing continuously increasing demand for high data rates and mobility required by new wireless applications, and therefore, have started research on fifth generation wireless systems that are expected to be deployed beyond 2020. The MoIC which is responsible for identifying and allocating the frequency bands for all technologies and the NTA which is responsible for implementing the decisions of the Ministry has been working in tandem to face the current challenges and make the country benefit from the recent technologies which are being successfully implemented elsewhere in the world. In this paper, we will discuss about the real data and position of each operators, the role and strategies of regulatory bodies in the context of Nepal. We will also touch upon the possible impact of upcoming 5G technology in the telecom sector.

Keywords: *4G, 5G, IoT Strategies*

Testing of Swedish Execution Time Analysis Tool (SWEET)

Bal Krishna Nyaupane, Jan Gustafsson

balkrishnanyaupane@gmail.com

School of Innovation, Design and Engineering

Mälardalen University

Västerås, Sweden

Abstract

Our testing mainly focuses on verifying two requirements for Swedish Execution Time Analysis Tool (SWEET). Firstly, we have created large programs (larger than 14 KLOC) to find the limits of the program size that can be handled by SWEET. Then after we observed the result produced by SWEET and compare it with the output produced by GCC compiler. In addition to this, we also analysed SWEET execution time for these programs. Secondly, we have created a number of useful examples to test special features of SWEET and to show how SWEET is capable to analyze different types of C programs. Furthermore we found some bugs in SWEET during our testing period.

Keywords: Real Time System, Execution Time, SWEET Capacity, SWEET Output, Flow Analysis, Merge Mechanism, Single Path Analysis, Multipath Analysis, Test Programs, Bugs

1. Introduction

1.1 Background

A real-time system processes information and must guarantee response within strict time constraints. The real-time system must meet the real time deadline regardless of the system load. Apart from being logically correct, they must also exhibit temporal correctness that means they must produce the correct functional output by the provided correct instant of time [2]. Depending on the deadline response to be met by the systems, real time systems are two types:

Soft real time systems: a soft real time system can miss a deadline occasionally, but the risk for missing a deadline should be low. The main objective of a soft real time system is to meet the certain subset of deadlines in order to optimize the some specific application criteria and the system's quality of service. In soft real time system a deadline misses is tolerable, even though not desirable [2, 4].

Hard real time systems: the system is not allowed to miss any deadline. If a deadline is missed, it can lead to the catastrophic results. The response time of the hard real time systems are often, but not always, in the order of milliseconds or microseconds. Examples of hard real-time systems are monitoring systems in nuclear power plants, flight control system, anti-lock braking controller (ABS), and Satellite Systems etc. For example, the car with anti- lock breaking system, the anti-lock breaking system must release the break with suitable frequency that depends on car speed and road surface. If these actions do not happen appropriately, it may lead to catastrophic consequences [2, 4].

1.2 Timing Analysis for Real-Time Systems

The main purpose of analysis of timing behavior of real time system is to guarantee that the system meets its timing requirements. An important step of this analysis is to find the worst case execution time (WCET) of the software in the system. The WCET of a program is the maximum execution time the program could take on a specific hardware platform. The WCET is, of course, a very crucial measure for the reliability and correct behavior of the real time system. It is very important to know the WCET of a program to guarantee that a program will finish its execution before its deadline. If the WCET of a program can be determined, then the program can be used as a part of a real time system to ensure that the system responds fast enough and guarantee that the system is highly reliable and safe [2].

Hence we need to analyze the WCET of a program before using it a real time system. To estimate the worst case execution time of a program, we need to consider the characteristics of both the software and the hardware which is used to execute the program code.

Measuring the WCET

The most common industrial practice for determining the WCET of a program code is by performing end-to-end measurements of execution times for the code [5]. The program is executed a number of times with different inputs with the assumption that some of these inputs are capable to produce the longest execution path of the program code. Unfortunately, end-to- end measurements do not give any guarantee that the WCET has been found, unless the program is very simple. In addition to this, this method is often time consuming and error prone.

Static WCET analysis

An alternative method to find the worst case execution time of the program is by using static WCET analysis. This method estimates the WCET by analyzing the program code without executing it directly on the computer hardware. To calculate the longest possible time of the program, the static WCET tool analyses all possible executions of a program, such as possible upper bounds of loops, possible if-else structures, and possible feasible and infeasible paths in the program. Furthermore, the tool also analyses special characteristics of the used hardware such as memory speed, pipelining, and processor architecture. Hence this analysis estimates the WCET of the program by considering possible program executions and models of the targeted hardware characteristics. This analysis guarantees that the resulting estimated time is longer than or equal to the actual longest execution time of the program [5]. This is the meaning of the concept “safe WCET estimation”.

The Three WCET Analysis Phases

Static WCET analysis can be divided into main three phases: flow analysis of the code which obtains the possible program execution path, low level analysis which finds the execution time for atomic parts of code from the targeted architecture, and finally a calculation phase, which combines the flow and timing information to derive the WCET.

1.3 WCET Analysis Tool: SWEET

The WCET research group at the Mälardalen Real-Time Research Center (MRTC) in Västerås has developed a static WCET analysis tool called SWEET (SWEdish Execution Time tool) as result of the extensive research since 2001 in the field of static time analysis [5].

The main objective of the SWEET tool is to perform flow analysis of the program code, which results in flow facts that contain information about the loop bounds and possible infeasible paths in

the program. Flow facts are necessary to find the WCET for the analyzed program. SWEET can also calculate the WCET and BCET (Best Case Execution Time) directly. The major functions of SWEET tool are to:

- Perform automatic flow analysis based on a program representation on the intermediate code level (ALF code).
- Provide means to integrate the flow analysis with a low level analysis.
- Provide connections between the flow analysis and the C program level
- Offer two ways to calculate WCET and BCET directly using timing models.

It is necessary to convert a program code into ALF format before it can be analyzed by SWEET. ALF is an intermediate program language developed for flow analysis. A C-code program is converted into ALF format to be analyzed by SWEET. SWEET can analyze programs for single core processor but do not support multi-core processors.

Flow Analysis

Most program code does not have fixed execution time. Often, the execution time depends on the input data for the program, the characteristics of the program and the hardware upon which the program is run. Hence, the program can be executed via different paths available inside the program code. To calculate the worst case execution time, SWEET needs to identify the possible paths in the code. This is called flow analysis. The main purpose of flow analysis is to calculate safe bounds on the execution behavior of the program and to calculate the flow information as automatically as possible.

Flow Facts

SWEET represents flow information in the form of flow facts. Flow facts use virtual execution counters for the nodes in the control flow graph in a scope. For each execution scope that is entered in scope hierarchy and for every node, the counter #N is initialized to zero and incremented at each execution of the node. The context-sensitive valid-at-entry-of flow fact format is the format for SWEET's flow information [8, 6]. The standard format is [7]: *CALL_STRING: VALID_AT_ENTRY_OF: FOREACH_OR_TOTAL: CONSTRAINT;*

Abstract Interpretation, Abstract Domains and Abstract Execution

Abstract interpretation is a method used to statically determine the possible run-time values of variables at different program points. An abstract domain is selected to represent the values of the program variables. The main goal of the abstract domain selected in SWEET is to find safe estimations of all possible values of the variables in the program code, and calculate the safe flow information using these variables.

The main analysis mechanism of SWEET is Abstract Execution (AE), which is a form of symbolic execution based on the abstract interpretation. AE is input sensitive, which means that input can influence the resulting flow facts. AE executes the program in the abstract domain, and uses abstract values of variables and abstract version of language operators. The main result of AE is flow facts that can be given as input to the subsequent calculation phase. AE extends the abstract states with recorders to collect flow information and analyses the program part with collectors to successively accumulate recorded information from the abstract states. A program might have different possible execution paths, and then AE must execute these paths in different abstract states to represent all possible execution paths.

By extending the abstract states of the AE we can keep track of the smallest and largest execution

cost for all in the particular abstract states. This method is used in SWEET for BCET/WCET calculations [1, 3].

The Merge Mechanism

Most programs have conditional branch statements. Condition expressions cannot always be decided using abstract values, since the evaluation can lead to both true and false outcome of the condition. In such cases, the abstract execution must execute both branches separately in different abstract states. With increasing number of possible execution paths, the corresponding number of abstract states also increases, often exponentially. We can apply different merge strategies based on the selection of different types of merge options [6]:

- Merge at function end: all different abstract states, representing possible execution paths, will be merged at the return statement at the end of functions.
- Merge at loop termination: all different abstract states, representing possible execution paths, will be merged at the termination points after loops.
- Merge at loop body end: all different abstract states, representing possible execution paths, will be merged at header after each loop iteration.
- Merge at if: all different abstract states, representing possible execution paths, will be merged at the join points after selection statements.

SWEET allows the user to specify different merge options using the following syntax [7]:

sweet –i= filename, -ae merge=<merge point>

merge=<merge point> is the merge options to be used. *<merge point>* can be one or more of:

- all : represents all merge options (fe, fr, le, be, je)
- none : no merging at all
- fe - Each function entry point.
- fr - Each function return point.
- le - Each loop exit edge.
- be - Each back-edge.
- je - Each point of joining edges.

If we do not select any merge option, SWEET takes merge=all as default.

Use case: Single path analysis

This use case explains how to write SWEET commands for single path analysis and how to produce output of the SWEET analysis. The syntax is described below.

sweet -i= file-name.alf, std_hll.alf outannot= file-name.oas func=main -d g=rsg -ae merge=all ffg=uhss ft=n -f lang=ff

Use case: Multipath analysis

Multipath analysis needs input annotations file for defining the possible values of the variables used in the program. The standard syntax is described below.

sweet -i=file-name.alf,std_hll.alf annot=file-name.ann outannot=file-name.oas func=main -d g=rsg -ae merge=all ffg=uhss ft=n -f lang=ais,ff

2. Literature Review

We have not found any other related reports on our theme “testing a WCET tool”. There has been a number of “WCET Tool Challenges” where WCET tools have been tested, but they are more

focused on the study, comparison and discussion of the properties of different WCET tools and approaches, to define common metrics, and to enhance existing WCET benchmarks.

3. Methodology

We have used different types of programs during the testing of SWEET. At first phase we search on the web to find existing programs to test SWEET. Then we describe three examples of test programs that were used to test SWEET. The first (Matrix Manipulation) tests the limits of programs size that can be handled by SWEET, the second (Merge) and third (File Handling) test particular features of SWEET.

3.1 Searching for Existing Programs

We wanted the programs to be large (greater than 10K LOC) to find the limits of the program size that can be handled by SWEET. So, extensive web surfing was carried out to find useful real time programs on the web. More than ten free real time projects with complete source code in C were found on the web. Some of them were image compression and decompression programs and others were audio/video encoder and decoder programs. Unfortunately, none of them could be fully analyzed by SWEET. There were mainly three reasons for this:

- SWEET did not (at the start of the thesis work) support any file operations such as fopen, fclose, fread, fwrite etc.
- SWEET does not support dynamic memory allocation.
- SWEET can only analyze programs written in ANSI C.

Because of the above reasons none of the found projects was used as a testing program. At the end phase of testing analysis, SWEET was updated so it now is possible to analysis most file operations in C (see section “File Handling Example” for an example). But, it was impossible to update SWEET to handle dynamic memory allocation in this short period of time.

3.2 The Matrix Manipulation Program

The main objective of the program *“Matrix_Manipulation.c”* is to find the limits of the program size that can be handled by SWEET. The program has two input functions; *“inputA()”* for matrix *“A”* and *“inputB()”* for matrix *“B"*. These two functions assign distinct random numbers in a given interval to each matrix element on each call of the function depending upon a seed value provided via a function argument. The program has 24 functions to compute different properties of the matrices.

The program contains calculations with different logic to perform different coding constructs such as nested for-loops, while loops, do-while loops, if-else ladders, and switch-case structures. Our main goal is to find how efficiently SWEET can analyze the code.

We have made a table for SWEET analysis times to show the analysis times for different sizes of the test programs. We see that the analysis time is roughly proportional to the size of the analyzed program and the total number of iterations. This is to be expected, since SWEET analyses programs by abstract execution of the code. This means that every piece of code is analyzed for every iteration. In addition to this, we have made a comparison of the GCC compiler output of the *“Counter”* variable with the SWEET single path analysis output.

Table 1: Comparison of SWEET output with GCC Compiler output and SWEET analysis time

Name of Program	LOC	GCC Compiler Output (Counter)	SWEET Analysis Output (Counter)	SWEET Analysis Time
Matrix_Manipulation.c	1,025	1,313	1,313	2 minutes
Matrix_Manipulation1.c	1,925	2,383	2,382	3 minutes
Matrix_Manipulation2.c	2,820	3,696	3,695	4 minutes
Matrix_Manipulation3.c	3,715	7,373	7,377	6 minutes
Matrix_Manipulation4.c	4,610	8,397	8,401	9 minutes
Matrix_Manipulation5.c	5,505	9,710	9,714	12 minutes
Matrix_Manipulation6.c	6,400	10,624	10,630	15 minutes
Matrix_Manipulation7.c	7,295	13,276	13,280	22 minutes
Matrix_Manipulation8.c	8,190	14,351	14,362	24 minutes
Matrix_Manipulation9.c	9,085	15,624	15,635	28 minutes
Matrix_Manipulation10.c	9,980	20,009	20,020	33 minutes
Matrix_Manipulation11.c	10,875	21,282	21,293	39 minutes
Matrix_Manipulation12.c	11,765	25,078	25,092	45 minutes
Matrix_Manipulation13.c	12,660	29,385	29,404	56 minutes
Matrix_Manipulation14.c	13,560	31,151	31,171	1 hour
Matrix_Manipulation15.c	14,455	30,091	30,108	1 hour 3 minutes

The difference in value for “Counter” is due to a bug in SWEET (see Section “Result and Discussion”).

3.3 The Merge Program

The merging feature in SWEET gives a possibility to speed up the analysis. However, this may come to the price of less precision. It would be interesting to have an example that illustrates this “trade-off” and which will produce different outputs for different types of merge points. This is the main objective of the program *“MergeExample.c”*.

This program has two input variables, “a” & “b” and one output variable “Flag”, which is the sum of the final values of "a" and "b" after some odd and random calculations. For multipath analysis, the abstract annotation input is provided via the “*MergeExample.ann"* file. The content of the input annotation file is: *FUNC_ENTRY Merge_Example ASSIGN "a" INT 10 15 || "b" INT 13 17;*

SWEET produces analysis output in the file “*MergeExample.out”*. The content of the output annotation file is: *STMT_EXIT main main:: entry::3 Flag;*.

We have executed the following SWEET multipath analysis command, with “x” replaced as described in the different cases: *sweet -i=MergeExample.alf,std_hll.alf annot=MergeExample.ann outannot=MergeExample.oas func=main -ae merge=x ffg=unsp ft=n -f lang=ais,ff*

Case I: merge=none or merge=fe or merge=fr

The output of the SWEET analysis tool is: STMT_EXIT main main::entry::3 0 ASSIGN "Flag" 0 32 INT 83 178 ;

Case II: merge=le or merge=all

The output of the SWEET analysis tool is: STMT_EXIT main main::entry::3 0 ASSIGN "Flag" 0 32 INT 78 305 ;

Case III: merge=be

The output of the SWEET analysis tool is:STMT_EXIT main main::entry::3 0 ASSIGN "Flag" 0 32 INT 81 305 ;

We have used different merge point settings during the analysis and found three different results (case I to III above). As can be seen from the table, there is really a trade-off. Case I gives a much better (tighter) result, but to the price of a much longer analysis time. Columns "gcc" gives the correct output, to be compared with.

Table 2: Three different merge point analysis

Item	Comment	Case I	Case II	Case III	gcc
Analysis time		1m 10s	0.8 s	0.7 s	-
while.end	Loop bound	15	40	40	-
while.cond1	-"-	19	44	44	-
while.body	-"-	4	4	4	-
while.cond4	-"-	58	158	158	-
while.cond	-"-	5	5	5	-
while.body3	-"-	15	40	40	-
while.body6	-"-	43	118	118	-
while.end25	-"-	1	1	1	-
while.end22	-"-	4	4	4	-
Flag	Value range	[83..178]	[78..305]	[81..305]	[115..130]

The flow facts for the loops are same as flow facts for the *merge=all* case.

When we use the setting *merge=je,* SWEET cannot produce an output because it hangs in an infinite loop. We do not know why it happens. The reason might be a bug in SWEET.

We have also executed this program using GCC to get the "real" result to compare with. We executed the program 24 times with all combinations of values of the variables "a" & "b" inside the multipath input range. For a selected from the range [10...15] and b from [13...17], we get results ("Flag" values) in the range of [115...130]. We see that the analysis result are safe (i.e., the real values are inside the range of the analysis result). This is what is expected.

3.4 File Handling Program

During the testing period, SWEET was extended so that file operations could be handled. We found one program on the internet that was used to test this new feature. The program shows that the SWEET can analyze file based project without any complains or warnings.

The program *"file.c"* was downloaded from the web and as we know that SWEET cannot analyze input/output functions such as *"scanf()", "printf()",* the program has been modified to make it workable for SWEET.

4. Result and Discussion

A software bug is an error or fault in a program code that produces an unexpected result or unwanted behavior. Most of the bugs come from errors made by the developer either in the programming phase or during program design. We have found a number of bugs during the testing of timing analysis of SWEET. These are presented below.

Bug 1: SWEET hangs in an infinite loop during multipath analysis but works perfectly in case of single path analysis.

We have developed a simple test program "*Loop_Analysis.c"* with two input variables, "a" and "b". We use 16 different combinations of " a" and" b" and execute the program 16 times with one execution for each combination of " a" and "b". To test SWEET analysis thoroughly, we have run this program in both single path and multipath analysis mode.

For single path analysis with SWEET, we have executed the following SWEET command:

sweet -i=Loop_Analysis.alf,std_hll.alf utannot=Loop_Analysis.oas func=main -ae merge=all

The variable "Sum" is used as a result of the program. It is the sum of the number of inner and outer loop iterations of the program. The results of single path analysis with SWEET and output from an executable using the GCC compiler are same.

To achieve multipath path analysis, we have used the following SWEET command: *sweet -i=Loop_Analysis.alf,std_hll.alf annot=Loop_Analysis.ann outannot=Loop_Analysis.oas func=main -ae merge=all*

For multipath analysis, the abstract annotation input is provided via the "Loop_Analysis.ann"

file. The content of the input annotation file is: *FUNC_ENTRY Infinite_Loop_Analysis ASSIGN "a" 0 32 INT 17 20 || "b" 0 32 INT 82 85;*

In case of multipath analysis, analysis of the program will never terminate. This is strange, since for single path analysis for the 16 different combinations of "a" and "b", the analysis works perfectly and give the same result as using the GCC compiler. But if we combine all 16 cases and execute in multipath mode, then the SWEET analysis does not terminate. This indicates a bug in SWEET.

Bug 2: The SWEET analysis output and output using GCC compiler for total loop iterations count of a program *"Matrix.c"* is different, despite the input is same for both.

The main objective of this program *"Matrix.c"* is to reveal that the total loop iterations count in

SWEET analysis output and the GCC compiler output are different. The *input()* function is responsible to assign random values for matrix elements. The matrix values are also dependent on "p" and "b". If we change the value of "p" or "b", the *input()* function will assign different values to the matrix elements.

We have studied three different cases and found three different results. For single path analysis, we have executed the following SWEET command: *sweet -i=Matrix.alf,std_hll.alf outannot=Matrix.oas func=main – ae*

Case I: p=37 and b=29

The output of the SWEET is: *STMT_EXIT main main::entry::3 0 ASSIGN "Counter" 0 32 INT 84;*

The output using the GCC compiler is: Total loop count is: 80

Case II: p=41 and b=19

The output of the SWEET is: *STMT_EXIT main main::entry::3 0 ASSIGN "Counter" 0 32 INT 80;*

The output using the GCC compiler is: Total loop count is: 81

Case III: p=1 and b=19

The output of the SWEET is: *STMT_EXIT main main::entry::3 0 ASSIGN "Counter" 0 32 INT 87;*

The output using the GCC compiler output is: Total loop count is: 81

Here, we see that total number of loop iterations for SWEET analysis and corresponding output using GCC compiler are different. Hence we conclude that the SWEET analysis might have some problems.

Bug 3: The SWEET calculates wrong result for the remainder operator (%)

We have developed a simple program that revealed that there is a problem with handling of the remainder operator in SWEET. This program has been analyzed in both single path and multipath mode. If we replace the remainder operator (%) by division operator (/) in this part of code "sum=sum + n/3;", the program works perfectly in both single path and multipath analysis. But if we use remainder operator, it works for single path analysis but not for multipath analysis.

This program has been executed in multipath analysis using the following SWEET command*: sweet -i=Remainder.alf,std_hll.alf annot=Remainder.ann outannot=Remainder.oas func=main -ae*

This program has been executed in single path analysis using the following SWEET command: *sweet -i=Remainder.alf,std_hll.alf outannot=Remainder.oas func=main -ae*

For multipath analysis we use the input annotation file *"Remainder.ann",* which has the following contents: *FUNC_ENTRY Calculation ASSIGN "a" INT 13 15 || "b" INT 19 21;*

This program has two input variables "a" and "b". We have made 9 different combinations of these two variables. Using the remainder operator, the output of the program using the GCC compiler and single path analysis are same. But the multipath analysis using the input annotation file *"Remainder.ann"* does not terminate which means there is an infinite loop somewhere inside the code.

Bug 4: SWEET hangs in an infinite loop for *merge=je* merging point, but not for the rest of the merge options such as *merge=all, merge=none* etc.

As has been mentioned before, SWEET hangs in an infinite loop for *merge=je* merge point when analyzing the "Merge" example.

Bug 5: SWEET's loop count is different than GCC compiler's loop count for a program.

The main objective of the program *"Max_Min.c"* is to reveal that SWEET count of number of loop iterations is different compared to the GCC compiler. We have analyzed this program in single path analysis mode. To analyse this program we have executed the following SWEET command: *sweet -i=Max_Min.alf ,std_hll.alf outannot=Max_Min.oas –ae*

The output of SWEET is: STMT_ENTRY main main::do.end 0 ASSIGN "Counter" 0 32 INT 2;

The output of the GCC compiler for the *"Counter"* variable is 6, however, when the attached program terminates. This means that there is a bug in SWEET.

5. Conclusion

We have created own large programs to test the capacity of SWEET in terms of LOC. A time analysis table has been produced to show the variation of SWEET analysis time according to the

number of LOCs.

We have used different kinds of program code to identify unknown problems in SWEET. Some bugs have been found by comparing SWEET analyzed output with output of the program compiled by the GCC compiler. In addition to this, we have found a number of bugs by comparing single path analysis output with multipath analysis output.

Moreover, a program has been created that produces different output for different merge points during analysis. In addition to this, we have created different kinds of example with complex C- code that includes nested while and do-while loops, deeply nested if-else structures, complex logical expressions and arithmetic expressions. The example programs are matrix manipulation, array based calculations, and string operations, to verify that SWEET can analyse any kind of ANSI-C programs and produce expected result during SWEET analysis.

To summarize, we have been successful in creating test programs for SWEET. We have not been able to find useful and large test code on the Internet, instead we have developed own test programs. Using them, we have demonstrated the capacity of SWEET in terms of size and complexity. We have also been able to identify around five bugs in SWEET. These bugs have been reported to the Bugzilla bug server that is used for SWEET.

References

1. Stefan Bygde. "*Abstract Interpretation and Abstract Domains with special attention to the Congruence domain."*Master Thesis, Malardalen University, Sweden, May 2006.
2. Daniel Sandell. "*Evaluating Static Worst-Case Execution-Time Analysis for a Commercial Real-Time operating System*." Master Thesis,,Malardalen University,Sweden, July 22, 2004.
3. Andreas Ermedahl, Jan Gustafsson, Björn Lisper. Deriving WCET Bounds by Abstract Execution. Proc. 11th International Workshop on Worst-Case Execution Time (WCET) Analysis (WCET 2011), July 2011.
4. Susanna Byhlin "*Department Evaluation of Static Time Analysis for Volcano Communications Technologies AB"*. Master Thesis, Malardalen University, Sweden, December 7, 2004.
5. Jan Gustafsson, Adam Betts, Andreas Ermedahl, and Björn Lisper. "*The Malardalen WCET Benchmarks: Past, Present and Future."* Proceedings of the 10th International Workshop on Worst-Case Execution Time Analysis, July 2010.
6. Jan Gustafsson, Andreas Ermedahl, and Björn Lisper. "*Towards a Flow Analysis for Embedded System C Programs*." The 10th IEEE International Workshop on Object-oriented Real- time Dependable Systems (WORDS 2005), February 2005.
7. SWEET Manual, compiled by Jan Gustafsson, Mälardalen University, Sweden. URL: http://www.mrtc.mdh.se/projects/wcet/

SUPER COMPUTING USING CLUSTER NETWORK (HYPE-II)

Santosh Pandey, Ram Sharan Chaulagain, Prakash Gyawali

069/BCT, Advanced College of Engineering and Management,

Supervised By

Prof. Dr. Subarna Shakya

Kupondole, Lalitpur, Nepal

Email Address: Santosh.pandey2222@gmail.com, rameskool@hotmail.com

hsageyolk@gmail.com

Abstract

"Super Computing Using Cluster Network" is a vision to achieve super computation speed through the network of simple commercial computers easily available in the market. The amount of data is increasing at a rapid rate and the need to compute these data at faster rate is also high. It deals with the speed and accuracy that is at high demand in sectors that handle large amount of data at a time or for large and complex computation and simulation tasks. With the help of this system the need of high performance at low cost and easy availability has been dealt with. The System is based on self-made distributed architecture without the use of any special libraries. The architecture performs the tasks of job division, handles task queue and result queue, schedules the tasks and supervises the worker nodes. The salient features of our architecture are plug and play software framework, dynamic worker addition and fault tolerance in case of Node failure. These features also make our system reliable for handling large amount of data that needs to be processed at fast rate without error.

1. Introduction

It is a vision to provide high performance computing for big data analysis, research and statistical usage. As we all know the amount of data in the world is increasing day by day. What we don't know is the rate of increase of this data. One of the study shows that this rate is "**The data doubles every 18-24 months**". This is something of concern as we might not be able to handle all these data with our current computers. We also know that the performance of a processor can be increased by increasing the number of transistors in a core of the processor. However, there is a limit to how many transistors we can put in a single core. At some instance, the transistor will be so small that quantum effect starts to show in our performance, i.e. the decrease in size results to decrease in performance. So, though we might be able to create smaller transistors, we will not get better performance. Also the lithography process of creating a transistor becomes very hard at that point to further decrease the transistor size.

So what can we do to solve these issues? We have two options:

- Use Multi-core processor systems
- Use Cluster of computers

This system is based on the second option where multiple computers are used to enhance the performance for a single user.

Though a simple concept in theory, designing cluster network and software architecture is a difficult task. We have to consider task distribution, flexibility of task for parallelizing, communication between computers, congestion in network and other multiple things that affect the performance of any system.

It is focused on providing high performance computing at a cheaper rate. So, instead of application side of supercomputing, the focus here is on creating an architecture that allows supercomputing to be possible. In other words, this is a platform for applications that make use of parallel processing and supercomputing.

Furthermore, along with the high computing aspect, it also comes with the package that includes fault tolerance and dynamic worker addition and removal. In other words, if a computer is unable to perform a task given, it is detected and the task is rescheduled to another computer. Also the support of dynamic worker means we can add any number of nodes to the system as per our need or task demand during the execution phase of the task.

2. System Design and Architecture

The system is based on Beowulf's cluster where the main server is connected to the worker nodes through Ethernet switch.

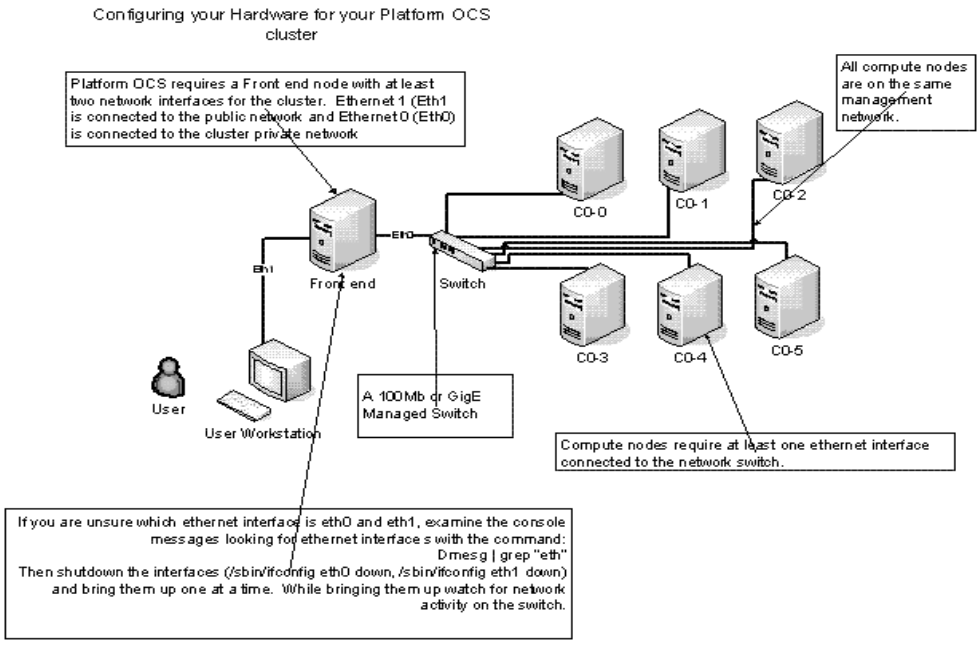

Figure 1: Beowulf Cluster

As it can be seen from the above figure the user can access to the main workstation which is the server and further communication and task distribution is handled by the server itself. This creates an environment where the user thinks they are using a single computer in contrast to the cluster network of multiple computers that they are using.

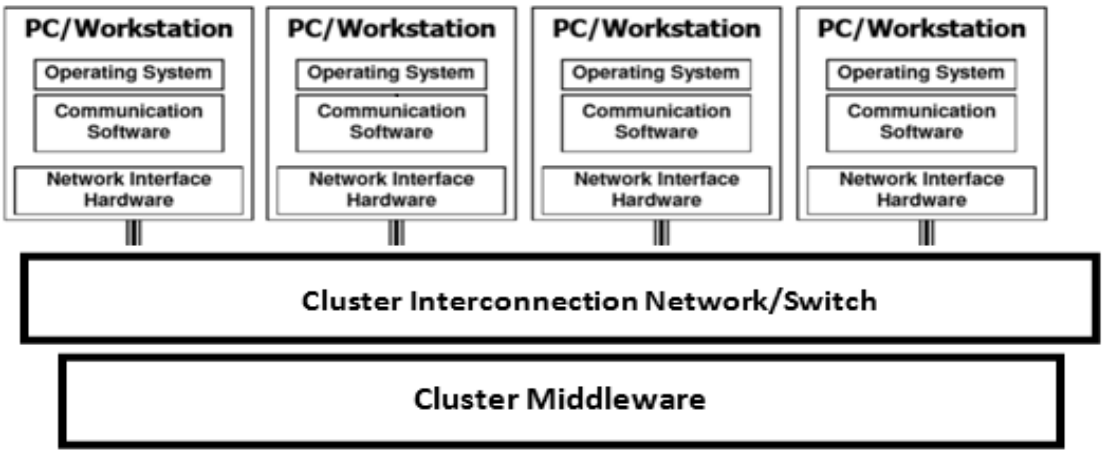

Figure 2: In-depth Architecture

The design is made such that the task is divided between the worker nodes by the server and once the worker nodes complete the tasks, the result is available to the server node which integrates the result to provide the user with the final output. The communication delay during the scheduling of task and retrieving of result can be minimized by either using high quality Ethernet switch or using of routing algorithms or by using some different means of communication like InfiniBand, Myrinet, QsNet II etc.

Further in depth study of the architecture is given by the figure below:

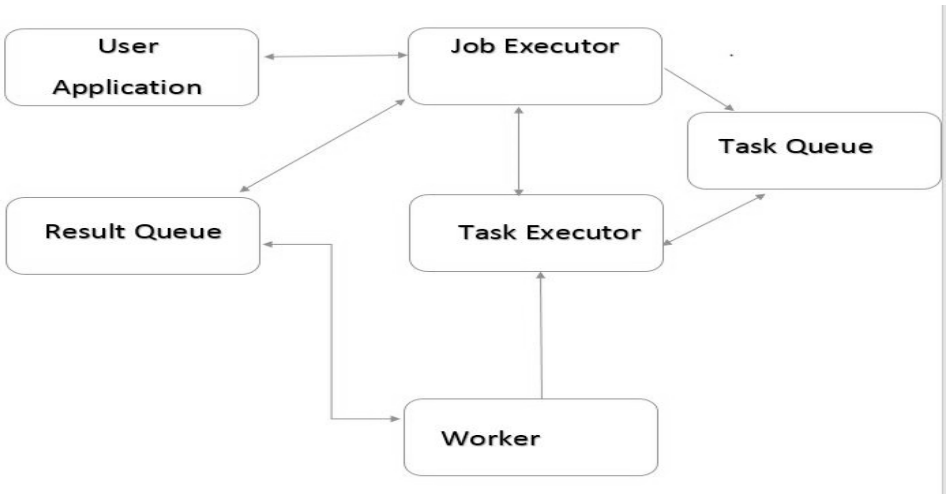

Figure 3: System Working

Initially, User chooses the application that they want to use in the supercomputer. After the user defines the job, the job is passed to the Job Executor. It divides the job into a number of chunks (defined as task) and stores it in a Task Queue. After that, the Executor starts parallely.

When a worker tries to connect to the Work Server, it is connected through the socket and it is given a specific ID. Then it runs in a different thread than main Server. The Executor passes the task to the distributed nodes located in the same network. The workers receive the work through the work and start the computation of the task. Each node runs multiple worker session parallely for a better resource utilization. When worker finishes the task, it passes the result to the Executor and the Executor writes the result to a Result Queue. After all threads are closed i.e. All worker finishes the work, the Job Executor reads the various values from the result queue and provides the final result to

the User. During the working of the Worker, if they crash or fault arises, the Executor detects it and throws exception to the Executor and again writes the task to the Task Queue overcoming the Fault.

The overall working of the cluster is shown in the figure. The user assigns the input to the Job Executor

The program forwards small chunks of tasks as per instruction to different nodes such that there is no problem in result or calculation process. The nodes perform task assigned to them. The results are returned and integrated to provide the user with the final result or solution.

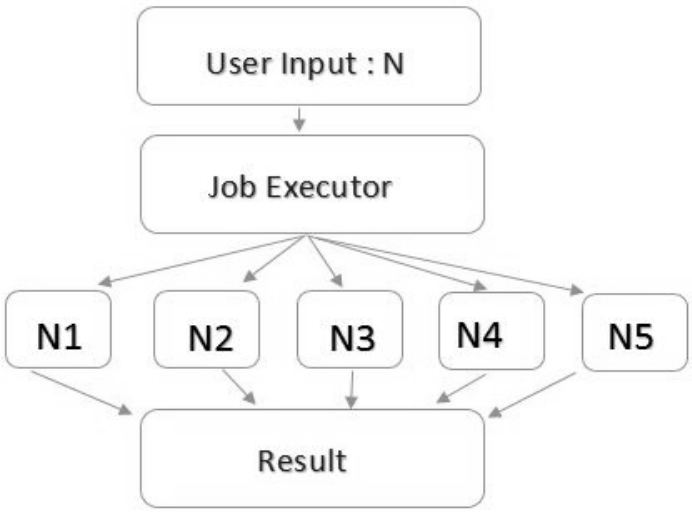

Figure 4: Task Sequencing

3. Methodology

No external libraries were used during the making of this system. It is mostly based on Java The construction phase on the basis of design was done by following iterative model of system development.

First, client server model was created for interaction between the nodes. This model focused only on interaction between the server and its client and the clients were unknown to each other. Then program to calculate the value of Pi in distributed mode was created and tested. Since the first version of client server model is the base of software architecture of the Hype II, this iteration was also used as a means to test the parallel processing, task distribution and application base of the system. The third version included optimization through management of task distribution along with introduction of minor fault tolerance system.

For the hardware connection of computers in cluster, star topology was followed. The system is related to close network of computers for better performance, thus better management of hardware connection was crucial. The topology has a single server computer connected to the rest of the computers where the other computers can only interact to the server but not with one another.

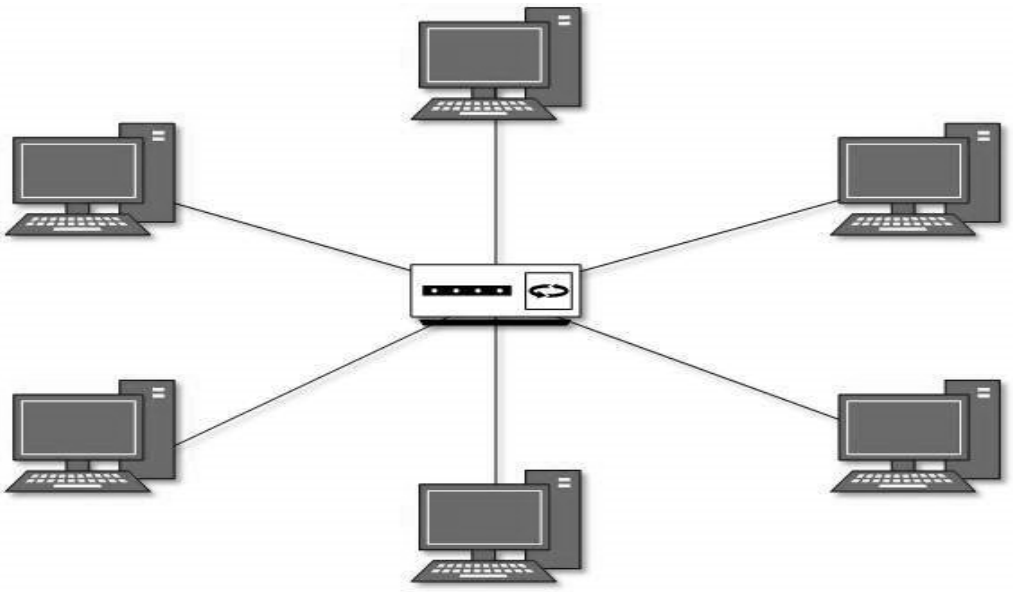

Figure 5: Star Topology

Server (Control node)

Server is the main computer which is available to the end user. The server ran on both windows and Linux OS for parallel computing containing middleware for handling and synchronizing all the tasks in the system. The server acts as a global broker for data flow management to the cluster. In other words, the server performs the task of work division and task scheduling. The actual working of the task takes place on the cluster. For better understanding, the cluster network can be taken as the hardware part of a computer and the server/middleware can be viewed as the operating system. So, the operating system is a resource manager and task scheduler. It manages and distributes the work load among the CPUs/nodes in cluster.

Node

The node is an individual computer in the cluster. These are normal computers which we use for basic requirements. The reason to use normal computer is to achieve high performance computing in cheap price rather than using expensive mainframe supercomputers. The worker node will be running on a customized version of Linux which will be capable to run only special functions required by the cluster. Every node will be containing dedicated graphics card for vector processing.

Memory Architecture

The cluster network uses distributed memory architecture. All the nodes are tightly coupled computers. The nodes have their own local memory for processing data. Initially while retrieving data from a network, the server collects all the data and distribute among the nodes. Message passage within process is done using our architecture for distributed computing.

Computation Architecture

This cluster is designed for high performance computing which requires parallel execution for faster computation. Single problem is divided into smaller independent tasks to be executed in parallel. GPU can also be added to the cluster for vector processing of the data for increasing the computation of the cluster. High performance arbitrary precision library was used for achieving higher precision in calculations.

Type of Parallelism

Various type of parallelism exists in parallel computing such as bit-wise parallelism, instruction wise parallelism and task wise parallelism. In our cluster system, a single program is broken into various independent parallelizable codes which have been distributed among the nodes for parallel execution. All the nodes are working for same task parallely.

Speed from the system

Using multiple computers rather than a single computer allows faster processing speed. But using large no of processors for a single task doesn't mean that it can be accelerated more and more with increase in no. of processors. The speedup depends upon the characteristics of the task. The acceleration in performance of the task depends on the level of parallism that we can gain on any task.

Data storage and management

The cluster has a distributed memory model. Every node has its own memory. The intermediate results are stored by the server in its memory**.** It is maintained by the server or the control node. For any application, which requires sets of data, the server distributes the data to the remote worker as instructed by the program. The data repository will also be used for inter-node communication between the remote worker nodes.

4. Result and Analysis

After completing the build, we tested the cluster in different scenarios where numbers of nodes were connected at a time with set cores utilized. The cluster was setup in the lab using 15 nodes. Every computer was connected to a switch along with a router in star topology. This setup of workers was connected to the server laptop which connected to the network through Wi-Fi of the router. CAT5 and CAT6 cables were used as Ethernet connection for the network. IP address of each computer was assigned by the switch. From the acquired data, the following graph was observed:

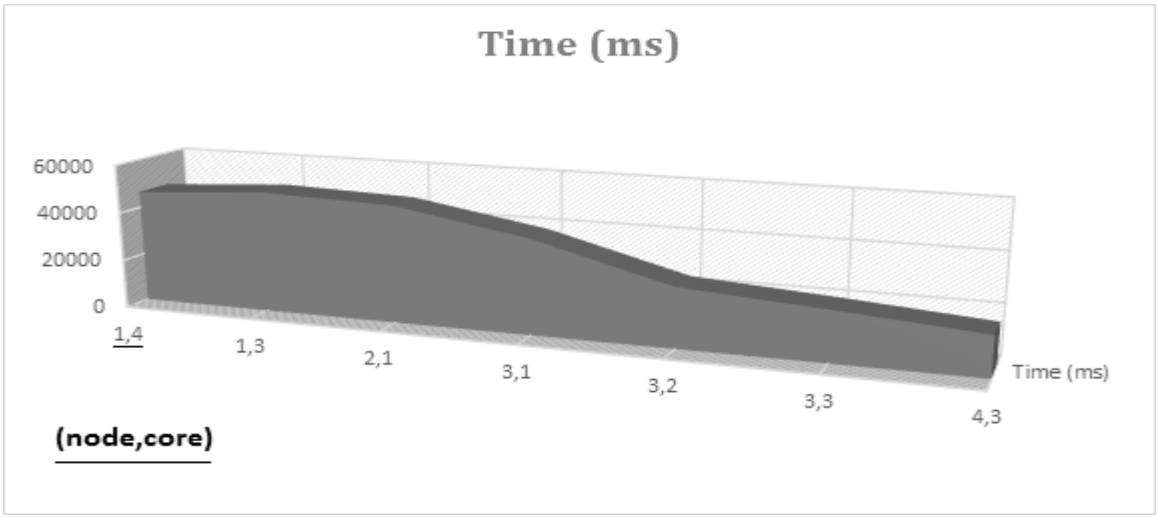

Figure 6: Node (core) Vs Time

The above graph shows the change in computing time of cluster with the change in number of Node and core of each node. The more nodes we use the faster speed we can achieve.

After all this was done, the resulting change in performance of the cluster came out for 10000000 iterations as:

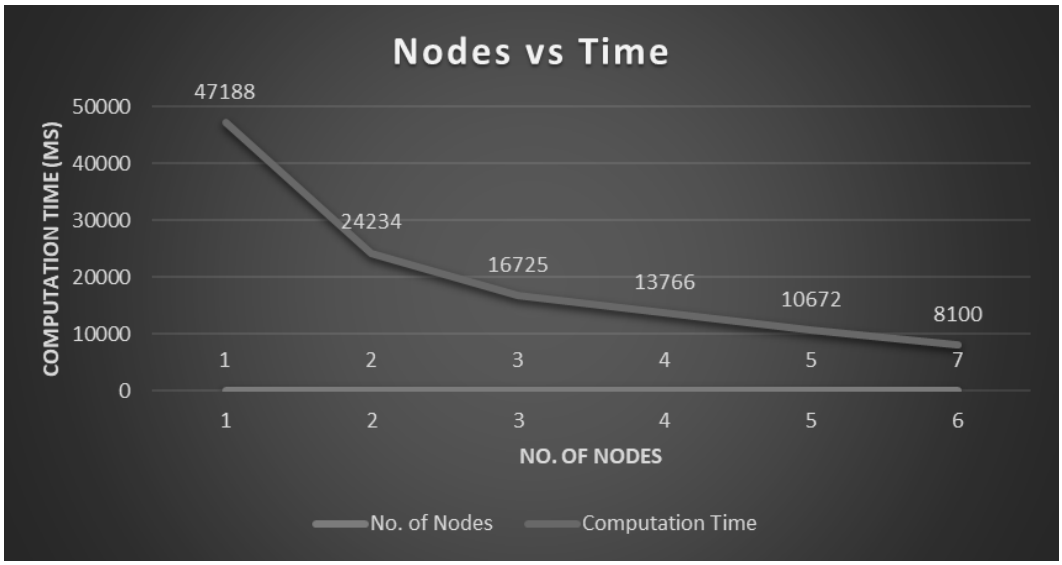

Figure 7: Node Vs Time graph

This graph shows the change in computation speed of cluster with the increase in number of node. The increase in speed as found is increasing at almost exponential rate. This also confirms that we achieved supercomputing as the same task required higher time to execute is completed at a far faster time frame.

The system was tested using multiple number of iteration of tasks and using that data, the speedup was determined on the system for computation comparing with single node. The graph below shows the speedup of the system. From the graph, it can be seen that the speedup is not liner but exponential. It is due to utilization of more resource and better task size received by each Worker.

For Speed-Up Comparison, the following curves shown below are perfect examples. It can also be seen that when no. of iterations is less i.e. only 10 million, significant speed up from 15 nodes could not be achieved, whereas on 100 million iterations, the speedup computation was by 18 times using only 15 nodes.

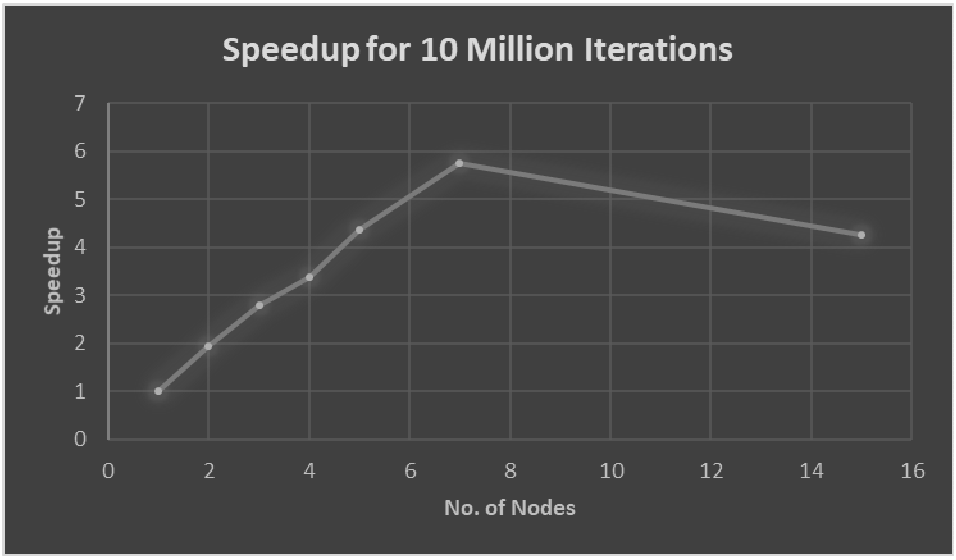

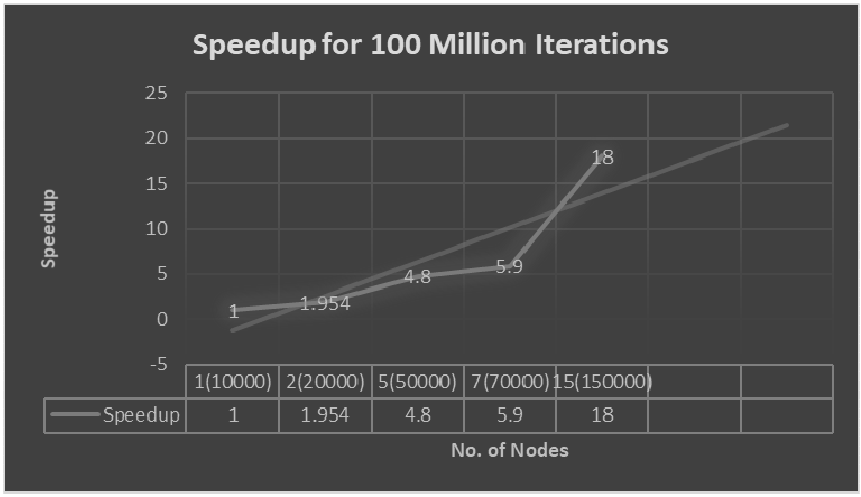

Figure 8: Comparison of Speedup of system

The above graph shows the final analysis of the system where both speedup and the cost required for getting that speedup using multiple computers.

5. Conclusion

Thus, supercomputing was achieved through the cluster of commercial computers. The original task of fulfilling the need of supercomputing at a cheaper rate was achieved as well was increasing the accuracy of computation when dealing large amount of data. The architecture was also found to be useful for distributed grid networks due to its certain features like platform independence, fault tolerance and scalability.

Future Works

For future works, we have set the following tasks:

- Optimizing every node for better performance
- Including the low parallizable and complex tasks

Limitations

There are a few limitations yet to be tackled. They are:

- The fault tolerance is only limited to restarting of a node or disconnecting form server, but not to shutting down of the node.
- Is not comparable with bigger super computer containing thousands of cores.

References

1. Don Berker. Robert G. brown. Greg Lindahl. Forrest Hoffman. Putchong Uthayopas. Kragen Sitaker. *Frequently Asked Questions* [Online]. Available: http://www.beowulf.org/overview.faq.html
2. Technopedia. *Computer Cluster* [Online]. Available: http://www.technopedia.com/definition/6581/computer-cluster
3. Dr. Wu-chun. Feng. (2015). *The Green500 List-November 2015* [Online]. Available: http://www.green500/list/green201511
4. Shiflet, *Introduction to Computational Science: Modeling and Simulation for Sciences*, Princeton University Press, 2014.
5. Kumar, Lenina, *MATLAB: Easy Way to Learning*, PHI Learning, 2016.
6. Etter, *Introduction to MATLAB*, Prentice Hall, 2015.
7. Lemay Laura, Charles L. Perkins, *Teach Yourself Java in 21 Days*, Samsnet, 1996.
8. Schildt Herbert, *JAVA: The Complete Reference*, 9th Edition, McGraw Hill Education, 2014.

A Comparative Study of Job Scheduling Algorithms in Cloud Computing

Narayan K.C.

Department of Graduate Studies, NCIT, Lalitpur, Nepal

Email Address: narayanck@gmail.com

Abstract

Cloud computing is a type of computing that relies on sharing computing resources rather than having local servers or personal devices to handle applications It is a kind of Internet-based computing that provides shared processing resources and data to computers and other devices on demand. It is a model for enabling ubiquitous, on-demand access to a shared pool of configurable computing resources which can be rapidly provisioned and released with minimal management effort. It is a new concept and based on the facts that reuse the resources of IT and its capabilities. This paper gives the brief introduction of cloud computing and also discusses the various issues in scheduling process in cloud computing and also proposes an optimal scheduling algorithm that could minimize the cost and completion time of a task. As we know that, Cloud computing is a technology where the user can pay only for the needed resources. Cloud computing is an attraction for many user as it offers access to computing resources form anywhere and anytime as they need.

Keywords: Cloud computing, CloudSim, Data Center, IaaS, PaaS, SaaS, Scheduling, Round Robin, Genetic Algorithms

1. Introduction

Today cloud has made it possible to access our data from anywhere, anytime. When compared to a traditional IT setup which requires same location for user and data storage device, in cloud we do not have such limitations. Cloud is very helpful for small & medium businesses which cannot afford bigger hardware and storage space. They can store their information in the cloud, reducing the cost of buying and storing memory devices. To run a cloud computing setup we need to have an internet connection. The benefit of this is that we can access that same document from wherever we are with any device that can access the internet. These electronic devices could be desktop, tablet, laptop or phone. This can also help our business to function more smoothly because anyone who can connect to the internet and your cloud can work on documents, access software, and store data.

2. Cloud Deployment Models

There are four deployment models which are as follows:

2.1 Private cloud

The private cloud is cloud infrastructure operated solely for a single organization, whether managed internally or by a third-party, and hosted either internally or externally.

2.2 Public cloud

A cloud is called a "public cloud" when the services are rendered over a network that is open for public use. Public cloud services may be free. Technically there may be little or no difference between public and private cloud architecture, however, security consideration may be substantially different for services that are made available by a service provider.

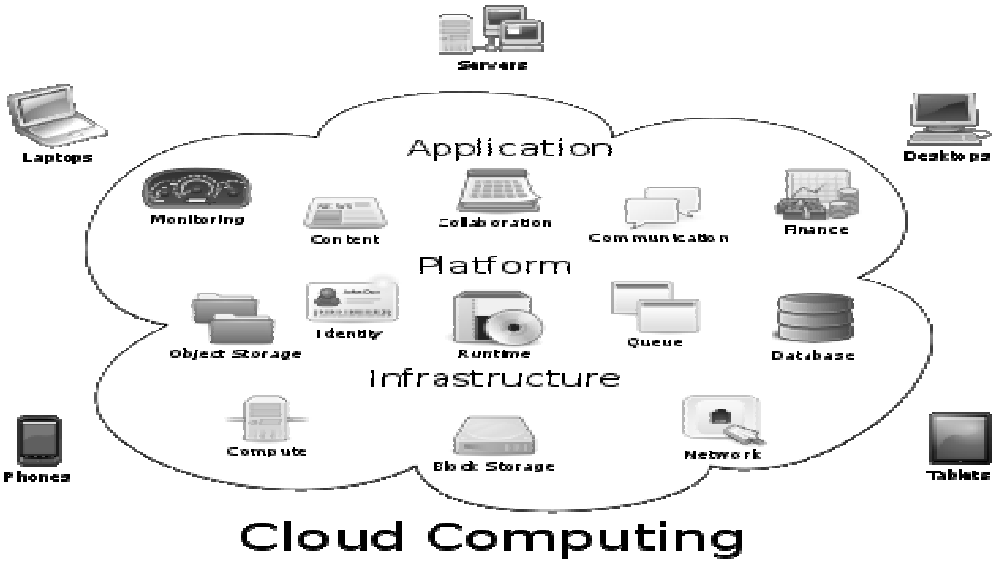

Fig. 1 overview of cloud computing

2.3 Hybrid cloud

The hybrid cloud is a composition of two or more clouds (private, community or public) that remain distinct entities but are bound together, offering the benefits of multiple deployment models. Hybrid cloud can also mean the ability to connect collocation, managed and/or dedicated services with cloud resources.

2.4 Community cloud

The community cloud shares infrastructure between several organizations from a specific community with common concerns, whether managed internally or by a third-party, and either hosted internally or externally.

3. Service Models

The cloud computing defines the service models as follows:

3.1 Software as a Service (SaaS)

The capability provided to the consumer is to use the provider's applications running on a cloud infrastructure. The applications are accessible from various client devices through either a thin client interface, such as a web browser or a program interface.

3.2 Platform as a Service (PaaS)

The capability provided to the consumer is to deploy onto the cloud infrastructure consumer-created or acquired applications created using programming languages, libraries, services, and tools supported by the provider. The consumer does not manage or control the underlying cloud infrastructure.

3.3 Infrastructure as a Service (IaaS)

The capability provided to the consumer is to provision processing, storage, networks, and other fundamental computing resources where the consumer is able to deploy and run arbitrary software, which can includes operating systems and applications. The consumer does not manage or control the underlying cloud infrastructure.

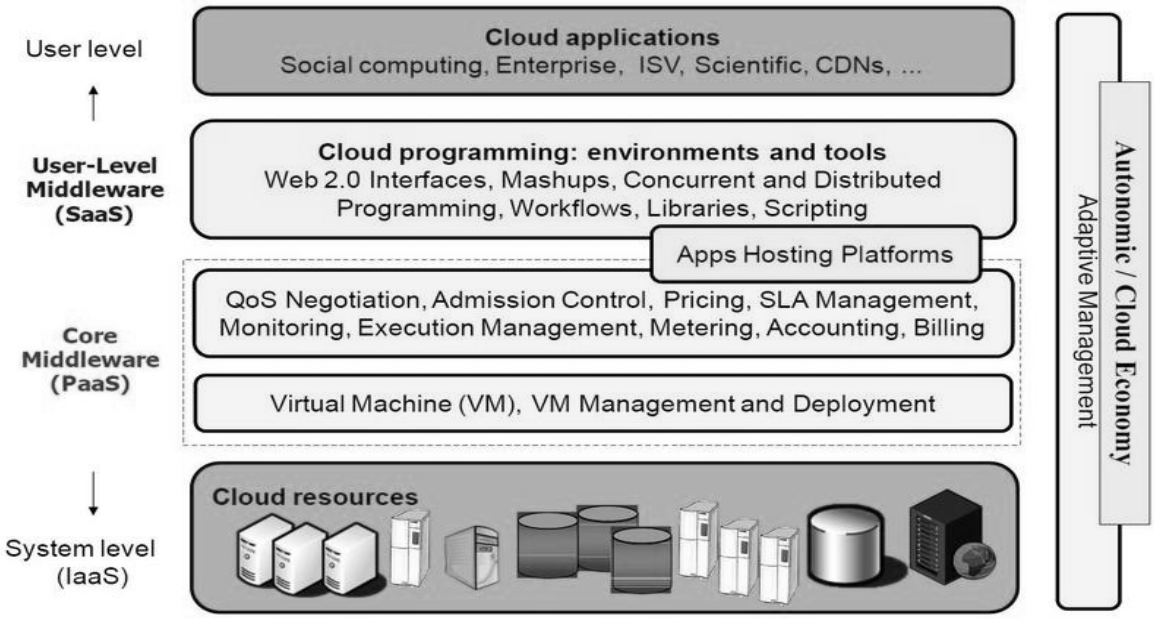

Fig. 2 Cloud Services

4. Procedure of Scheduling

Scheduling in cloud computing can be categorized into three stages.

- Discovering a resource and filtering them.
- Selecting a target resource (Decision stage).
- Submission of a particular task to a target resource.

5. Job Scheduling

The Job management is the fundamental concepts of cloud computing systems ask scheduling problems are main which relates to the efficiency of the whole cloud computing system. Job scheduling is a mapping mechanism from users' tasks to the appropriate selection of resources and its execution. Job scheduling is flexible and convenient. Jobs and job streams can be scheduled to run whenever required, based on business functions, needs, and priorities. Job streams and processes can set up daily, weekly, monthly, and yearly in advance, and run on demand jobs without need for assistance from support staff.

6. Existing Job Scheduling Algorithms

Job Scheduling Algorithms are as follows:

6.1 First come first serve scheduling algorithm

It is also known as First in First out. Shortest job next is advantageous because of its simplicity and because it minimizes the average amount of time each process has to wait until its execution is complete. It is one of the simplest Scheduling algorithms we have it allocate the CPU in the order in which the process arrive.

6.2 Shortest job first scheduling algorithm

Shortest job first (SJF) also known as Shortest Job Next (SJN) or Shortest Process Next (SPN) is a scheduling technique that selects the job with the smallest execution time. The jobs are queued with the smallest execution time placed first and the job with the longest execution time placed last and given the lowest priority.

6.3 Round robin scheduling algorithm

It is one of the oldest, simplest, fairest and most widely used scheduling algorithms, designed especially for time- sharing systems. A small unit of time, called time slices or quantum is defined. All run able processes are kept in a circular queue. The CPU scheduler goes around this queue, allocating the CPU to each process for a time interval of one quantum. New processes are added to the tail of the queue. The CPU scheduler picks the first process from the queue, sets a timer to interrupt after one quantum, and dispatches the process.

6.5 Priority scheduling algorithm

This Scheduling algorithm is preemptive in which all things are based on the priority in this scheduling algorithm each process in the system is based on the priority whereas highest priority job can run first whereas lower priority job can be made to wait, the biggest problem of this algorithm is starvation of a process.

6.5 Genetic algorithm

The genetic algorithm is a problem solving method that uses genetics as its model of problem solving. It is a search technique to find optimized solution. GA handles a population of possible solution. Each solution is represented through a chromosome. Genetic algorithm is a method of scheduling in which the tasks are assigned resources according to individual solutions, which tells about which resource is to be assigned to which task.

Table 1. Comparison of task scheduling algorithm

Algorithms	Complexity	Allocation	Waiting Time	Type of system
FCFS Algorithm	Simplest Scheduling Algorithm	CPU is allocated in the order in which the	More	Suitable for Batch system.
SJF Algorithm	Difficult to understand and code	CPU is allocated to the process with least CPU burst time	Lesser than FCFS	Suitable for Batch system
Priority Algorithm	Difficult to understand	Based on priority, So the higher priority job can run first.	Lesser	Suitable for both Batch and time sharing systems
Round Robin Algorithm	Performance heavily depends upon the size of time quantum	The preemption take place after a fixed interval of time	More than all	Suitable for time sharing system
Genetic Algorithm	Complexity depends on the task to be scheduled	This is a greedy algorithm and pick the best job to allocate the CPU	Waiting time is less	It deals with problem where the search space is large

The above given table presents the number of task scheduling algorithms and comparison between them on the basis of complexity, allocation, waiting time and type of system. The number of task scheduling algorithms and comparison between them on the basis of complexity, allocation, waiting time and type of system. Complexity defines which type of algorithm is simple or easy to use in processing. Allocation defines how the jobs are assigned to the resources. Waiting Time defines which of the algorithm takes more time for processing. Type of System defines which algorithm is suitable for which type of system. The FCFS algorithm is a simplest algorithm for scheduling but waiting time to process the tasks is much more in this. This algorithm is work on the basis of first come first serve, it means which process or task arrives first will processed first and it is suitable for batch type of systems. SJF algorithm is not a simple algorithm but their waiting time is less than FCFS. This algorithms process the task first having least CPU burst time and it is also suitable for batch systems. Priority algorithm works on the basis of priority. It is difficult to understand because how priority can be assigned to the task is a difficult task. Here waiting time is less because task with higher priority processed first. It is suitable for both batch and time sharing systems. Round robin algorithm works accordingly its fixed intervals of time. Here waiting time is more than all because after a fixed time interval the next task will execute. So problem faced when one task is very heavy and other one is with very simple and small calculations. Genetic algorithm is a bio inspired artificial intelligent scheme. Its complexity depends on the task. The best selected task executes first so waiting time is less here. This algorithm deals with large problems.

7. Proposed Framework and Methodology

The resource allocation and scheduling of resources have been an important aspect that affects the performance of networking, parallel, distributed computing and cloud computing. Many researchers have proposed various algorithms for allocating, scheduling and scaling the resources efficiently in the cloud. Scheduling process in cloud can be generalized into three stages namely

- Resource discovering and filtering
- Resource selection
- Task submission

7.1 Generalized priority algorithm

Customer defines the priority according to the user demand you have to define the parameter of cloudlet like size, memory, bandwidth scheduling policy etc. In the proposed strategy, the tasks are initially prioritized according to their size such that one having highest size has highest rank. The Virtual Machines are also ranked (prioritized) according to their MIPS value such that the one having highest MIPS has the highest rank. Thus, the key factor for prioritizing tasks is their size and for VM is their MIPS. This policy is performing better than FCFS and Round Robin scheduling.

Consider a five computational specific Virtual Machines represented by their Id and MIPS as follows:

V = {{0, 250}, {1, 1000}, {2, 250}, {3, 500}, {4,250}}. Here Vm2 will get first preference because of the highest MIPS, second preference is given to Vm4 and then Vm1, Vm3 and Vm4 get rest preferences.

The algorithm is given in stepwise below. This algorithm stores all suitable Virtual Machines in a VM List.

Create VM to different Datacenter according to computational power of host/physical server in term of its cost processor, processing speed, memory and storage.

Allocate cloud length according to computational power.

VM Load Balancer maintain an index table of VMs, presently VM has zero allocation. Cloudlet bound according to the length and respective MIPS. Highest length of cloudlet gets highest MIPS of virtual machine. Datacenter broker sends the request to the VM identified with id. Update the available resource.

8. Experiment and Evaluation

In order to verify our algorithm, the experiment on Intel(R) core(TM) i5 Processor 2.6GHz, windows 7 platform and using Cloudism 3.0.3 simulator. The Cloud Sim toolkit supports modeling of cloud system components such as data centers, host, virtual machines, scheduling and resource provisioning policies. A tool kit is the utilization which opens the possibility of evaluating the hypothesis prior to software development in an environment where one can reproduce tests.

Five Virtual Machines using VM component and set the property of RAM as 512 MB for all Virtual Machines, and the MIPS as 250, 1000, 250, 500 and250 respectively. We have created 12 tasks using Cloudlet component and set the property of Cloudlet length as 20000, 10000, 20000, 10000, 10000, 20000, 10000, 20000, 10000, 10000, 20000 and 10000 respectively. For this we considered 5 Virtual Machines with MIPS 1000, 500, 250, 250, 250 and RAM size of all Virtual Machine as 512 MB. Experiment is conducted for varying number of tasks like 100, 200, 300, 400 and 500 respectively. For comparison and analysis, we implemented the FCFS, Round robin, generalized priority algorithm.

Table 2. Experimental evaluation of Algorithms

FCFS Algorithm			**Round Robin Algorithm**			**Generalized Priority Algorithm**		
Execution Time	Data Center id	VM	Execution Time	Data Center id	VM	Execution Time	Data Center id	VM
80	2	1	239.99	2	1	20	2	2
10	2	2	119.99	2	2	20	3	1
80	2	3	160	2	3	40	3	4
20	3	4	40	2	4	40	2	3
40	3	5	20	3	5	40	3	5
80	2	1	239.99	2	1	20	2	2
10	2	2	119.99	2	2	40	2	1
80	2	3	160	2	3	40	3	4
20	3	4	40	2	4	40	2	3
40	3	5	20	3	5	40	3	5
80	2	1	239.99	2	1	20	2	2
10	2	2	119.99	2	2	10	2	4
45.8			114.16			30		

The scheduling is one of the most important tasks in cloud computing environment. The analysis of various scheduling algorithm shows the scheduling of the computational tasks in cloud environment. Among the FCFS, Round robin scheduling algorithm and new proposed scheduling algorithm is (GPA) generalized priority algorithm, Priority is an important issue of job scheduling in cloud environments. The experiment was conducted for varying number of Virtual Machines and workload traces. The experiment conducted is compared with FCFS and Round Robin. The result shows that the proposed algorithm is more efficient than FCFS and Round Robin algorithm.

9. Conclusion

In cloud computing, the job is executed on resources that are geographically distributed then there are need to schedule the tasks for better utilization of resources. The scheduling of tasks in better way that is beneficial for service provider and user is also a challenge in cloud environment. Hence, this paper has given the overview of cloud computing environment and also proposes an algorithm that groups the incoming tasks and schedule on basis of execution time.

References

1. https://en.wikipedia.org/wiki/Cloud_computing
2. http://cloud-simulation-frameworks.wikispaces.asu.edu/
3. R. Kaur and S. Kinger" Analysis of Job Scheduling Algorithms in Cloud Computing" in International Journal of Computer Trends and Technology, vol. 9, Mar 2014.
4. Agarwal and S. Jain" Efficient Optimal Algorithm of Task Scheduling in Cloud Computing Environment" in International Journal of Computer Trends and Technology, vol. 9, Mar 2014
5. Sashka Davis" in Priority Algorithms" June 2003
6. Seema Gusain and Rupak Kumar" An Optimization in Cloud Computing for Job Forecast" in International Journal of Computer Science and Mobile Computing, Vol. 3, Issue. 5, May 2014, pg.304 – 309

Extraction and Analysis of Retinal components using Morphological Operation

Pratik Shrestha

Department of Electronics and Computer Engineering

Advanced College of Engineering and Management

Kupondole, Lalitpur, Nepal

Email: pratikstha440@gmail.com

Abstract

This paper presents the way of extracting the retinal components using morphological operation. The major retinal components include Blood vessel and Optical Disc. The main significance of extraction of these components is to use it in biometric authentication system. Besides that, it can also be used in retinal disease diagnostics. In this paper firstly the image is desaturated, then it is enhanced. For the Blood vessel detection, Canny edge detection method is used with suitable parameters and later dilation is done. Similarly, for the Optical disc, binary threshold technique along with image dilation with suitable factor is used to segment the region of interest (ROI). For the analysis of obtained result, a desired image is drawn using a Adobe Photoshop and then the obtained image is compared with desired image along with every pixel and matched pixel accuracy is calculated. Peak Signal To Noise (PSNR) value and Mean Square Error (MSE) is also calculated for both blood vessel and optical disc. Error in centroid of optical disc is also calculated between obtained centroid and desired centroid. In this paper, the whole experiment is conducted over 10 retinal fundus images.

Keywords: Image processing, Retina, Blood vessel detection, Morphological operation, Authentication system, Optical disc, Biometric

1. Introduction

Retina is the innermost layer of the eye which can be visualized using adequate apparatus such as fundus camera. Just like other conventional biometric authentication systems like face, fingerprint, voice, facial thermo gram , palm print, hand geometry etc , retina scan also be used as a biometric authentication system. Comparing to other authentication system retina may provide higher level of security due to its inherent robustness against imposture. On the other hand, retinal pattern of each subject undergoes less modification during life [2]. The two main structures used in retinal image analysis are blood vessels and optic disc. Optic disc is the brightest region in the retinal image and the blood vessels originate from its center [1]. It can be seen as a pale, round or vertically slightly oval disk. Optic disc and blood vessels are the key reference for recognition algorithms and diagnosing some diseases such as diabetic retinopathy [2].

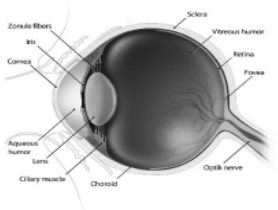

Fig (1) Anatomy of eye [4]

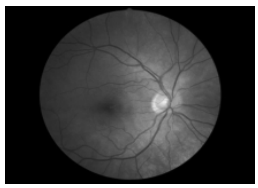

Fig (2) Fundus image of retina [11]

The above figure (1) shows the anatomy of eye and figure (2) shows the fundus image of retina. As shown in figure (1), the iris is located in the front of the eye, and the retina is located towards the back of the eye. Because of its internal location within the eye, the retina is not exposed to the external environment, and thus it possesses a very stable biometric. It is the blood vessel pattern in the retina that forms the foundation for the science and technology of retinal recognition which is as unique as finger print patterns [2].

The paper mainly concerns with the extraction and analysis of major retinal components, Blood vessel and Optical disc. In this paper a morphological method along with canny edge detection is used to segment the blood vessels of retina from fundus image. Similarly, for the optic disc, binary thresholding technique is used to segment out the optic disc which is the Region of Interest (ROI). To match the obtained image with desired image, a desire image is drawn in Adobe Photoshop and it is then compared pixel wise. The total matched pixel percentage is then calculated. Regarding the localization of optic disc, distance between obtained centroid and desired centroid is calculated and hence the error from this process is estimated. Peak Signal to Noise (PSNR) value and Mean Square Error (MSE) is also calculated for the components, Blood vessel as well as Optic disc.

2. Literature Review

In 1935, a paper was published by Simon and Goldstein [6], in which they discovered that every retina possesses a unique and different blood vessel pattern. They even later published a paper which suggested the use of photographs of these blood vessel patterns of the retina as a means to identify people. The second study was conducted in the 1950s by Dr. Paul Tower. He discovered that even among identical twins, the blood vessel patterns of the retina are unique and different [7].

In V.Vijaya Kumari and Dr. N. Suriyanarayanan‘s work [1] a similar experiment was done. They used morphological operation along with canny edge detection for blood vessel extraction. They have extracted the blood vessel using Weiner filter and morphological operation. They concluded that PSNR of morphological method is high, hence it is better than Weiner filter method. They have also suggested to localize the optic disc in future which has been done in this paper.

Osareh [5] proposed a method based on template matching for localizing the center of optic disc. In this algorithm, some of retinal images in dataset were used to create a template and the correlation between each image and template is computed. The point which has the maximum correlation value is selected as the center of optic disc.

In the work of P. Choukikar, A.K. Patel and R.S. Mishra [8], the true color Retinal images were converted to gray image and then image was enhanced using histogram equalization. This improves the efficiency of the conventional thresholding method. The method of segmentation utilizes gray level thresholding for segmentation and then morphological operators were used for extracting the optical disk. The method was less complex and efficiently recognized the boundary of the optic disc and also evaluated the optical center. The optical centers were tabulated for original and corrupted images.

Some methods are based on the Hough transform which is capable of finding geometric shapes. Therefore, the circular shape of optic disc was detected using Hough transform and other algorithms such as thresholding and morphological operations [9, 10].

3. Methodology

In this paper, like mentioned above, two major retinal components have been extracted. Method for extraction and analysis of those two components i.e Blood vessel and Optic Disc is slightly different. In the upcoming sections, it is described in detail.

3.1 Detection of Blood Vessel

Segmentation and extraction of blood vessel is one of the major and difficult task of retinal image processing for retinal authentication system and retinal disease diagnostics. The process of blood vessel detection is presented using block diagram in figure (3). In this method, firstly the fundus image is taken. The input retina fundus image is as shown in figure 4 (a). Then the input retinal image is pre-processed. In pre-processing stage, the input image is resized and cropped according to necessity and the green channel image is separated as the blood vessel appears brighter in the reen channel image. Then filter is used to remove the noise in the input image. Then histogram equalization is applied to the filtered image to make the segmentation work easier. Then our image looked something like shown in figure 4(b). The Canny edge detection is applied in the resultant image to detect the image with suitable parameter.

The primary morphological operations are dilation and erosion. The more complex morphological operations are opening and closing. Dilation is an operation that grows or thickens objects in a binary image. The specific manner and extent of this thickening is controlled by shape referred to a structuring element. In this method, a structuring element of disk shaped with size 1 to 2 pixels is created. Dilation is defined in terms of set operation. Erosion shrinks or thins objects in a binary image. The manner and extent of shrinking is controlled by a structuring element. Image after Canny edge detection and final dilation looked something like figure 4(c).

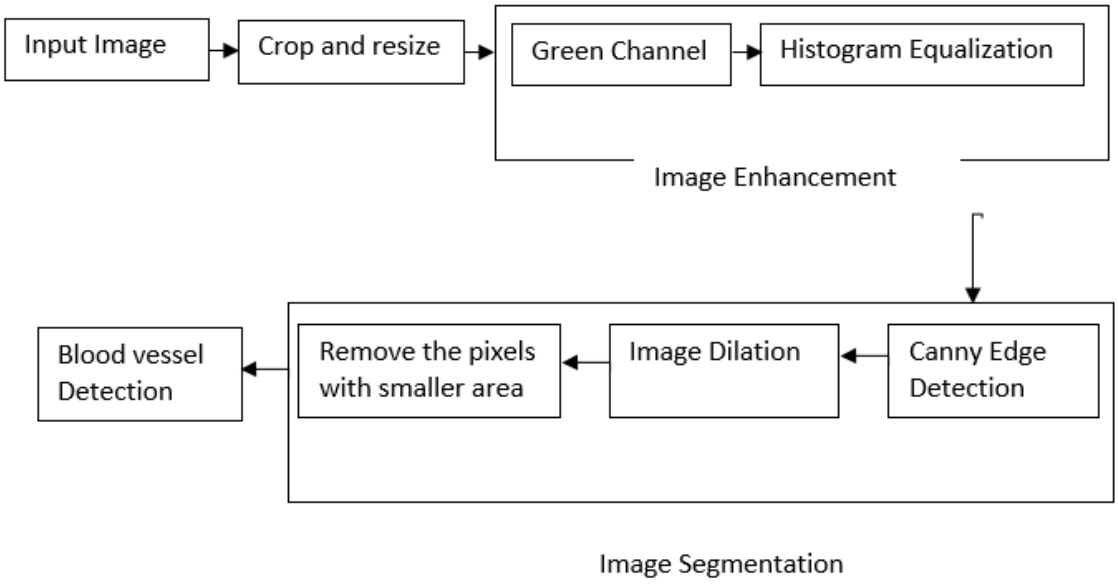

Fig (3): Block diagram of overall method for Blood vessel extraction

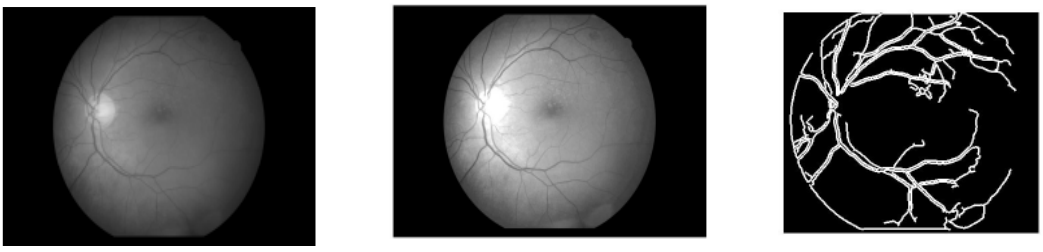

(a) (b) (c)

Fig (4). Steps of blood vessel detection. (a) Input Image of retina fundus. (b) Enhanced Image after histogram equalization. (c) Image obtained after Canny edge detection and dilation.

The above method is tested for 10 images which are standard images taken from Google and result is then calculated along with accuracy, Peak Signal to Noise value (PSNR) and Mean Square Error (MSE).

3.2 Detection of Optic Disc

Similar to detection of blood vessel, even optic disc has important role to play in retinal authentication and other retinal disease diagnostics. The key feature to detect the optical disc is that it is the brightest part of retina and also of shape ellipse or oval, almost round. Considering these key features in mind firstly the image is taken and then green channel is separated. The obtained green channel image is then enhanced using histogram equalization so that the details of the image get more clear and distinct. The resultant image is shown in figure 6 (b). Binary thresholding is done with suitable parameter to segment the desired area of interest. After that it is then dilated with structural element of disc shape to make the shape of blob more round and free from unwanted noise and holes. The resultant image after binarizing and dilation appeared as figure 6 (c). Moreover, a centroid of that blob, which is considered to be centroid of the optic disc, is also calculated. This is displayed in figure 6 (d). Figure 6 (e) shows the distance between obtained centroid and desired centroid. All of this mentioned process is shown in block diagram of figure (5).

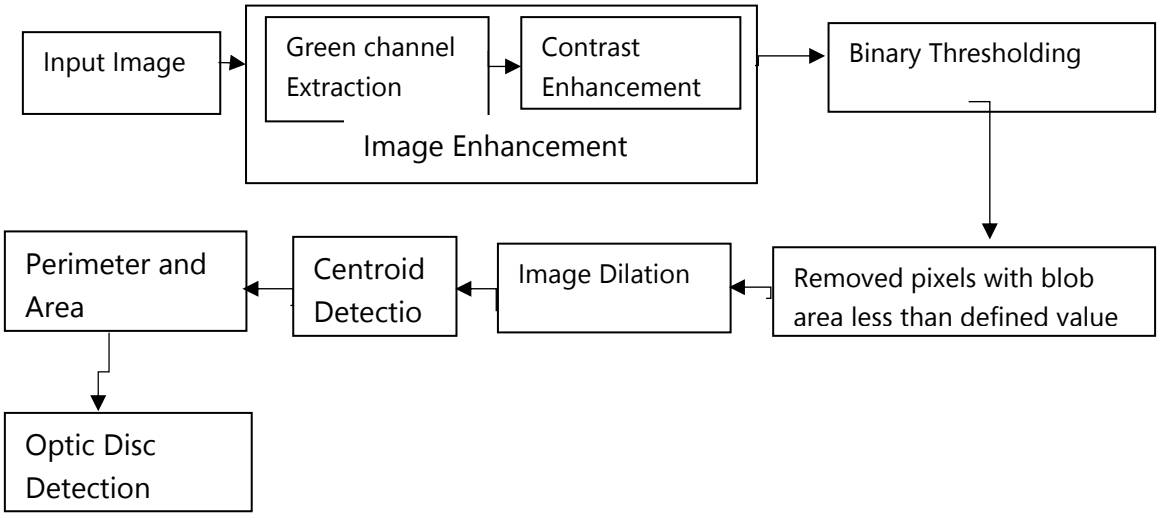

Fig (5): Block diagram of overall method for Optic Disc extraction

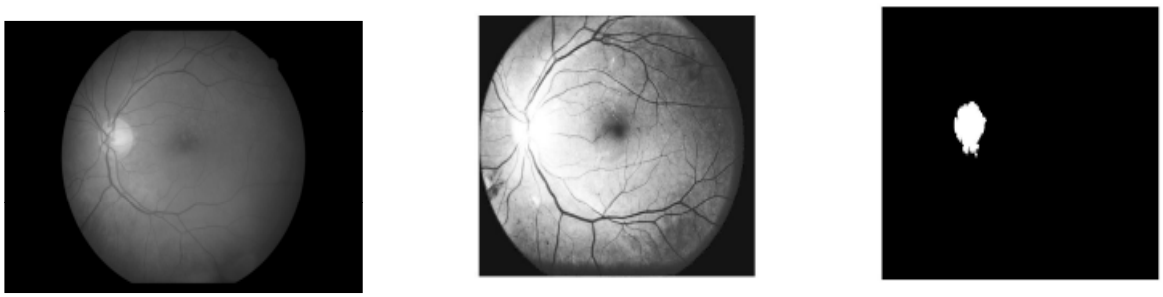

(a) (b) (c)

(d)

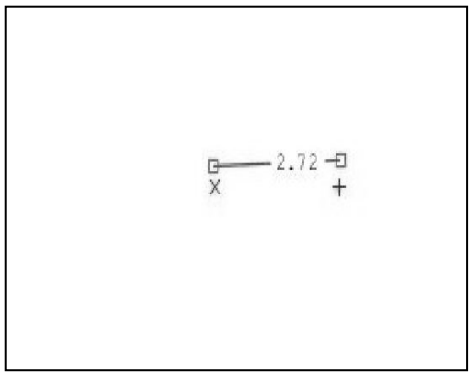

(e)

Fig (6). Steps for Optic Disc detection. (a) Input retina fundus image. (b)Enhanced Grayscale image (c) Thresholded and segmented image of optic disc (d) Detection of centroid. (e) Distance between desired centroid and Obtained centroid which shows the error

For the detection of area, the total number of ones (whites) in an image is counted and hence that is the obtained area. Similarly, for the calculation of the centroid, the rows and columns with value one are found. [3]. Eg: let a matrix be A= $\begin{matrix} 1 & 0 & 1 \\ 0 & 1 & 0 \\ 1 & 1 & 1 \end{matrix}$

Row = [2 1 3]

Column = [2 2 2]

Centroid [X, Y] = [(2+1+3)/3 (2+2+2)/3]

= [2 2]

The roundness of the blob (segmented region) is calculated using following formula:

Roundness = (4*Area*pi)/ (Perimeter^2)

If the Roundness is greater than 0.90 then, the object is circular in shape.

4. Result and Discussion

The above method is tested in Matlab with over 10 random fundus images which are standard and are taken randomly from Google. To measure the accuracy of this method, a desired pattern of blood vessel is drawn in Adobe Photoshop. Then it is converted into binary image by thresholding the required level. Now the two images, the desired image and obtained image, is compared pixel wise. In this method, corresponding pixels of two images are compared and the number of matched pixels are counted. The result is table (a). On the basis of matched pixels and Total pixels, accuracy percentage is calculated using following formulae mentioned by Equation (i):

$$\text{Accuracy (\%)} = \frac{Matched Pixels}{Total Pixels} \times 100\% \qquad \text{(i)}$$

Table (a): Result obtained for Blood vessel detection

Image	Match Count	Size	% Matched	PSNR	MSE
1_jpg	190,689	427x516	86.54	8.995	8.19E+03
2_jpg	73,050	293x316	78.89	6.7567	1.37E+04
3_jpg	143,130	412x410	84.732	8.1623	9.93E+03
4_jpg	127,942	360x420	84.61	8.1298	1.00E+04
5_jpg	80,062	290x320	86.27	8.7172	8.74E+03
6_jpg	201439	432x504	92.51	11.26	4.86E+03
7_jpg	164790	401x468	87.8	9.1397	7.93E+03
8_jpg	108707	353x353	87.23	8.941	8.30E+03
9_jpg	192294	466x466	88.55	9.4124	7.44E+03
10_jpg	113768	337x381	88.6	9.4334	7.41E+03

Similarly, for the optic disc detection, a desired image is drawn in the Adobe Photoshop and it is compared with obtained image just like above mentioned method. The distance between the centroid of obtained optic disc and desired optic disc is also calculated which shows the error. Moreover, the PSNR value and MSE value is also calculated. The result obtained is Table (b) and (c).

Table (b): Result showing the distance between obtained centroid and desired centroid in optic disc

Image	**Perimeter**	**Roundness**	**Desired Centroid**	**Obtained Centroid**	**Distance between two points**
1_img	360.8772	0.4816	224.6509 ,189.2904	229.7385 ,187.2805	5.47
2_img	313	0.2515	259.4356 ,164.0992	255.6677 ,162.1423	4.25
3_jpg	357.0193	0.7752	226.4658 ,200.1581	227.9847 ,197.8872	2.73
4_jpg	142.4092	0.5292	275.8643 ,180.1593	271.4734 ,180.1755	4.39
5_jpg	167.7229	0.7185	251.7146 ,140.5327	238.8004 ,138.0851	13.14
6_jpg	310.6518	0.3829	158.6446 ,195.5741	170.3939, 199.0584	12.26
7_jpg	399.6884	0.4122	63.5018 ,279.9919	72.8400, 277.3928	9.69
8_jpg	189.6224	0.5371	107.8738,167.0036	109.2130, 167.1455	1.35
9_jpg	208.5929	0.6164	130.8691 ,213.8973	138.7314, 207.1206	10.38
10_jpg	370.0071	0.4869	227.6071 ,213.0918	230.2775 , 213.0890	2.67

Table (c): Result for Optic Disc detection

Image	Match count	Size	%Matched	PSNR	MSE
1_jpg	270674	427x640	99.04	20.2	620.0789
2_jpg	120821	304x400	99.35	21.934	416.5664
3_jpg	167106	412x410	98.92	19.6904	698.2912
4_jpg	110883	309x360	99.67	24.9359	208.6833
5_jpg	93781	298x320	98.34	17.8	1.08E+03
6_jpg	216252	432x504	99.32	21.6883	440.811
7_jpg	331412	535x624	99.27	21.3829	472.9233
8_jpg	123913	353x353	99.44	22.5294	363.1953
9_jpg	189015	437x437	98.97	19.9004	665.3376
10_jpg	348422	483x725	99.49	23.005	325.5196

According to the above obtained result, for blood vessel detection the average values are as follows:

Average PSNR = 8.89475

Average MSE = 8650

Average accuracy percentage = 86.57 %

Similarly, for the optic disc, the average result is as follows:

Average PSNR = 21.306

Average MSE = 528.81

Average accuracy percentage = 99.181%

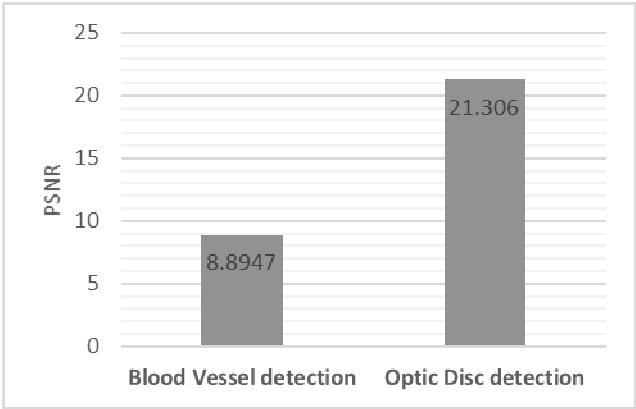

Chart (a)

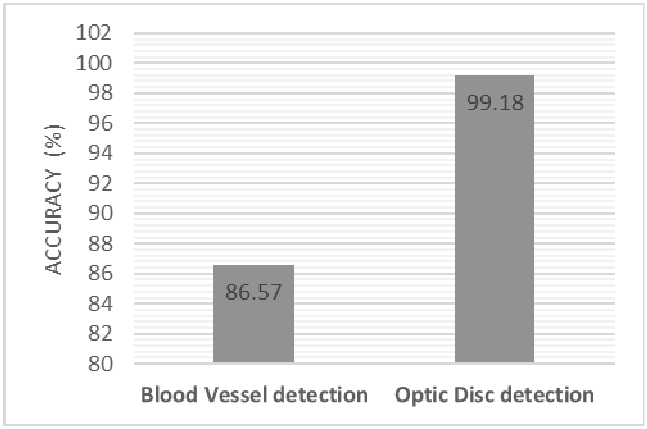

Chart (b)

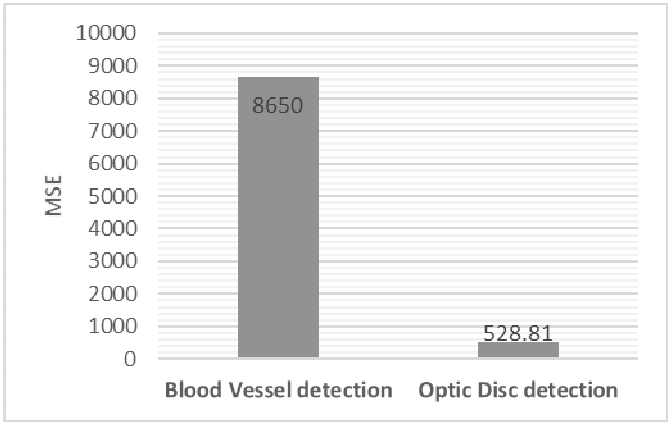

Chart (c)

Chart 1. (a) Comparison of PSNR between Blood vessel detection and optic disc detection. (b) Comparison of Accuracy percentage between Blood vessel detection and optic disc detection. (c) Comparison of MSE between Blood vessel detection and optic disc detection.

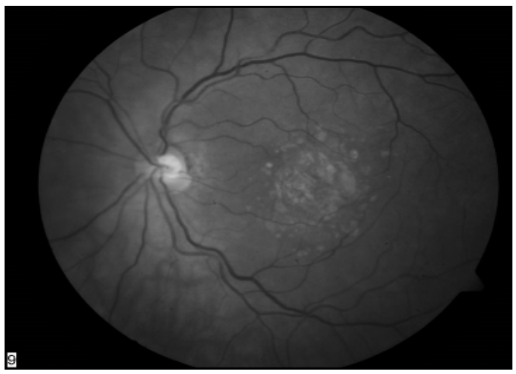

(a)

(b)

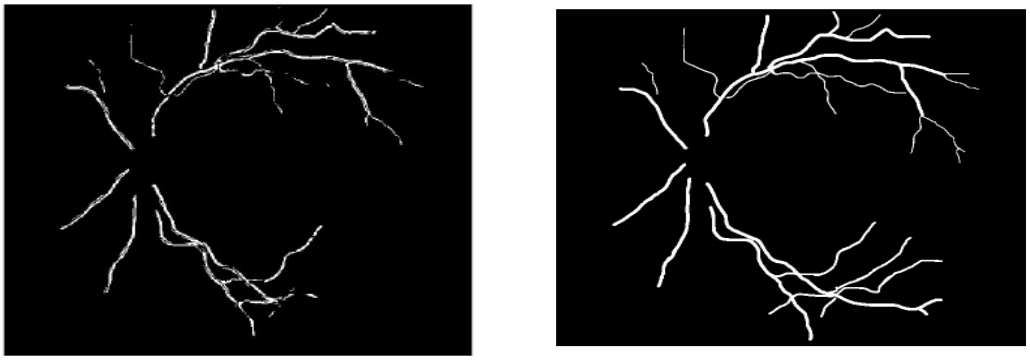

(c) (d)

Fig (7). (a) The input retina fundus image. (b) The obtained binary image of segmented blood vessel. (c) The image of desired blood vessel drawn in Adobe Photoshop. (d) The image of result obtained from ANDING fig (b) and (c).

The above figure 7(d) is obtained from ANDING fig 7(c) and 7(b). This image shows the matched pixels between desired image and obtained image.

5. Conclusions

In this paper, the green channel image from RGB image is taken and the blood vessel is extracted from the retinal fundus image. The extraction is done using gray image thresholding and morphological operation. The optic disc is also extracted along with its centroid and other parameters like roundness and area. Chat 1(a) and 1(b), which show the average PSNR and accuracy percentage, obtained from the 10 retinal fundus images show that the performance is better in extraction of optic disc than extraction of blood vessel using this image thresholding and morphological operation. Chart 1(c) shows that Mean Square Error is less in case of Optic disc extraction than in Blood vessel extraction.

6. Suggestions and Recommendations

The drawback of this method is that it uses different values for canny edge detection, thresholding and noise removal. In the future these things can be made automatic using neural network where the system itself will adjust these values. As we can see in above results that the blood vessels with softer edge is not visible to the system. Hence in future the enhancement work can be done with higher efficiency which makes every softer blood vessel appear brighter and sharper which will ultimately increase the accuracy.

References

1. Kumari VV, Suriyanarayanan N: Blood vessel extraction using wiener filter and morphological operation. Int. J. Comput. Sci. Emerg. Technol. 2010, 1(4):7-10.
2. Farzin H, Abrishami Moghaddam H, Moin M-S: A novel retinal identification system. EURASIP J. Adv. Signal Process 2008, 2008: Article ID 280635. 10.1155/2008/280635
3. http://angeljohnsy.blogspot.com/2012/05/find-area-perimeter-centroid.html, October 14, 2016
4. http://www.savesightcentre.com/images/anatomy%20big.jpg, October 14, 2016
5. Osareh A: Automated identification of diabetic retinal exudates and the optic disc. Ph.D. dissertation. Department of Computer Science, Faculty of Engineering, University of Bristol, Bristol, UK; 2004.

6. C. Simon and I. Goldstein, “A new scientific method of identification,” New York State Journal of Medicine, vol. 35, no. 18, pp. 901–906, 1935.
7. P. Tower, “The fundus oculi in monozygotic twins: report of six pairs of identical twins,” Archives of Ophthalmology, vol. 54,no. 2, pp. 225–239, 1955.
8. Prashant Choukikar, Arun Kumar Patel and Ravi Shankar Mishra ,”Segmenting the Optic Disc in Retinal Images using Thresholding”, International Journal of Computer Applications (0975 – 8887) Volume 94 – No 11, May 2014
9. M Niemeijer, B van Ginneken, F Ter Haar, MD Abramoff, Automatic detection of the optic disc, fovea and vascular arch in digital color photographs of the retina. Proceedings of the British Machine Vision Conference, 109–118 (2005)
10. S Sekhar, W Al-Nuaimy, AK Nandi, Automatic localization of optic disc and fovea in retinal fundus. 16th European Signal Processing Conference (2008)
11. http://triadeyecenter.com/wp-content/uploads/sites/1990/2015/07/digitalretinallefthealthy.jpg

HUMAN AND WILDLIFE CONFLICT PREDICTION OF CHITWAN NATIONAL PARK USING DATA MINING TECHNIQUES

Samir Pokharel[1], Kshitij Wagle[2]

[1,2]Department of Electronics and Computer, Pashchimanchal Campus, Pokhara, Nepal

[1]Email Address: samir.pokhrel02@gmail.com

[2]Email Address: kshitij.wagle@gmail.com

Abstract

Human and Wildlife Conflict (HWC) has negative impact on socio-economic and cultural life. Knowledge discovery from past data records of human and wildlife conflict is vital in area near to the National Parks and Conservation Areas, which is quite challenging. In this paper, we predicted the maximum conflicted months and areas in Chitwan National Park. This is carried out using K Mode Clustering Algorithm with the help of data collected between 2064 and 2072 from Chitwan National Park, Nepal. This paper examines species-specific catastrophes, including buffer zones along with months or seasons of maximum attack which will be helpful to enhance preventive measures around park.

Keywords*: HWC, Clustering, K-modes algorithm, Buffer zone, Categorical data*

1. Introduction

Chitwan National Park (CNP) is being encroached by enormously increasing human settlement which has affected the flora and fauna of that particular region. It consists of more than 700 species of wildlife. Losses of crops and depredation on livestock near national parks are increasing day by day. With increasing urbanization and demand of resources, conflict between human and wildlife is more pronounced.

Human-Wildlife Conflict (HWC) is defined as any interaction between humans and wildlife that results in negative impacts social, economic or cultural life, on the conservation of wildlife populations, or on the environment [1]. Conflicts arise when the activities of wild animals coincide with those of people [2]. It is more in developing countries where livestock holdings and agriculture are an important part of rural livelihoods. HWC arises mainly because of the loss, degradation and fragmentation of habitats through human activities such as logging, animal husbandry, agricultural expansion, and developmental projects. Reduction in the availability of natural prey/food sources leads to wild animals seeking alternate sources.

Damages by wildlife can have catastrophic effect in various sectors. Crop and property damage, livestock toll, harassment to the people, trophic cascade and destruction of habitat, collapse of wildlife population and reduction of geographic ranges are more pronounced effects. Although presently, the Buffer Zone Management Committee of the Chitwan National Park (CNP) and the Bardia National Park (BNP) are allocating small amounts of money as compensation for livestock depredation and human casualties [3]

Data mining is the computational process of discovering patterns in large data sets involving methods at the intersection of artificial intelligence, machine learning, statistics, and database systems [4]. It is the process of analysing data from different perspectives and summarizing it into useful information.

Its theme is finding unknown patterns and others which is the part of knowledge discovery phase. This technique is used in many research areas like wildlife, mathematics, bio informatics, customer relationship management etc. Data, information and knowledge are three things that we can obtain from raw data stored in database. Data are any facts, numbers, text etc. that can be processed by a computer. The patterns, associations, or relationships among all this data can provide information. Information can be converted into knowledge about historical patterns and future trends.

2. Literature Review

Causes and consequences of Human and Wildlife Conflict:

The report on Human-Elephant Conflict in Eastern and Western Terai regions by [5] provides the information about the adverse effect of conflict on Jhapa and Bardiya district. Moreover, research did by The Rufford Foundation gives the spatial and temporal patterns of human casualties and livestock depredations of Chitwan National Park. The report of compensation provided to the people, prepared by Chitwan National Park shows that the major wildlife species causing conflict are Royal Bengal Tiger, One Horned Rhino, Leopard, Crocodile, Bear, Elephant and Wild Pig.

A study on "Park people conflict- A case study from Beldandi VDC adjacent to Suklaphanta Wildlife Reserve of western lowlands, Nepal" showed that the park people conflict was due to resource use problem, grazing problem, wildlife damage and resettlements problems. The study by IUCN, shows the Demographic and social changes place more people in direct contact with wildlife: as human populations grow, settlements expand into and around protected areas as well as in urban and sub-urban areas. These crops create favorable habitats for predators and play a major role in influencing the natural distribution and growing densities in livestock populations can create an overlap of diets and forage competition with wild herbivores, resulting in overgrazing and decline or local extinction in wild herbivore populations.

Data mining concept and application:

Understanding in the concept of data mining was obtained from Data Mining Concept and Technique [4]. Several papers about data mining published in Indian Journal of Computer Science and Engineering makes us familiar about the concepts and algorithms. The book Advances in Knowledge Discovery and Data Mining, edited by Fayyad, is the collection of later research result on knowledge discovery and data mining. KD Nuggets is a regular electronic newsletter containing information relevant to knowledge discovery and data mining, moderated by Piatetsky-Shapiro since 1991 has become prior for our knowledge.

The statistical understanding of large number of data was obtained from various papers including The Elements of Statistical Learning by Hastie, Tibshirani, and Friedman. Good summary of statistical descriptive data mining method include Freedman, Pasani and Purves. The visualization technique of data is described in The Visual Display of Quantitative Information [6]. Large number of research published in Transaction on Visualization and Computer Graphic and IEEE Computer Graphic and Application provides concept in data visualization.

Srikanta and Agrawal [7] provides in depth knowledge in Association rule mining and about frequent item set. Many algorithms have been proposed that adapt frequent pattern mining to the task of classification. Early studies in association classification include the CBA algorithm purposed in Lau, Hsu, and Ma [8]. Algorithm like k means, decision tree, ID3 etc. was known from [4]. Several textbook dedicated to method of cluster analysis, including Hartigan [9], Jan and Dubes [10] gives the concept about clustering and its types.

Wildlife data mining

The research article published in International Journal of Computer Applications about Wild Life Protection by Moving Object Data Mining - Discover with Granular Computing by Rawat, Sodhi and Tyagi makes us familiar about the process of extraction of knowledge from wildlife [11]. Research on Data-Mining Discovery of Pattern and Process in Ecological Systems [12] makes us familiar about pattern on ecology. Several other papers published in IEEE and Springer Link provides knowledge about the wildlife data mining.

3. Methodology

We used R programming language for data mining process. R is widely used in both academia and industry. It is a free software environment for statistical computing. R can be easily extended with 6,600+ packages available on CRAN. The CRAN Task Views provide collections of packages for different tasks. We used K Mode Clustering Algorithm by the use of package available in the R Studio.

K-modes algorithm

Let X, Y be the two categorical object described by m categorical attributes. The simple dissimilarity measure between X and Y is defined by the total mismatched of the corresponding attribute values of the two object, the smaller the number of mismatches is, the more similar the two objects. Formally,

$$d(X,Y) = \sum_{j=1}^{m} \delta(x_i, y_i)$$

Where,

$$\delta(x_j, y_j) = \begin{cases} 0 & (x_j = y_j) \\ 1 & (x_j \neq y_j) \end{cases}$$

Let S be a set of categorical objects described by m categorical attributes $A_1 \ldots A_m$. A mode of $S = \{X_1, X_2, \ldots\ldots X_n\}$ is a vector $Q = [q_1, q_2, \ldots\ldots, q_m]$ that minimizes.

$$D(S,Q) = \sum_{i=1}^{n} d(X_i, Q)$$

Here, Q is not necessarily an object of S.

Let $n_{c_{k,r}}$ be the number of objects having the kth category ck,r in attribute Ar and $f(A_r = C_{k,r}) = \frac{n_{c_{k,r}}}{n}$ the relative frequency of category $n_{c_{k,r}}$ in S. The function D(S,Q) is minimized iff $f(A_r = q_r) \geq f(A_r = c_{k,r})$ for $(q_r = c_{k,r})$ and all r = 1,…,m.

The optimization problem for partitioning a set of n objects described by m categorical attributes into k clusters S1, S2,……,Sk becomes

Minimize $\sum_{i=1}^{k} \sum_{X \in S_i} d(X_i, Q_i)$

Where, Qi is the mode of cluster Si.

In above k-modes clustering problem, the representative point of each cluster Si, i.e., the mode Qi, is not necessarily contained in Si. If we restrict the representative point to be in Si, it becomes well-known k-median problem. In the next section, we will show that the optimum of k-median is at most

the twice optimum of k-modes for the same categorical data clustering problem. Hence, the loss is modest even restricting representatives to points contained in original set.

Data selection and data processing

Basically CNP prepares annual report on topic “Compensation provided on behalf of wildlife damage in Chitwan National Park”. It contains a lot of attribute and some of them the lacks proper data. The report was prepared in Nepali and some of the record lacks date. Also the date needs to be converted into AD. So we select some of the attribute which is useful in data mining process as our requirement.

Table 1: Original Data Source retrieved from Chitwan National Park

सि.नं.	निवेदकको नाम	ठेगाना	उपभोक्ता समिति	घटना मिति	घटनाको विवरण	माग गरेको रकम	मध्यवर्ती क्षेत्र व्यवस्थापन समि		
							मानविय क्षति	पशुधन क्षति	घर गोठ क्षति
११११	जितकुमारी महत्तो	अग्यौली ५,न.प.	अमलटारी	२०६३।१२।८	बाघले भेडा मारेको	२०००		१०००	
१११२	मिना कुमारी महत्तो	अग्यौली ५,न.प.	अमलटारी	२०६३।१२।८	बाघले भेडा मारेको	२०००		१०००	
११११	पुरन चौधरी	अग्यौली ५,न.प.	अमलटारी	२०६३।१२।८	बाघले भेडा मारेको	७०००		३५००	
११११	शोभा महत्तो	अग्यौली ५,न.प.	अमलटारी	२०६३।११।२२	बाघले गोरु मरेको	८०००		४०००	
११११	ओम बहादुर थापा	कुमारवर्ती ८,न.प.	अमलटारी	२०६४।७।१४	बाघले भैसी मारेको	२०००		१०००	
११११	तुल बहादुर वि.क.	पिठौली ७,न.प.	लामिचौर	२०६४।५।५	बाघले बाख्रा मारेको	३४५०		१७५०	
११११	चुरामणी थारु	काबासोती १,न.प.	लामिचौर	२०६४।४।११	चितुवाले बाख्रा मारेको	३०००		१५००	
११११	सिखाराम महत्तो	पिठौली ६,न.प.	लामिचौर	२०६४।३।३०	बाघले बंगुर मारेको	४०००		२०००	
११११	हरिभक्त घिमिरे	बछौली १,चितवन	मृगकुञ्ज	२०६४।६।५	हात्तीले घर भत्काएको	१०००			१०००
१२१०	बुद्ध गिरी	बछौली २,चितवन	मृगकुञ्ज	२०६४।६।५	हात्तीले घर भत्काएको	८१००			४०००
१२११	फागु महत्तो	बछौली २,चितवन	मृगकुञ्ज	२०६४।६।६	हात्तीले घर भत्काएको	१५००			१५००
१२१२	लालकान्ता न्यौपाने	मेघौली ९,चितवन	मेघौली	२०६४।६।२९	चितुवाले बाख्रा मारेको	२४००		१२००	
१२१३	सुकमाया राई	अयोध्यापुरी ४,चितवन	अयोध्यापुरी	२०६४।५।२९	हात्तीले घर भत्काएको	२९९०			१४९५
१२१४	जंग बहादुर वि.क.	अयोध्यापुरी ४,चितवन	अयोध्यापुरी	२०६४।५।२९	हात्तीले घर भत्काएको	६००			३००

The original format is converted to the following format.

Table 2: Conversion table of original data source

	A	B	C	D	E
1	place	predetor	prey	month	season
2	Meghauli	tiger	domestic	june	spring
3	Lamichow	rhino	man	march	spring
4	Daunnede	leopard	domestic	march	spring
5	Panchpan	leopard	domestic	jan	winter
6	Panchpan	leopard	domestic	feb	winter
7	Amaltari	tiger	domestic	march	spring
8	Lamichow	tiger	domestic	march	spring
9	Amaltari	tiger	domestic	march	spring
10	Amaltari	tiger	domestic	march	spring
11	Amaltari	tiger	domestic	march	spring
12	Amaltari	tiger	domestic	march	spring
13	Sisauwar	tiger	domestic	oct	autumn

The number of data and its types are shown below:

'data.frame': 1539 obs. of 5 variables:

$ place : Factor w/ 26 levels "Amaltari","Ayodhyapuri",..: 14 12 6 20 20

1 12 1 1 1 ...

$ predetor: Factor w/ 10 levels "bear","crocodile",..: 8 6 5 5 5 8 8 8 8 8

.

$ prey : Factor w/ 4 levels "crops","domestic",..: 2 4 2 2 2 2 2 2 2 2 .

.

$ month : Factor w/ 13 levels "74","april",..: 8 9 9 6 5 9 9 9 9 9 ...

$ season : Factor w/ 4 levels "74","autumn",..: 3 3 3 4 4 3 3 3 3 3 ...

The summary of our data is shown below:

place	predetor	prey	month	season
Ayodhyapuri:373	elephant:449	Crops :445	dec :197	74 : 1
Lamichowr :136	tiger :362	Domestic :647	oct :163	autumn:408
Rewa :127	leopard :338	House :170	feb :159	spring:618
Bagauda : 95	rhino :292	Human :277	jan :156	winter:512
Panchpandav: 94	bear : 55		july :149	
Nandavauju : 71	wildpig : 23		nov :137	
(Other) :643	(Other) : 20		(Other):578	

Statistical test:

a) Test for place and predetor:

Number of cases in table: 1539
Number of factors: 2

Test for independence of all factors:

Chisq = 1661.1, df = 225, p-value = 3.93e-217

b) Test for place and prey:

Number of cases in table: 1539
Number of factors: 2

Test for independence of all factors:

Chisq = 813.3, df = 75, p-value = 2.101e-124

c) Test for place and month:

Number of cases in table: 1539
Number of factors: 2

Test for independence of all factors:

Chisq = 990.8, df = 300, p-value = 9.477e-75

d) Test for place and prey:

Number of cases in table: 1539
Number of factors: 2

Test for independence of all factors:

Chisq = 813.3, df = 75, p-value = 2.101e-124

e) Test for place, predator, prey and month :

Number of cases in table: 1539
Number of factors: 2

Test for independence of all factors: Chisq = 38376, df = 13470, p-value = 0

4. Simulation and Results

RStudio output: Model based clustering

Model based clustering is used to visualize the dependency of attributes. In above graph, various color and shapes shows the data of attributes and circular line represent that two attributes are dependent to each other. In between place and predator from second row first column circular line between them shows the dependency which is graphically shown as stated above from chi square test.

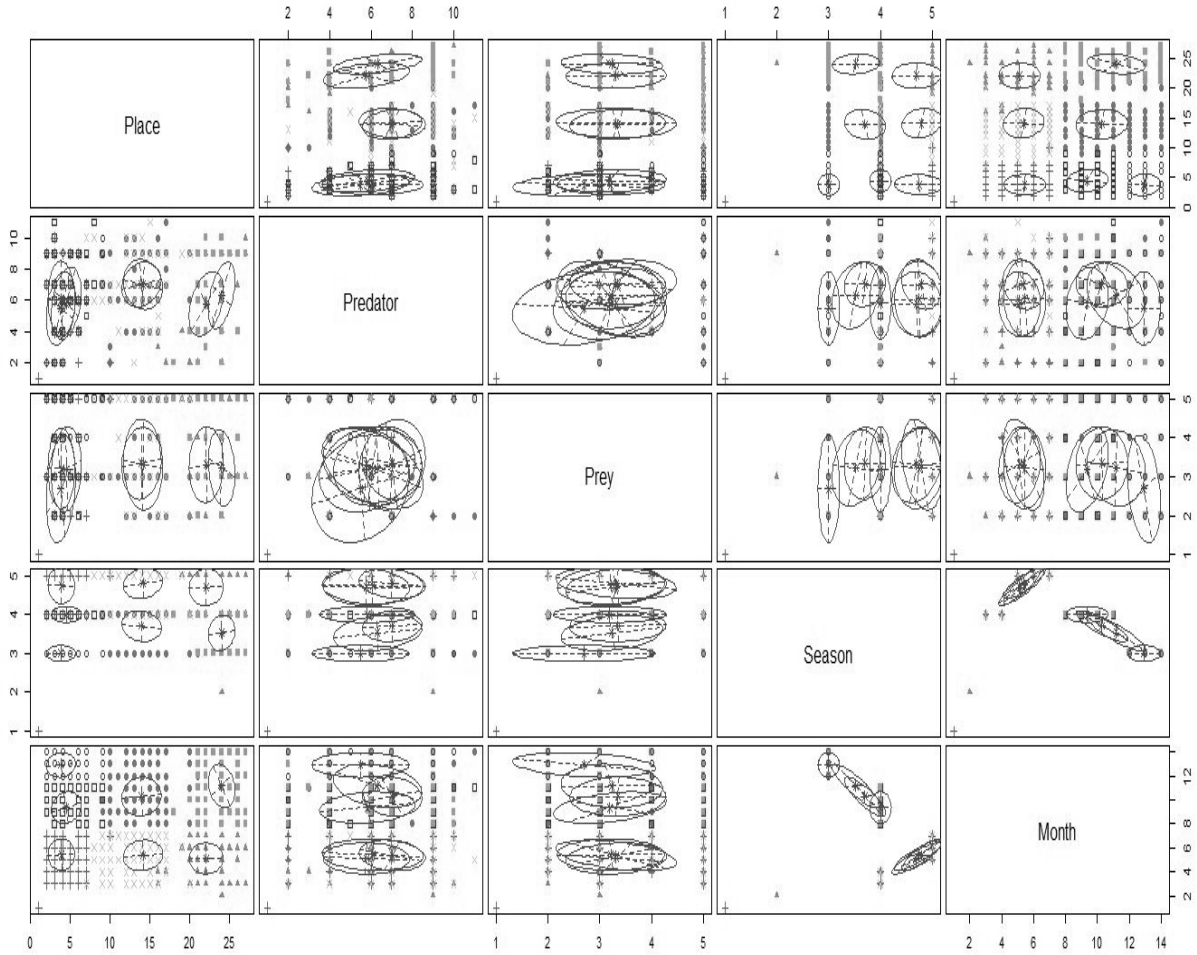

Figure 1: Model based clustering of various attribute

RStudio output: k-mode clustering

From the huge categorical data sets, the k-mode clustering algorithm has been applied which counts frequent item of the same attribute from where following knowledge has been discovered. This can predict the month or season that the maximum conflict. Also we can see that the species-specific list of catastrophes which as shown below.

Cluster modes:

	place	predetor	prey	month season
1	Lamichowr	rhino	human	dec winter
2	Ayodhyapuri	tiger	domestic	feb winter
3	Khagendramalli	leopard	domestic	july spring
4	Lamichowr	tiger	domestic	march spring
5	Lamichowr	rhino	crops	jan winter
6	Ayodhyapuri	elephant	crops	oct autumn

7	Panchpandav	leopard	domestic	dec winter
8	Ayodhyapuri	bear	human	may spring
9	Rewa	rhino	crops	nov autumn
10	Ayodhyapuri	rhino	crops	feb winter
11	Nirmalthori	tiger	domestic	july spring
12	Amaltari	tiger	domestic	april spring
13	Nandavauju	rhino	human	july spring
14	Nirmalthori	elephant	house	dec winter
15	Ayodhyapuri	elephant	crops	july spring
16	Mrigakunga	rhino	human	april spring
17	Mrigakunga	leopard	human	dec winter
18	Budirapti	leopard	domestic	sept autumn
19	Rewa	elephant	crops	june spring
20	Panchpandav	elephant	human	oct autumn
21	Rewa	tiger	domestic	dec spring
22	Daunnedevi	leopard	domestic	feb winter
23	Rewa	rhino	human	feb winter
24	Sisauwar	tiger	human	june spring
25	Nikunja	bear	human	june spring
26	Budirapti	tiger	domestic	april spring
27	Khagendramalli	leopard	human	jan winter
28	Ayodhyapuri	tiger	domestic	nov autumn

5. Conclusion

In this paper we examined species-specific catastrophes, including buffer zones along with months or seasons of maximum attack. From these results it is concluded that human and wildlife conflict is maximum during winter and spring season. Also it is seen that especially the elephant destroys households and crops, tiger and leopard especially attacks domestic animals, rhino especially attacks to human and destroys crops.

The destruction by rhino is especially during winter season. Attack by tiger and leopard is during spring season. In case of destruction by elephant, the season is random. There might be many reasons behind it. As we got the partial information from different papers that this might be due to the lack of food inside park. Also the elephant especially comes out during their erotic period etc. So, from these information, related sectors might be beneficial to enhance preventive measures around park.

References:

1. "*Human Wildlife Conflict Manual-Wildlife Management Series*", World Wildlife Fund (WWF), Switzerland.
2. "*Balancing the Needs of People and Wildlife: When Wildlife Damage Crops and Prey on Livestock*" J. People and wildlife. No. 7; August 2007.
3. "*Draft Report on Elephant- Human Conflict in Nepal Terai Park areas with Particular emphasis to Western Terai Arc Landscape*," Kathmandu, Nepal.
4. J. Han, M. Kamber and J. Pei, "*Data Mining Concepts and Technique*," MK publishers, 2012.
5. "*When Mega Vertebrates Makes Ranch their Home*,"Vol 1 (3), Kathmandu, Nepal, August 2007.
6. E.R.tufte, "*Envision information and graphic*," 1990.
7. R. Srikant, R. Arawal, "*Mining Generalized Association Rule*," IBM Almaden Research Centre,San Jose, CA 95120,1995.
8. B Lau, W. Hsu and Y. Ma, "*Integration classification and association Rule*," AAAI, Department of Information Systems and Computer Science National University of Singapore Lower Kent Ridge Road, Singapore 119260,1998.
9. J.A Hartign, "*Clustering algorithm*," John Wiley and Sons, 1975.
10. A.K. Jain and R.C. Dubes "*Algorithm for clustering data*," John Wiley and Sons, 1985.
11. N. Rawat, J. Sodhi, R. Tyagi, "*Wild Life Protection by Moving Object Data Mining - Discover with Granular Computing*," Development of Reliable Information Systems, Techniques and Related Issues (DRISTI), 2012.
12. W. Hochachka, R. Caruana, D. Fink, A. Munson, M. Riedewald, D. Sorokina, S. Kelling, "*Data-Mining Discovery of Pattern and Process in Ecological Systems*," 2009.

STUDY ON EFFECT OF SINTERING TIME ON THE PHASE TRANSITION BEHAVIOR OF $(Ba_{0.998}La_{0.002})TiO_3$ CERAMICS

N. Shrestha[1], B. P. Pokharel[2]

[1]Department of Science and Humanities, Advanced College of Engineering and Management, Kupondole, Lalitpur, Nepal

Email: 1narendra.shrestha@gmail.com

[2]Department of Science and Humanities, Pulchowk Campus – Institute of Engineering, Pulchowk, Lalitpur, Nepal

Email: bhadrapokharel@gmail.com

Abstract

We have carried out an extensive study on the effect of sintering time on the phase transition behavior of the Lanthanum doped Barium Titanate Ceramics. The $(Ba_{0.998}La_{0.002})$ TiO3 (BLT2) powders were synthesized using a dry route involving solid state thermo-chemical reaction in a mixture of $BaCo_3$, La_2O_3, and TiO_2. The powders were calcined at temperature 1100°C and are compacted to pellets using hydraulic press. The samples then were sintered at temperature 1300°C for 1hr, 3hr and 5hr to achieve above 96% of theoretical density. The structure of samples as obtained by XRD is tetragonal and the lattice parameter "a" was found to be decreasing with the increase of sintering time. During the heating mode at frequency 10 KHz the transition temperature from ferroelectric to paraelectric phase for BLT2 was found to be 136°C, 134°C and 132°C sintered for 1hr, 3hr and 5hr respectively. During cooling at 10 KHz the transition temperature decreases which gives the thermal hysteresis of 3°C and 2°C for BLT2 sintered for 3hr and 5hr respectively. The study confirms the first order type of phase transition. Also the Curie temperature obtained from Curie-Weiss behavior sintered for 3hr and 5hr are 105°C and 98°C respectively which are lower than the transition temperature, also confirming the transition is first order type.

Keywords: Barium titanate (BT), Lanthanum, Dielectric properties, Perovskite.

1. Introduction

Since the discovery of ferroelectricity intensive research in the sphere of polycrystalline ceramics has lead to great technological progress and success in the field of ferroelectric materials. The ferroelectric perovskites belong to large group of ferroelectric material and they have very important role due to its wide application in electronics and optics [1-3]. Barium titanate has special place in this group of compound because it can be formulated in a large number of system and solid solution that provide a wide range of various application. The perovskite structure has capacity to host ions of different size, so a large number of different dopants can be accommodated in the $BaTiO_3$ lattice which makes $BaTiO_3$ semiconducting.

Barium titanate (BT) is versatile composition that exhibits high permittivity (ε') making it desirable material for multilayer capacitors, ferroelectric thin-film memories, piezoelectric transducers etc [4-5]. On heating, it undergoes a ferroelectric-paraelectric phase transition to the cubic polymorph at Curie temperature T_c of ~130^{0}C, at which ε' passes through a maximum ε'_{max} and typically reaches value of ~10000 in undoped ceramic samples. The phase transition is of the first order, and the peak in ε' is correspondingly sharp.

Doped of BT ceramics is very important to obtain required characteristics for different applications. Interesting changes can be observed with partial substitution of A-site ion with suitable impurities. Multiple ion occupied in A and/ or B-site of ABO_3 compound is expected to bring in changes in the Curie temperature and other physical properties. This kind of substitution can affect the lattice parameters, tetragonal distortion (c/a), polarization, ferroelectric transition and electro mechanical conversion characteristics of the samples.

The ionic radius is one of the main parameter that determines the substitution site. The La^{3+} (1.15 Å) is exclusively incorporated at the Ba^{2+} (1.35 Å) site, as its size is incompatible in ABO_3 compounds with that of Ti^{4+} (0.68 Å), La^{3+} produces n-type semiconductors. Addition of Lanthanum as a donor dopant at a relatively low concentration (< 0.5 at %) leads to room temperature semiconducting ceramics with positive temperature coefficient of resistivity (PTCR) properties, whereas higher dopant concentration leads to insulating materials.

So we prepared La-doped $BaTiO_3$ samples with 0.02% of lanthanum sintered for different time. In the present study the real (ε ') and imaginary (ε ") part of dielectric permittivity were investigated at frequency 10 KHz and temperature range of 35^0C to 180^0C.

2. Literature Review

X. Chou, J. Sun and Xi Yao [6] have studied the Dielectric properties of Mg-Doped $Ba_{0.6}Sr_{0.4}4TiO_3$ Ceramics sintered at a low temperature with Li_2O additive. Phase and microstructure of these samples were analyzed using XRD and SEM.

Muller et al [7] have studied x-ray diffraction on $Ba(Ti_{0.95}Sn_{0.05})O_3$ (BTS-5) revealing phase coexistence in barium stannate titanate. It is reported that the orthorhombic tetragonal phase transition at T_c = 306 K is found to proceed in a considerably wider temperature range than expected from the dielectric anomaly.

D. Mancic, V. Paunivic, M. Vijatovic, B. Stojanovic and Lj. Zivkovic [8] have studied the electrical characterization and impedance response of Lanthanum Doped Barium titanate Ceramics.

Tadas Ramoska, Juras Banys, Ricardas Sobiestianskas, Mirjana Vijatovic Petrovic, Jelena Bobic and Biljana Stojanovic [9] have studied the influence of Lanthanum concentration on dielectric behavior.

D. D. Gulwade, S. M. Bobade, A. R. kulkarni and P. Gopalan [10] have studied the Dielectric properties of A- and B- site doped $BaTiO_3$: La- and Ga- doped solid solution.

N. P. Sharma [11] dopped Mg ion on A site for x=0.00, 0.04 and 0.08 of $BaTiO_3$ to study phase transition behavior. Here, I have attempted to study the dielectric properties and phase transition behavior of $(Ba_{0.998}La_{0.002})TiO_3$ ceramics by substituting La-ions in A-site.

3. Methodology

Barium titanate doped with Lanthanum i.e. ($Ba_{0.998}La_{0.002}TiO_3$) was prepared by the dry route method involving solid state thermochemical reaction between $BaCo_3$, La_2O_3 and TiO_2, with assay 99%, 99.9% and 98% respectively. The powders and agglomerate characteristics of the raw material play a very important role as they affect the structure (grain size) and properties (strength) of the final component. The compositions in powder form are mixed in desired molar ratios properly in acetone. These solid mixtures are milled for 6 hours in indigenously designed ball-mill to produce a final powder. Acetone is used as the milling agent.

The dried powder was calcined at an optimize temperature 1100^0C for six hours in alumina crucible. The powders were isostatically pressed into pellets of 8mm in diameter and average thickness of about 2.5 mm using pressure of about 80KN. Sintering was performed at 1300^0C for 1, 3 and 5hr (in

the tube furnace "Lenton", UK) and the heating rate was 10^0C/min. with nature cooling in air, which means that sample was cooled down in air, without particular cooling rate.

The sample was polished for the study of dielectric behavior. Silver paste was used for electroding. Dielectric permittivity was measured at the frequency 10 KHz with a HIOKI 3532-50 LCR HI-TESTER in a temperature range between 35^0C to 180^0C.

The density of doped Barium titanate powders was measured by using Archimedes principle. The density of the sample can be calculated using the formula

$$\rho = \frac{W_{air} \times \rho_{glycerine}}{W_{air} - W_{glycerine}}$$

where,

$$W_{air} = \text{Weight of the sample in air}$$

$$W_{glycerine} = \text{Weight of the sample n glycerine}$$

$$\rho_{glycerine} = \text{Density of glycerine at the laboratory temperature}$$

The structure of the samples was investigated using X-ray diffraction (D2 PHASER Diffractometer).

4. Result and Discussion

In this section, we have presented the result and discussion of $Ba_{0.998}La_{0.002}TiO_3$ (BLT2) ceramic samples whose compositional homogeneity can be controlled using powders obtained by dry route method. In the BLT samples where the typical separation between barium and lanthanum ions is of the order of several tens of thousands of unit cells due to complete mixing the powder very carefully and hence a homogeneous distribution of barium and lanthanum ions in the final product, which consequently decreases the degree of optimization of temperature for reaction. The experimentally observed values and the corresponding results for structure of the sample; its density, porosity and electrical properties are also presented here.

Density and Porosity Measurement

Density Measurement

The density of the sample is measured by liquid displacement method using glycerin of density 1.255 gm/cc at 25ºC and of purity of 99%.

Since the atomic size of La (1.95Å) is less than that of Ba (2.173Å) [12]. So when La^{3+} atom is inserted into the lattice of $BaTiO_3$ matrix unit cell volume will decrease according to Vegard's rule [13], where the density of La is 6.162 gm/cc and that of Ba is 3.6 gm/cc. Obeying this rule the density of BLT samples should also decrease as La^{3+} content increases.

Table1: Theoretical and bulk densities of BLT2 samples

Sample	Theoretical density (gm/cc)	Bulk density (gm/cc)	% Densification
BLT2 3hr	6.112	6.013	98.38
BLT2 5hr	6.216	6.132	98.65

The density increases with the increase of sintering time which may be due to more compaction of the samples.

Porosity Measurement

The ceramics are not always fully dense however the open pores can create a problem in measuring not only the density but also dielectric constant, resistance etc. Porosity reflects not only defectiveness of the samples in device fabrication but also is useful in some applications like filter candle etc [14]. The table shows the variation of soaking time versus porosity and density of the sample. The variation of densification with time is as shown in figure 1. It is evident from figure that the soaking of water is fast upto 1 hour then increases slowly up to 2 hours and remains constant for further increment of time.

Table 2: Variation of soaking time versus porosity and density of the sample

Soaking time (hrs)	Wt. of sample (gm)	Density (gm/cc)	% density	% porosity
0	0.321	6.013	98.38	1.62
1	0.325	6.087	99.59	0.14
2	0.326	6.106	99.90	0.1
3	0.326	6.106	99.90	0.1
4	0.326	6.106	99.90	0.1
5	0.326	6.106	99.90	0.1

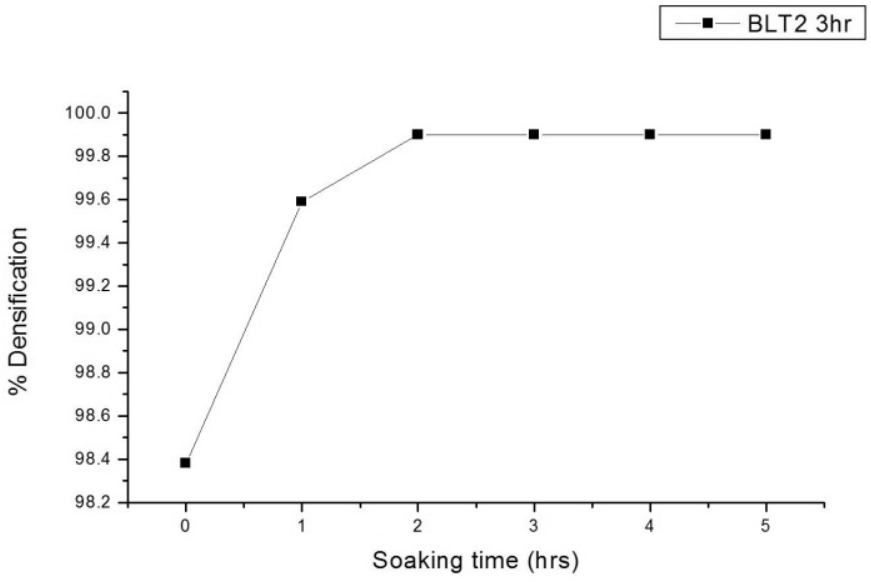

Figure 1: The variation of Densification vs soaking time XRD-data analysis

We have carried out the XRD using D2 Phaser Diffractometer (Bruker) and the lattice parameters for $Ba_{0.998}La_{0.002}TiO_3$ (sintered for 3hr and 5hr) were calculated for tetragonal phase by embedded into the computer program Unit cell (1998). The refined parameters obtained by the refinement of XRD data for BLT2 are given in table below. The strong perovskite reflections can be indexed with respect to tetragonal structure [15]. With indices 100, 110, 111, 200, 210, 211 and 220 as shown in figure 2 and 3.

Table 3: Refined parameters obtained by the refinement of XRD data for BLT2

Samples	Lattice Parameter (a=b)	Lattice Parameter (c)	Unit cell Volume (V)
BLT2 3hr	(3.8907 ± 0.0912)Å	(4.1842 ± 0.9291)Å	(63.3388 ± 13.6469)Å
BLT2 5hr	(3.8748 ± 0.0893)Å	(4.1485 ± 0.8989)Å	(62.2872 ± 13.0964)Å

The decrease in volume is due to incorporation of La^{3+} of lower atomic radii into Ba of higher atomic radii as per Vegard's Rule.

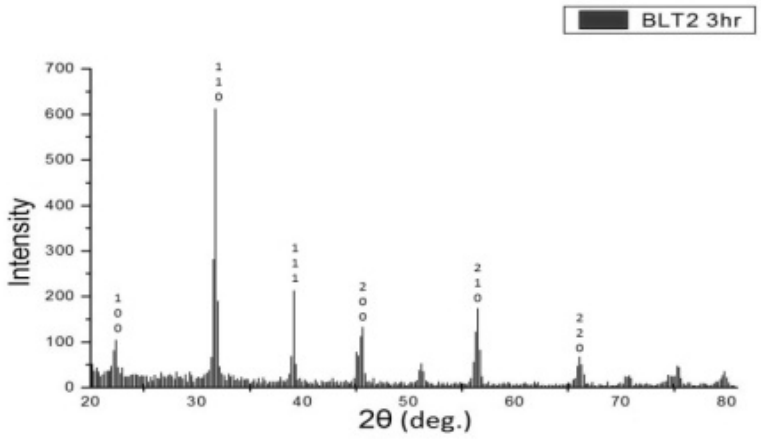

Figure 2: XRD-data of BLT2 sintered for 3hr

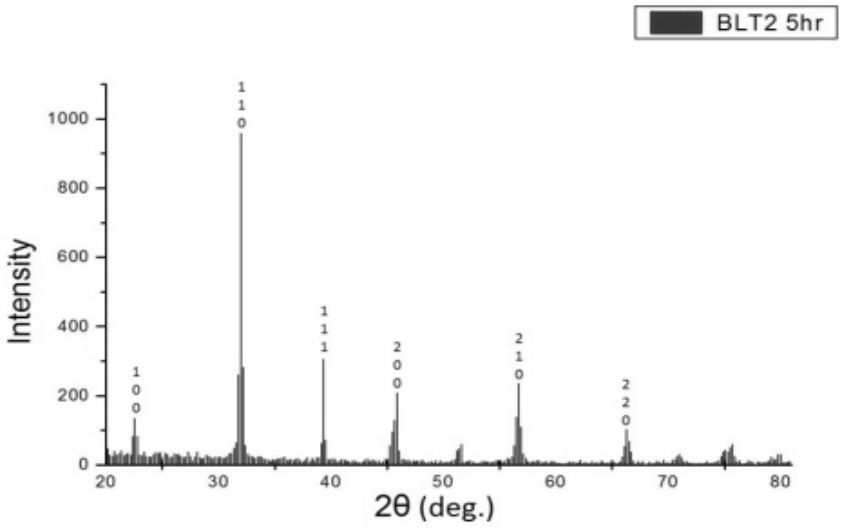

Figure 3: XRD-data of BLT2 sintered for 5hr

Electrical Properties

Ferroelectric to paraelectric phase transition

The dielectrics measurement was carried out at different frequencies. The variation of real part of dielectric constant with temperature for samples BLT2 sintered for different time at 10 KHz is shown in figure 5. The figure 5 shows that for the BLT2 sample, the value of dielectric constant is maximum when sintered for 3hr. The BLT2 sample sintered for 1hr is not perfectly sintered, so it is less dense and hence low dielectric constant, while the BLT2 sintered for 5hr is over sintered due to which its density is high but its dielectric constant is low which may be due to change in orientation of dipoles of the ferroelectric materials.

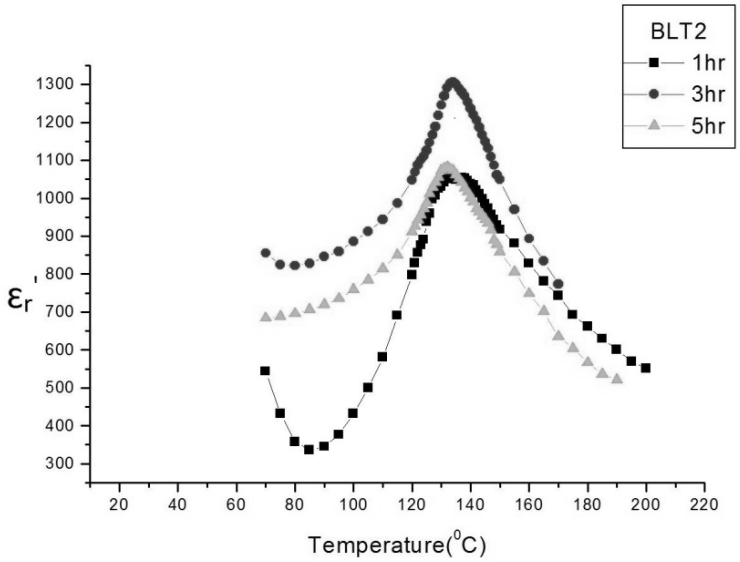

Figure 4: Variation of real part of dielectric constant with temperature at 10 KHz

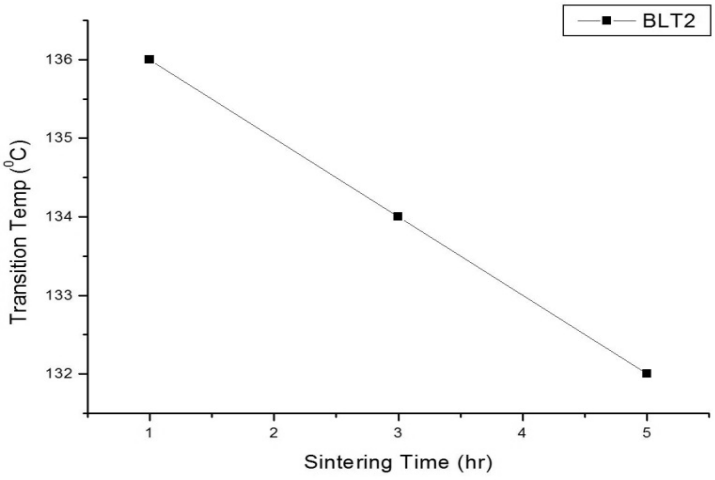

Figure 5: Variation of transition temperature with sintering time

Real and Imaginary part of dielectric constant

The transition temperatures for real and imaginary parts of dielectric constant are nearly same for BLT2 sintered for 3hr and 5hr as shown in figure 6 and 7. This indicates that the ferroelectric

transition is first order type but slightly diffused. The real part of dielectric constant represents the static part of the dipoles whereas the dynamic part of the dipoles is represented by imaginary part of the dielectric constant which provides good knowledge of kinetic properties of dipoles [16].

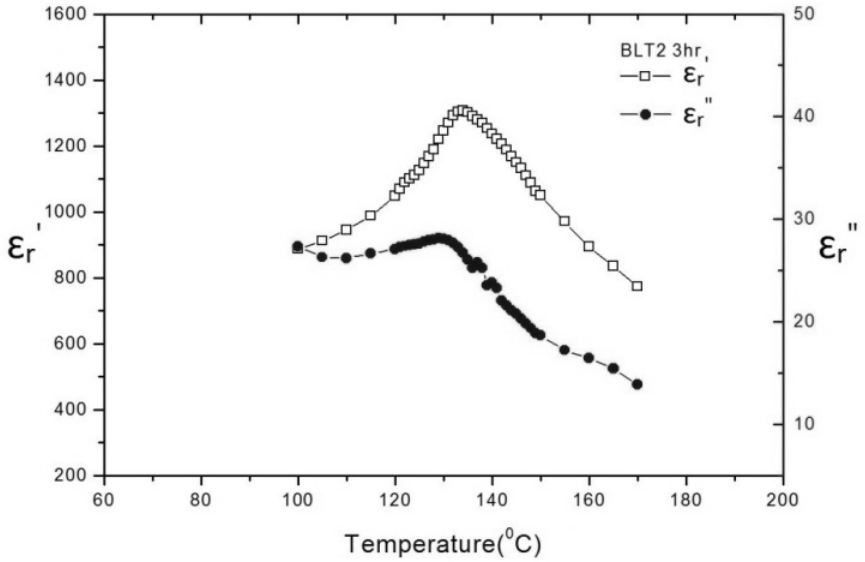

Figure 4: Variation of real and imaginary parts of dielectric constant with temperature for

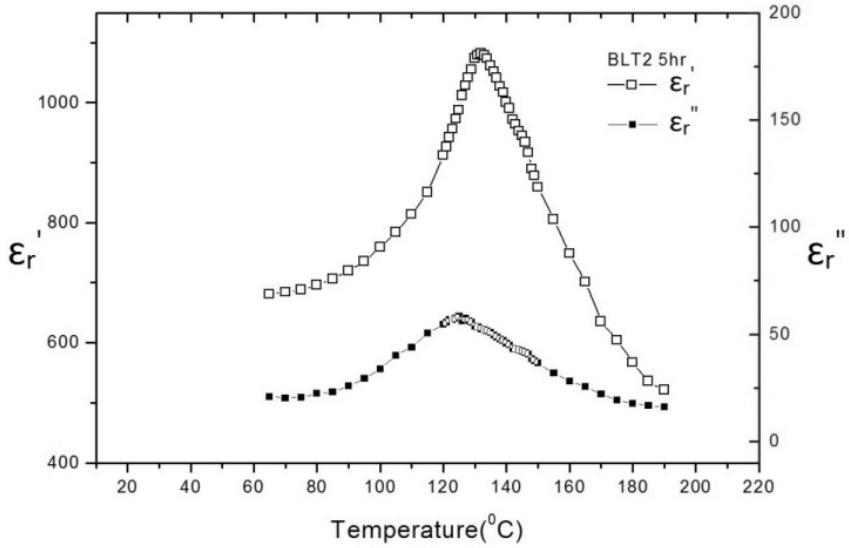

Figure 5: Variation of real and imaginary parts of dielectric constant with temperature for sintering time 5hr

Thermal Hysteresis

The hysteresis is obtained from the difference between the transition temperature during heating and cooling modes i.e. gives the value of thermal hysteresis. The value of thermal hysteresis observed in BLT2 sintered for 3hr and 5hr are 3^0C and 2^0C respectively. It is also confirmed that the value of dielectric constant in cooling cycle is more than that of heating cycle. Simple Landau theory [17]

argument suggests that the dielectric anomaly during the cooling cycle should be more than that of heating cycle. The existence of thermal hysteresis indicates the ferroelectric transition is first order type.

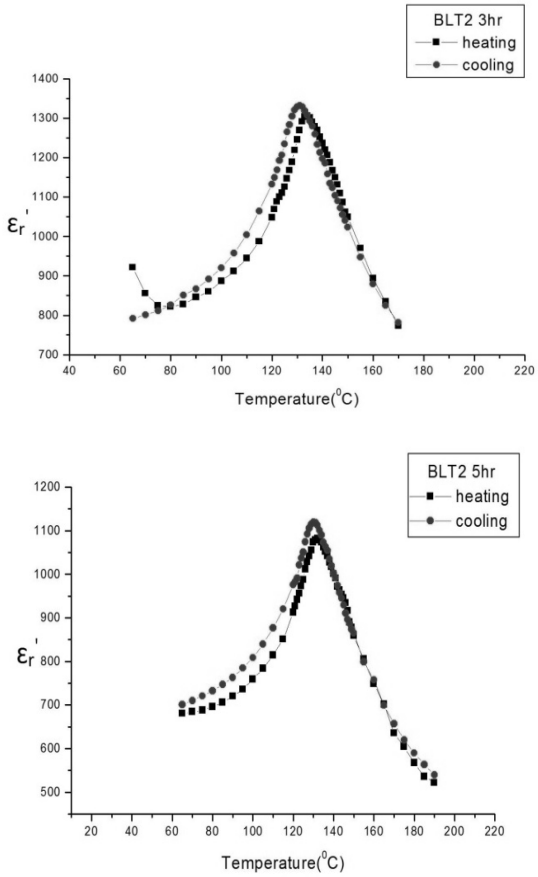

Figure 8: Variation of real part of dielectric constant with temperature for both heating and cooling cycle

Curie – Weiss Law

The dielectric constant of BLT samples exhibits Curie - Weiss behavior [18, 19] followed by the relation

$$\varepsilon_r' = \frac{C}{T - T_0}$$

Where C is Curie constant and T_0 is Curie temperature. The Curie temperature observed from the graphs for BLT2, sintered for 3hr and 5hr are 118^0C and 115^0C respectively. The observed values of Curie constant are 2.0895×10^4 ^{0}C and 1.8396×10^4 ^{0}C sintered for 3hr and 5hr respectively. The Curie temperature of our sample is less than that of transition temperature in the ferroelectric to paraelectric phase which is the characteristic of the first order phase transition. The Curie temperature decrease as the sintering time is increased confirming the phase transition tending towards diffuse type transition or relaxor.

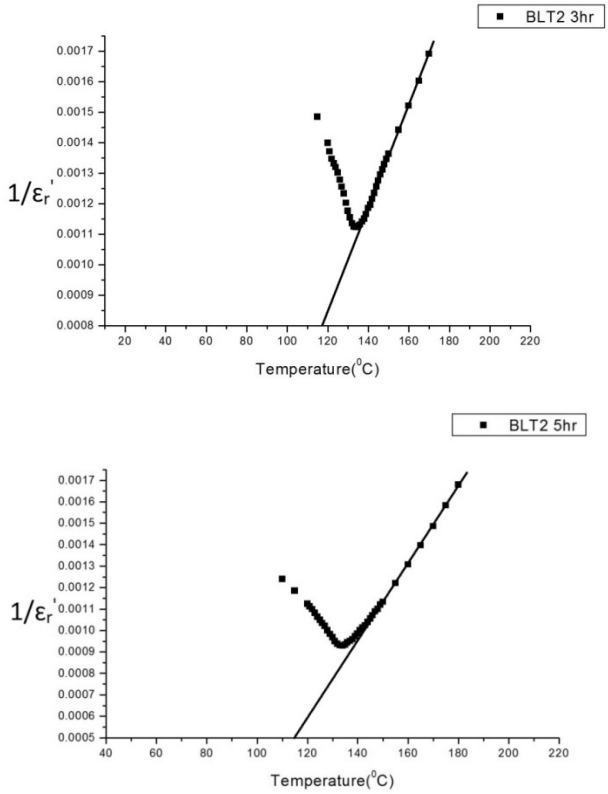

Figure 9: The variation of dielectric stiffness ($1/\varepsilon_r'$) with temperature at 10 KHz

To define the diffuseness of phase transition, modified Curie – Weiss law proposed by Uchino and Nomura [20] is used. This is defined as,

$$\frac{1}{\varepsilon_r'} = \frac{1}{\varepsilon_m'} + \frac{(T - T_c)^\gamma}{C}$$

where γ and C are assumed to be constant. The parameter γ gives the information on the character of phase transition. For sharp transition or regular phase γ should be nearly equal to 1 and for diffused transition it lies in the range $1 \leq \gamma \leq 2$ [21]. It is evident from the graph of $\ln(\frac{1}{\varepsilon_r'} - \frac{1}{\varepsilon_m'})$ vs $\ln(T - T_c)$ the values of slope i.e. γ are 0.49845 and 1.54235 for BLT2 sintered for 3hr and 5hr respectively.

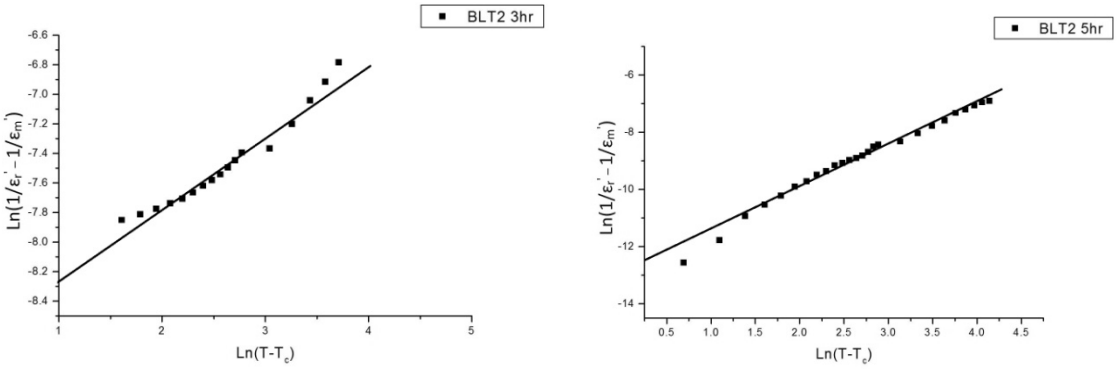

Figure 10: Variation of $\ln(\frac{1}{\varepsilon_r'} - \frac{1}{\varepsilon_m'})$ with $\ln(T - T_c)$ at 10 KHz

Impedance Spectroscopy

To confirm above result, impedance spectroscopy study was also carried out in which real and imaginary part of impedance are plotted with temperature as shown in figure 11.

For the circuit containing one parallel RC component total impedance Z^* is given by the relation,

$$Z^* = \frac{1}{i\omega C + \frac{1}{R}}$$

$$Z^* = \frac{R}{i\omega C + 1} = Z' - iZ''$$

Where

$$Z' = \frac{1}{1 + \omega^2 C^2 R^2}$$

$$Z'' = \frac{\omega C R^2}{1 + \omega^2 C^2 R^2}$$

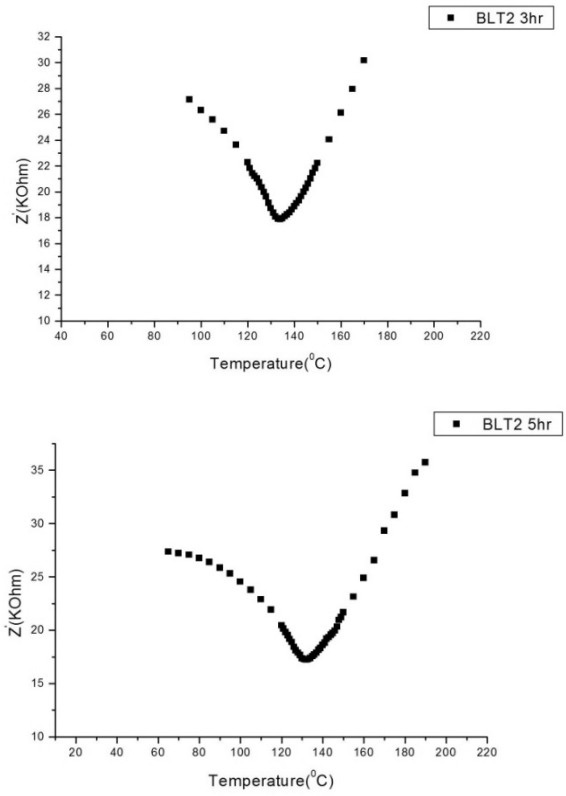

Figure11: Variation of real part of impedance ($Z^{'}$) with temperature at frequency 10 KHz

It is evident from the figure 11 that the impedance of BLT2 sample decreases up to transition temperature and starts increasing.These plots confirm the result of transition from ferroelectric to paraelectric phases as obtained in dielectric studies.

References

1. F. Jomni, P. Gonon, F. E. Kamel, B. Yangui, Integr. Ferroelectr., **97**, 121, (2008).
2. W. Zhu, C. C. Wang, S. A. Akbar, R. Asiaie, J. Mater. Sci., **32**, 4303, (1997).
3. S. Kim, O. Y. Kwon, J. Mater. Sci., **34**, 707, (1999).
4. Z. Wei, M. Noda, Integr. Ferroelectr., **52**, 111, (2010).
5. W. B. Luo, J. Zhu, Integr. Ferroelectr., **406**, 56, (2010).
6. X. Y. Wei, Y. J. Feng, and X. Yao, Appl.Phys.Lett., **83**, 203, (2003).
7. V. Muller, H. Beige, H. P. Abichat, C. Eisenschmidt, "Mater. Res. Soc., **19**, 2834, (2004).
8. Science of Sintering, **40**, 283-294, (2008).
9. Processing and Application of Ceramics, **4**[3], 193-198, (2010).
10. Journal of applied Physics, **97**, 074106, (2005).
11. N. P. Sharma, "An experimental Study on Phase Transition Behavior of $(Ba_{1-x}Mg_x)TiO_3$ (x = 0.00, 0.04, 0.08) Ceramics" Goldengate Msc. Phy. Thesis, (2013).
12. J. D. Lee, "Concise Inorganic Chemistry", 5^{th} ed., Blackwell Science Ltd., U.K., (1996)
13. F. S. Galasso, "Structure, Properties and Preparation of perovskite – type compounds", Pergamon Press, Hungery, (1969).
14. D. Pandey, "Key Engineering Materials", Trans. Tech. Switzerland, 101 – 102, (1995).
15. Z. Zhigang, Z. Gang "Ferroelectrics", **81**, 43 - 54, (1990).
16. A. Chelkowski: "Dielectric Physics", Elsevier Scienctific Publishing Company, Oxford, (1983).
17. H. Eisaki, H. Takagi, R. J. Cava, B. Batlogg, J. J. Krajewski, W. F. Peck, K. Mizuhashi, J. O. Lee, and S. Uchida. Competition between magnetism and superconductivity in rare – earth nickel boride carbides. Phys. Rev. B, **50(1):** R647 50, (1994).
18. Xiaoyong Wei, Xi Yao, Material Science and Engineering, **B 137**, 184 – 188, (2007).
19. V. S. Tiwari, N. Sing and D. Pandey, "Phys., Condensed Matter", **7**, 1441 – 1460, (1995).
20. K. Uchino and S. Namera, " Ferroelectric Lett.", **44**, 56, (1982).
21. Zhi Yu, Ang C, Guo R and Bhalla A S J. Appl. Phys., **92**, 265, (2002).

Similarity analysis of images in Secret Fragment visible mosaic for Steganography – A study

S. Poudyal[1], S. P. Panday[2]

Masters in Computer System and Knowledge Engineering, Central Campus, Pulchowk, Lalitpur

Email Address: shambhabi.poudyal@gmail.com

Department of Electronics and Computer Engineering, Central Campus, Pulchowk, Lalitpur

Email Address: sanjeeb77@hotmail.com

Abstract

Steganography is the science of hiding secret messages into cover media so that no one can realize the existence of the secret data. Image mosaicing is a technique which enables to combine together many small images into one large image, from which, more information can be collected easily. "Similarity analysis of images in Secret Fragment visible mosaic for Steganography – a study" is basically focused on the necessity of the use of similarity analysis techniques for images when used for secret-fragment-visible mosaic for secured transfer of information containing images. A number of experiments have been performed using visibly similar and dissimilar images to analyze the importance of the use of similarity analysis techniques. The result obtained shows the necessity of similarity analysis techniques to identify the target image most similar to the secret image so that the error between the mosaiced image and the target image is as least as possible.

Keywords: Secret-fragment-visible mosaic, Similarity analysis techniques, Steganography

1. Introduction

A new type of art image, called secret-fragment-visible mosaic image, which contains small fragments of a given source image is proposed in this study. Observing such a type of mosaic image, one can see all the fragments of the source image, but the fragments are so tiny in size and so random in position that the observer cannot figure out what the source image looks like. Therefore, the source image may be said to be secretly embedded in the resulting mosaic image, though the fragment pieces are all visible to the observer. And this is the reason why the resulting mosaic image is named secret-fragment-visible, which is the result of random rearrangement of the fragments of a secret image in disguise of another image called target image, creating exactly an effect of image steganography. The difficulty of hiding a huge volume of image data behind a cover image is solved automatically by this type of mosaic image. It is useful for the application of covert communication or secure keeping of secret images. Specifically, after a target image is selected, the given secret image is first divided into rectangular fragments, which then are fit into similar blocks in the target image according to a similarity criterion based on color variations. Next, the color characteristic of each tile image is transformed to be that of the corresponding block in the target image, resulting in a mosaic image which looks like the target image. Such a type of camouflage image can be used for securely keeping of a secret image in disguise of any pre-selected target image. Relevant schemes are also proposed to conduct nearly-lossless recovery of the original [1].

Steganography is the science of hiding secret messages into cover media so that no one can realize the existence of the secret data. Existing steganography techniques may be classified into three categories – image, video, and text steganographies, and image steganography aims to embed a secret image into a cover image with the yielded stego-image looking like the original cover image. Lai and Tsai proposed a new type of computer art image, called secret-fragment-visible mosaic image, which is the

result of random rearrangement of the fragments of a secret image in disguise of another image called target image, creating exactly an effect of image steganography [2].

2. Literature Review

In traditional methods, secret text can be hidden into image which is called as Steganography. Mosaic image technique is one of the efficient techniques to hide the secret images. This methodology needs another image which is said to be cover image. An image is fragmented into small tiles. Then, these tiles are randomly embedded onto a cover image. Secret key is used for embedding the small tiles of secret image onto cover image. LSB (least significant bit) replacement scheme is a technique mainly used for embedding process. LSB technique reduces or avoids the blur effect of encrypted mosaic image [1].

The original idea of the mosaic image steganography has been proposed by Secret-Fragment- Visible Mosaic Image-A New Computer Art and Its Application to Information Hiding by Lai and Tsai [2]. A new type of art image, called secret-fragment-visible mosaic image, which contains small fragments of a given source image is proposed in this study by Lai and Tsai. Observing such a type of mosaic image, one can see all the fragments of the source image, but the fragments are so tiny in size and so random in position that the observer cannot figure out what the source image looks like. Therefore, the source image may be said to be secretly embedded in the resulting mosaic image, though the fragment pieces are all visible to the observer. And this is the reason why the resulting mosaic image is named secret-fragment-visible.

A new type of image similarity method was proposed in "New Image Steganography by Secret Fragment Visible Mosaic Image for Secret Image Hiding", which created embedded image automatically by composing small fragments of given secret image in mosaic form in the target image. The mosaic image is yielded by dividing the secret image into fragments and transforming the color characteristics of secret image to that of target image. Skillful techniques are used in the color transformation process so that secret image may be recovered nearly lossless [3].

3. Methodology

The secret image is embedded into the target image as shown in figure 3.1. The basic working principle for secret fragment visible mosaic and recovery is as described in section 3.1. The detailed algorithm is described in section 3.2.

3.1 Working Principle

3.1.1 Color Transformations between Blocks

Suppose that in the first phase of this method, a tile image T in a given secret image is to be fit into a target block B in a pre-selected target image. Since the color characteristics of T and B are different from each other, how to change their color distributions to make them look alike is the main issue here. More specifically, let T and B be described as two pixel sets {p1, p2, …, pn} and {p1′, p2′, …, pn′}, respectively, assuming that both blocks are of the same dimensions with size n. Let the color of pixel pi in the RGB color space be denoted by (ri, gi, bi) and that of pi′ by (ri′, gi′, bi′). First, we compute the means and standard deviations of T and B, respectively, in each of the three color channels R, G, and B by the following formulas:

$$\mu c=\frac{1}{n}\sum_{i=1}^{n} ci, \quad \mu c'=\frac{1}{n}\sum_{i=1}^{n} ci' \qquad \text{Eq. 3.1}$$

$$\sigma c=\sqrt{(1/n)\sum_{i=1}^{n}(ci-\mu c)^2}\ ,\ \sigma c'=\sqrt{(1/n)\sum_{i=1}^{n}(ci'-\mu c')^2} \qquad \text{Eq. 3.2}$$

Where, ci and ci′ denote the C-channel values of pixels pi and pi′, respectively, with c denoting r, g, b.

Next, we compute new color values (ri″, gi″, bi″) for each pi in T by:

$c_i'' = (\sigma_{c'}/\sigma_c)(c_i - \mu_c) + \mu_{c'}$ with c = r, g, and b.……Eq. 3.3

This results in a new tile image T′ with a new color characteristic similar to that of target block B. Also, we use the following formula, which is the inverse of Eq. 3.3, to compute the original color values (ri, gi, bi) of pi from the new ones (ri″, gi″, bi″):

$c_i = (\sigma_c/\sigma_{c'})(c_i'' - \mu_{c'}) + \mu_c$ with c = r, g, and b.……..Eq. 3.4

Furthermore, we have to embed into the created mosaic image sufficient information about the transformed tile image T′ for use in later recovery of the original secret image.

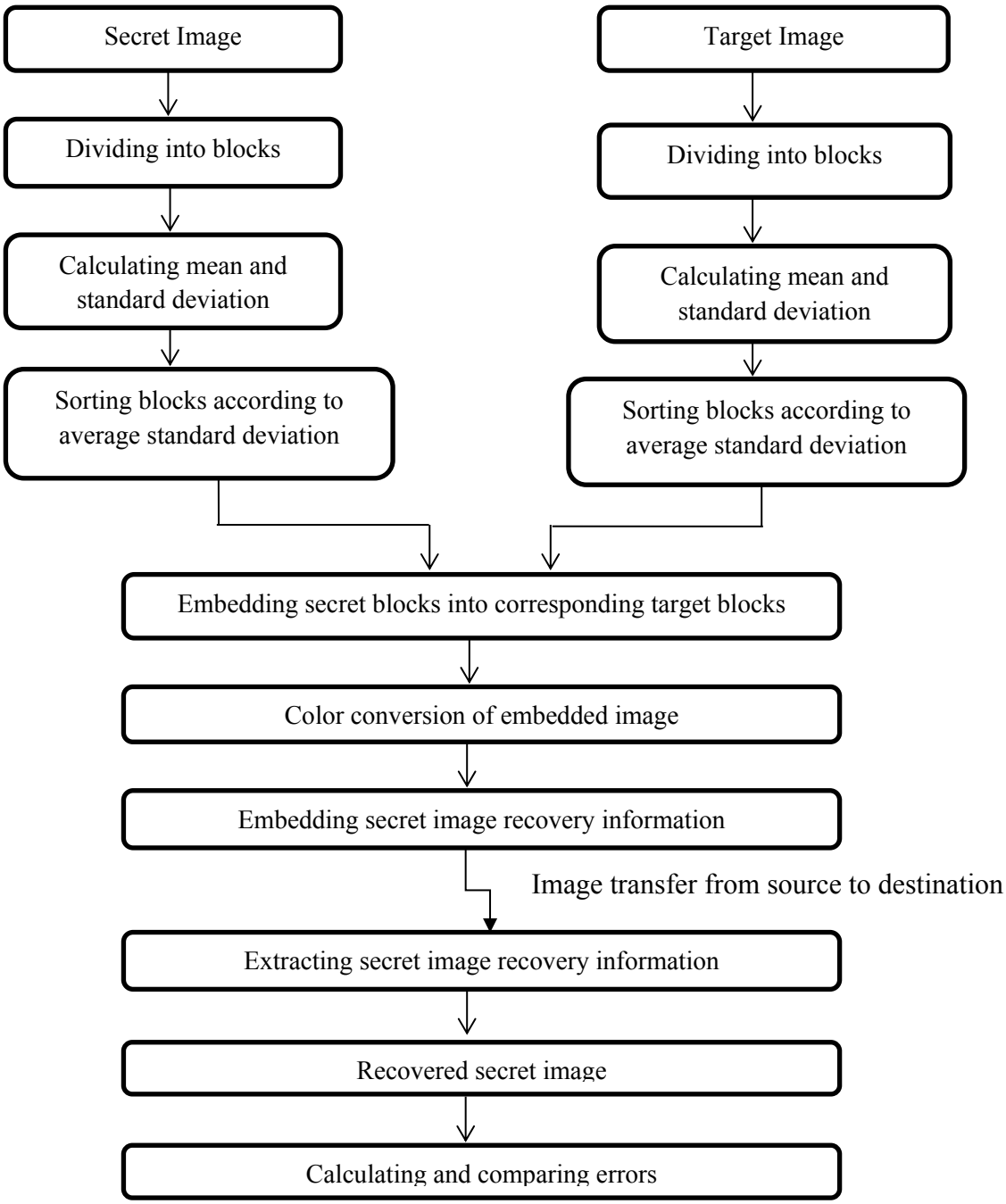

Figure 3.1 Process Flow for secret image embedding and recovery

3.1.2 Choosing Appropriate Target Blocks to Fit Better

In transforming the color characteristic of a tile image T to be that of a corresponding target block B as described above, how to choose an appropriate B for each T (i.e., how to fit each T to a proper B) is an issue. If two blocks are more similar in color distributions originally, a better transformation effect will result. For this, we use the standard deviation of block colors as a measure to select the most similar target block B for each tile image T. First, we compute the standard deviations of every tile image and target block for each color channel. Then, we sort all the tile images to form a sequence, Stile, and all the target blocks to form another, Starget, according to the mean of the standard deviation values of the three colors. Finally, we fit the first tile image in Stile to the first target block in Starget; fit the second in Stile to the second in Starget and so on.

3.1.3 Embedding Secret Image Recovery Information

In order to recover the secret image from the mosaic image, we have to embed relevant recovery information into the mosaic image. The information required to recover a tile image T which is mapped to a target block B includes: (1) the sorted rows and columns of secret image; (2) the sorted rows and columns of target image; and (3) the means and the related standard deviation quotients of all color channels of mosaiced image.

After embedding the bit stream into the mosaic image, we can recover the secret image back. But some loss will be incurred in the recovered secret image (i.e., the recovered image is not identical to the original one).

3.1.4 Image Comparison

Similarity analysis is one of the important portions of this thesis. Following approaches have been implemented for image comparison.

Mean Square Error (MSE)

The mean square error (MSE) of an estimator measure of the average of the square of the errors, that is difference between estimator and what is estimated.

In this thesis, MSE is used to compare original images with recovered and with mosaiced image. MSE is calculated as:

$$MSE = \frac{\sum_{x=1}^{M}\sum_{y=1}^{N}[Im(x,y)-Im'(x,y)]^2}{(M.N)} \quad \text{.....Eq. 3.5}$$

Where, M, N stands for the size of the image in both horizontal and vertical axes, I_m is the original image and I_m' is the reconstructed image that is to be examined.

Peak Signal to Noise Ratio (PSNR)

PNSR is defined as the ratio between the maximum possible power of signal and the power of corrupting noise that affects the fidelity of representation. Because many signal have wide dynamic range PNSR is usually expressed in term of logarithmic decibel scale.

PSNR is calculated using following formula:

$$PSNR = 20 * log_{10}[\frac{255}{\sqrt{MSE}}] \quad \text{.....Eq. 3.6}$$

3.2 Mosaic Image Creation and Secret Image Recovery Algorithms

Based on the above discussions, detailed algorithms for mosaic image creation and secret image recovery may now be described as:

Algorithm 1. Secret-fragment-visible Image Mosaic

Algorithm 1.1. Secret-fragment-visible mosaic image creation

Input: a secret image S with n tile images of size N_T; a pre-selected target image T of the same size of S;

Output: a secret-fragment-visible mosaic image F.

Steps:

Stage 1.1.1 — fitting tile images into target blocks.

1. Divide secret image S into a sequence of n tile images of size N_T, denoted as $S_{tile}=\{T_1, T_2, \ldots, T_n\}$; and divide target image T into another sequence of n target blocks also with size N_T, denoted as $S_{target} = \{B_1, B_2, \ldots, B_n\}$.
2. Compute the means (μ_r, μ_g, μ_b) and the standard deviations $(\sigma_r, \sigma_g, \sigma_b)$ of each Ti in Stile for the three color channels according to Eqs. 3.1 and 3.2; and compute the average standard deviation $\sigma_{Ti} = (\sigma_r + \sigma_g + \sigma_b)/3$ for Ti where i = 1 through n.
3. Do similarly to the last step to compute the means $(\mu r', \mu g', \mu b')$, the standard deviations $(\sigma r', \sigma g', \sigma b')$, and the average standard deviation $\sigma_{Bj} = (\sigma r' + \sigma g' + \sigma b')/3$ for each Bj in Starget where j = 1 through n.
4. Sort the blocks in Stile and Starget according to the average standard deviation values of the blocks; map in order the blocks in the sorted Stile to those in the sorted Starget in a 1-to-1 manner.
5. Create a mosaic image F by fitting the tile images of secret image S to the corresponding target blocks of target image T.

Stage 1.1.2 — performing color conversion between the tile images and target blocks.

6. For each pair Ti → Bji, let the means μ_c and $\mu_{c'}$ of Ti and Bji respectively and the standard deviation be σ_c and $\sigma_{c'}$

7. For each pixel pi in each tile image Ti of mosaic image F with color value ci where c = r, g, b, transform ci into a new value ci″ by Eq. 3.3

Stage 1.1.3 — embedding the secret image recovery information.

8. For each tile image Ti in F, construct a bit stream Mi for recovering Ti as described in Section 3.1.3, including the bit-segments which encode the data items of: 1) the sorted rows and columns of secret image; (2) the sorted rows and columns of target image; and (3) the means and the related standard deviation of all color channels of mosaiced image.

Algorithm 1.2 Secret image recovery.

Input: a mosaic image F with n tile images used in Algorithm 1.1.

Output: the secret image S embedded in F using Algorithm 1.1.

Steps:

Stage 1.2.1 — extracting the secret image recovery information.

1. Extracting from mosaic image F, the bit stream Mt′ for secret image recovery by a reverse version of the LSB replacement scheme
2. Decomposing Mt into n bit streams Mi for the n to-be-constructed tile images Ti in S, respectively, where i = 1 through n.
3. Decoding the bit stream Mi of each tile image Ti to obtain the following data: 1) the sorted rows and columns of secret image; (2) the sorted rows and columns of target image; and (3) the means and the related standard deviation of all color channels of mosaiced image.

Stage 1.2.2 — recovering the secret image.

4. Recovering each block from the tile images Ti, i = 1 through n, of the desired secret image S by using the received information.
5. Composing all the final tile images to form the desired secret image S as output.

Finally, calculating RMSE and PSNR values between the original secret image and the recovered secret image and between the mosaiced target image and original target image and comparing them.

4. Result and Discussion

10 experiments are performed in total using visibly similar and dissimilar images. The results obtained are then compared and analyzed. The images used are collected from various sources including reference papers, online databases and real life images captured using normal cameras. Two sample experiments have been presented here.Experiment no. 01:

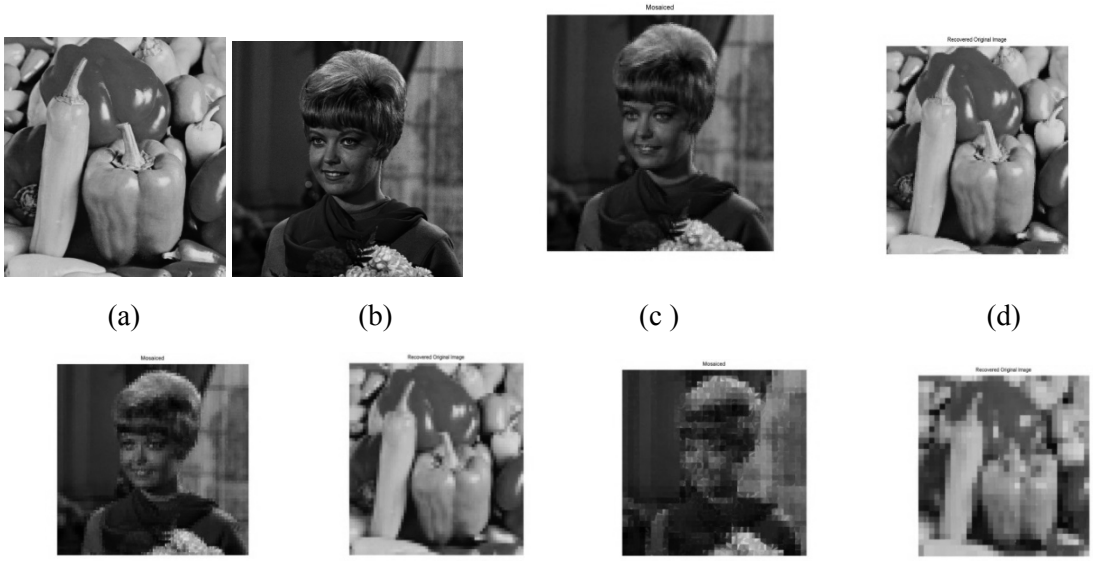

(a) (b) (c) (d)

(e) (f) (g) (h)

Figure 4.1: Images for Experiment no. 01 (a)secret image (b)target image (c)mosaiced image for block size 4x4 (d)recovered secret image for block size 4x4 (e)mosaiced image for block size 8x8 (f)recovered secret image for block size 8x8 (g)mosaiced image for block size 16x16 (h)recovered secret image for block size 16x16

Figure 4.1 shows the results obtained using secret image and target image for Experiment no. 01 for three block sizes. It shows the results of the mosaicing process by combining secret image and target image that does not seem much similar to each other as compared to the similarity of the secret and the target image in Experiment no. 02. It shows that the mosaiced image obtained by combining secret image and target image is similar to that of the target image. As seen from the figure, also illustrated by Table 4.1 and Figure 4.3, the mosaiced images are more similar to the target images and recovered

images to the secret images for lower block sizes than compared to higher ones. Table 4.1 shows the tabulation of rmse and psnr errors for different block sizes and images.

Experiment no. 02:

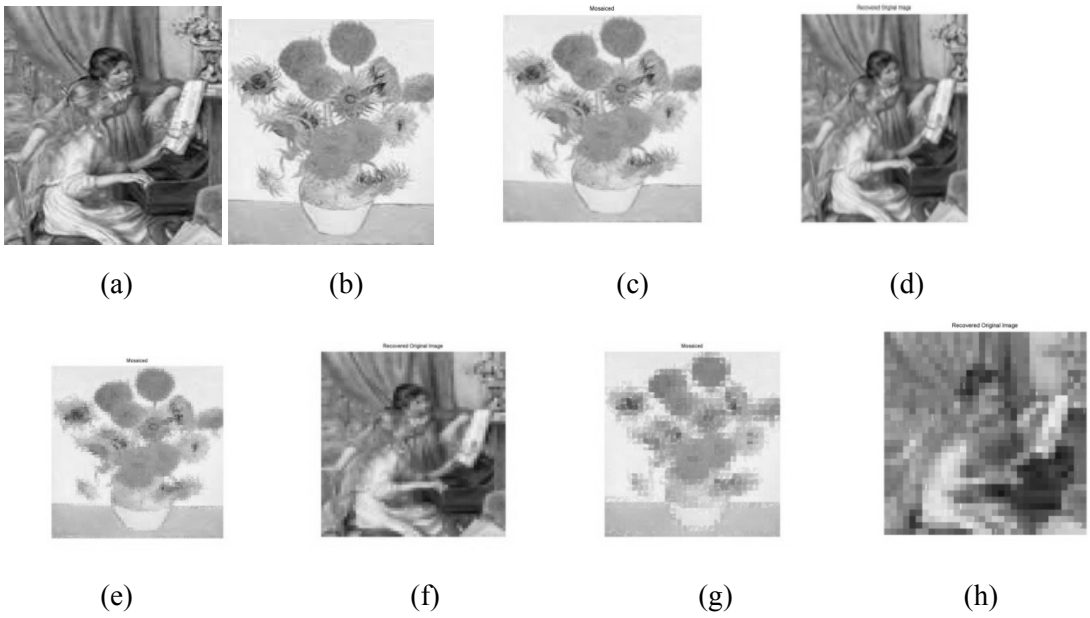

(a) (b) (c) (d)

(e) (f) (g) (h)

Figure 4.2: Images for Experiment no. 02 (a)secret image (b)target image (c)mosaiced image for block size 4x4 (d)recovered secret image for block size 4x4 (e)mosaiced image for block size 8x8 (f)recovered secret image for block size 8x8 (g)mosaiced image for block size 16x16 (h)recovered secret image for block size 16x16

Figure 4.2 shows the results obtained using secret image and target image for Experiment no. 02 for three block sizes. It shows the results of the mosaicing process by combining secret image and target image that seem quite similar to each other as compared to the similarity of the secret and the target image in Experiment no. 01. It shows that the mosaiced image obtained by combining secret image and target image is similar to that of the target image. As seen from the figure, also illustrated by Table 4.2 and Figure 4.4, the mosaiced images are more similar to the target images and recovered

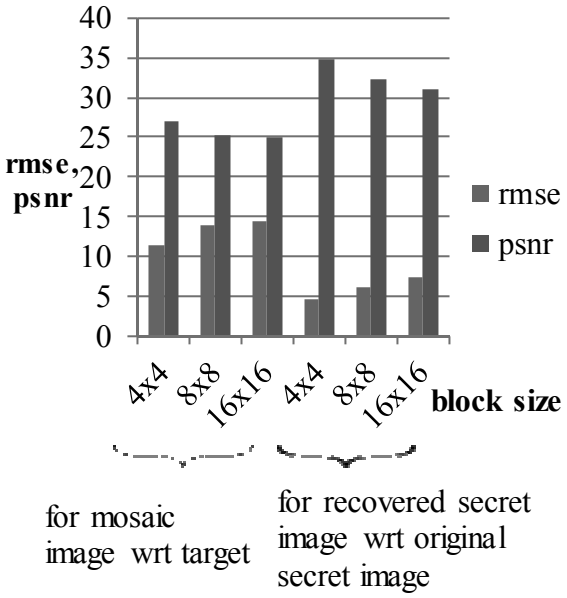

Figure 4.3: Plot of Table 4.1

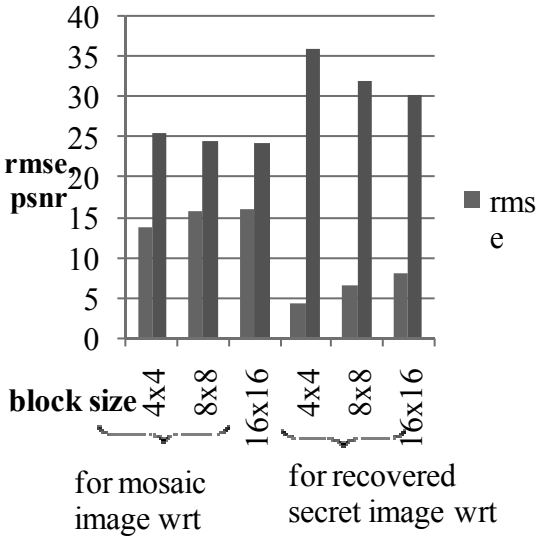

Figure 4.4: Plot of Table

images to the secret images for lower block sizes than compared to higher ones. Table 4.2 shows the

Table 4.1: Comparison of errors for images of Experiment no. 01

Block size	Error		Images
	rmse	Psnr	
4x4	11.377331	27.009996	for mosaic image wrt target image
	4.601257	34.873275	for recovered secret image wrt original secret image
8x8	13.873150	25.287302	for mosaic image wrt target image
	6.163121	32.334790	for recovered secret image wrt original secret image
16x16	14.398690	24.964344	for mosaic image wrt target image
	7.256016	30.916839	for recovered secret image wrt original secret image

Table 4.2: Comparison of errors for images of Experiment no. 02

Block size	Error		Images
	rmse	Psnr	
4x4	13.747725	25.366187	for mosaic image wrt target image
	4.173219	35.721379	for recovered secret image wrt original secret image
8x8	15.543497	24.299829	for mosaic image wrt target image
	6.485659	31.891722	for recovered secret image wrt original secret image
16x16	15.833678	24.139167	for mosaic image wrt target image
	8.054228	30.010325	for recovered secret image wrt original secret image

tabulation of rmse and psnr errors for different block sizes and images.

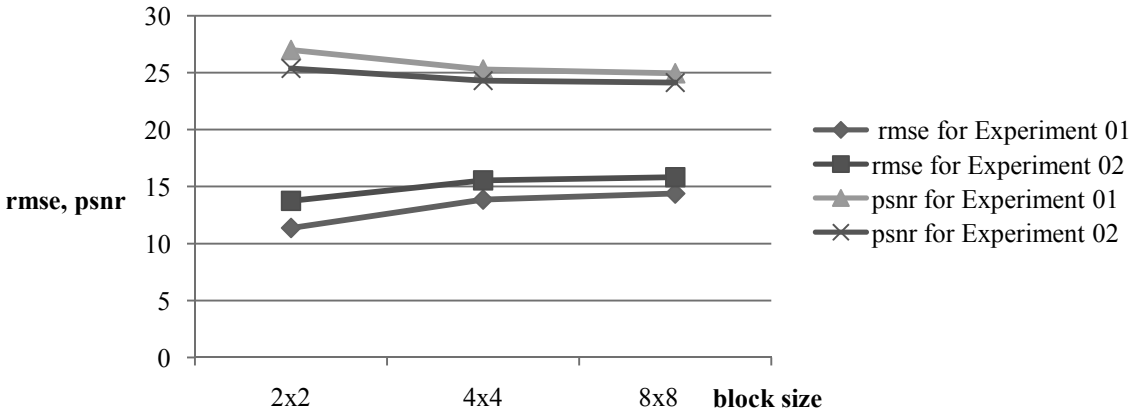

Figure 4.5: Plot of rmse and psnr errors for mosaiced image wrt target image for Experiment no. 01 and Experiment no. 02

When comparing the results, less rmse errors for mosaiced image compared to target image are obtained in Experiment no. 01 than Experiment no. 02, while visible observations show that images in Experiment no. 01 are less similar to each other than those in Experiment no. 02. This leads to the necessity of an algorithm which can actually analyze the similarity of the secret and target images prior to the application of the algorithm.

5. Conclusion

This study is meant for combining small tiles of secret image to form a target in the sense of mosaic for images which are visibly similar and dissimilar to each other. The experiments conducted conclude that the images which look similar in visual observation might not be similar when viewed comparing the image pixels and blocks. The experiments show that the images which look similar might have higher rmse value between the mosaiced image and the target image whereas the images which look dissimilar might have lower rmse value between the mosaiced image and the target image. Hence, image similarity analysis algorithm is to be applied to the images at the very beginning of the process while selecting the proper target image for the given secret image. This study only evaluates the necessity of such algorithms but the application of such algorithms is not included.

References

1. Lisha L, Kavitha M, "An Efficient Steganography with Mosaic Images for Covert Communication", in IOSR Journal of Engineering (IOSRJEN) Volume 3, Issue 3, March 2013
2. Ya-Lin Li, Wen-Hsiang Tsai, "New Image Steganography via Secret-fragment-visible Mosaic Images by Nearly-reversible Color Transformation", IEEE Transactions On Circuits And Systems For Video Technology, Volome 24, No. 4, April 2014
3. Fasna C. K., Nisha Narayanan, "New Image Steganography by Secret Fragment Visible Mosaic Image for Secret Image Hiding" in IJSRD - International Journal for Scientific Research & Development, Volume 1, Issue 6, 2013
4. Tsung-Chih Wang, Wen-Hsiang Tsai, " Creation Of Tile-Overlapping Mosaic Images For Information Hiding**",** Institute of Multimedia Eng., National Chiao Tung University, Hsinchu, Taiwan
5. Shan-Chun Liu and Wen-Hsiang Tsai, " Line-based Cubism-like Image - A New Type of Art Image and Its Application to Lossless Data Hiding" in IEEE Transactions on Information Forensics and Security, Volume 7, Issue 5 , June 2012
6. Suprith S., M. N. Ravikumar,"Secure Image Transmission based on Fragmenting and Mosaicing Image by RCT using Secret Key" in International Conference on Computer Science, Electronics & Electrical Engineering-2015
7. Dinu Coltuc and Jean-Marc Chassery," Very Fast Watermarking by Reversible Contrast Mapping", in IEEE Signal Processing Letters, Volume 14, April 2007
8. Ms. Parul M. Jain and Prof. Vijaya K. Shandliya, “A Review Paper on Various Approaches for Image Mosaicing”, in International Journal of Computational Engineering Research Volume 3, Issue 4, April 2013

Advance College of Engineering and Management, SET Conference 2016

GENETIC ALGORITHM FOR IMPROVING CLASS TIME TABLE

Ram P. Sapkota

Department of Computer and Electronics Engineering

Advanced College of Engineering and Management, Kupondole, Lalitpur, Nepal

Email: ramsapkota3721@gmail.com

Abstract

Timetable involves scheduling different set of resources by avoiding the conflict. Manual way of timetabling is more time consuming and laborious task. The paper describe about the solution of class timetable scheduling by implementing Genetic Algorithm, which comprises of various operations like chromosome representation, population generation, selection, crossover and mutation. Timetable is generated by satisfying all the hard constraints and soft constraints as much as possible, in which events are arranged into a number of timeslots such that conflicts in using the given set of resources are avoided. The optimized timetable is obtained as the number of generation increases on the basis of fitness value compared.

Keywords: Timetable, Genetic Algorithm, Chromosome, Fitness Function, Selection, Crossover, Mutation.

I. Introduction

The class timetable problem is a typical scheduling problem that appears to be arduous and time consuming task in every academic institute once or twice a year [1]. Traditionally, timetable problem is solved manually with a single person or some group, which takes a lot of effort and time; however, the valid solution is not guaranteed and even if found, it is likely to miss far better solutions [1,2]. So, manual planning of timetables do not produce much effective and better solutions. This motivated for the scientific study of the problem, and to develop an automated solution technique for it [1].

A. Wren define timetabling as," Timetabling is the allocation, subject to constraints, of given to objects being placed in space time, in such a way as to satisfy as nearly as possible a set of desirable objectives" [3]. An academic institution has a set of teachers, a set of students and a set of activities [4]. The activities need to be followed by both the teachers and the students according to their scheduled time in specified class. That means, class timetabling is the allocation of subjects, teachers and students into appropriate timeslots and classrooms in such a way that conflicts in using a given set of resources are avoided and they satisfy a set of predefined set of constraints [4, 5]. There are basically two types of constraints, soft constraints and hard constraints. Soft constraints are those if we violate them in scheduling, the output is still valid, but hard constraints are those which if we violate them; the schedule is no longer valid [6].

Class timetabling is an optimization problem because for the better solution it is necessary to satisfy more number of constraints and efficient utilization of resources. It is also found that the search space of timetabling problem is huge and among the many solutions it is necessary to select the feasible and better solution which satisfy the hard constraints and try to satisfy the soft constraints. So, using Genetic Algorithm for such large and multimode search space, optimized solution can be obtain for better timetabling [1, 7, 8].

2. Background

A. Genetic Algorithm

Genetic Algorithms (GA) is the part of evolutionary computation which is based on Darwin's theory of natural selection and evolution. It starts with a set of solutions called population, which are represented by chromosomes [8]. Solutions from one population are taken (parents) to form better and new solution (offspring). Parents are selected from the population based on the fitness value. The more suitable and better the fitness of parents, the more chances they can survive and reproduce. The process is repeated until the optimal solution is found.

GA is adaptive method which is used to solve search and optimization problems [9]. Individuals of the population, coupled with the genetic operators, combine to perform an efficient domain-independent search strategy that makes few assumptions about the search space [10].The performance of GA is usually evaluated in terms of convergence rate and the number of generations to reach the optimal solution [11]. The top level description of GA [12] is shown as:

1. Create a population
2. Evaluate the fitness of each chromosome
3. Create a new population by repeating the following steps:

a). Selection: Select two parent chromosomes from the population, the better fitness value is selected.

b). Crossover: Combine the parents to form a new offspring.

c). Mutation: New offspring are mutated.

d). Accepting: Place new offspring in the new population.

4. If the optimal solution is obtained, stop otherwise use new generated population for further run of algorithm.

B. Chromosome Representation

The chromosome consists of gene that encodes unique traits and provides information about the solution of the problems. The chromosome is represented as a binary string, '0' and '1' or integer or real numbers. The number represents some traits or characteristics of the solution. For example, a typical chromosome may look like this: 11011011

C. Initialization

The initialization of GA begins with creating the initial population. Each individual in the population is assigned with the fitness value and consider as the feasible solution of the problem.

D. Fitness Function

For the better solution, each individual is evaluated by determining the fitness value. Fitness value is the weighted sum of the violation of soft constraints [7]. After each round of testing, the worst solution is deleted and the best one is used for breeding. Thus, the better chromosome is determined by applying the fitness function to the test result obtained from the solution.

E. Selection

According to the Darwinian's Theory of Natural Selection "Only the organism best adapted to their environment tend to survive and transmit their genetic characteristics in increasing numbers to succeeding generations while those less adapted tend to be eliminated."

Selection operator plays a driving role to obtain an optimal solution [7]. The chromosomes are selected by determining the fitness value. The better chromosome has high chances of selection whereas the worst one is discarded. The operator can be found at two stages: one to select parents to form the off springs and other after the manipulation of some individuals where a best population is chosen for the next generation [7]. There are several selection methods:

1. Roulette Wheel Selection: It is also known as proportionate selection by fitness value where the individual is selected on the basis of fitness value [11]. In this method the chromosomes are placed in the roulette wheel. The chromosome which has the better fitness value occupies the larger size in the wheel and has a greater chance of survival.
   (i.e. the individuals' selection is based on the fitness value occupying larger portion of the roulette wheel)
2. Ranking and Scaling Method: In this selection method, first the individual is sorted according to their fitness value and then computes the selection according to their rank rather than their fitness value thus providing uniform scaling across the population [11].
3. Tournament: In this selection method, individual are selected randomly from the population and provide the selection pressure by holding the tournament among the competitors, competing in each tournament called tournament size [11,14]. The individual with the highest fitness win and inserted as one of the next generation population [11, 14].

F. Crossover

The exchanging of genetic materials between parents to produce new off springs is termed as crossover. This operator helps to narrow down the search space to look for the feasible solution. The point for exchange could be single/one point, two points or uniform [7].

1. Single/One point crossover: A single crossover point is selected on both parents and all the data beyond that point is exchanged between two parents. (| is crossover point)

Parent 1	**1 1 0 1 1 | 0 1 1**
Parent 2	1 1 0 1 0 | 1 1 1
Offspring 1	**1 1 0 1 1** | 1 1 1
Offspring 2	1 1 0 1 0 | **0 1 1**

Figure 1: Single point crossover [18]

2. Two point crossover: Two crossover points are selected on both parents and all the data between two points are exchanged between the parents.

Parent 1	**1 1 | 0 1 1 | 0 1 1**
Parent 2	1 1 | 0 1 0 | 1 1 1
Offspring 1	**1 1** | 0 1 1 | **0 1 1**
Offspring 2	1 1 | **0 1 1** | 1 1 1

Figure 2: Two point crossover [18]

3. Uniform Crossover: Multiple crossover points are selected and the data are randomly exchanged between the two parents.

Parent 1	**1 | 1 0 | 1 1 | 0 1 | 1**
Parent 2	1 | 1 0 | 1 0 | 1 1 | 1
Offspring 1	**1 |** 1 0 **| 1 1 |** 1 1 **| 1**
Offspring 2	1 | **1 0** | 1 0 | **0 1 |** 1

Figure3: Uniform crossover [18]

G. Mutation

Mutation alters one or more gene value from its previous state in the chromosome. For example: if the previous gene value is '1' then mutation alters it to '0'. This alteration helps to maintain the genetic diversity and allows a search space towards convergence. Mutation can occur at each bit position in a string with some probability, usually very small (for e.g., 0.001) [13].

Original offspring 1	1 **1** 0 1 1 0 1 1
Original offspring 2	1 1 **0** 1 0 1 **1** 1
Mutated offspring 1	1 **0** 0 1 1 0 1 1
Mutated offspring 2	1 1 **1** 1 0 1 **0** 1

Figure 4: Mutation [18]

3. Methodology

The scheduling of the timetable is very much attached with the number of the constraints. Constraints are almost employed by people dealing with timetabling problems [15]. So, the definition of the constraints is the main task in the problem. Both the hard constraints and the soft constraints are different for different academic institution, which are define according to their needs. But some of the hard constraints can be similar for all the institutions. For examples,

1. No student can attend more than one class at the same time.
2. No teacher/lecturer should have different classes at the same time.
3. No room can be booked for more than one lecture at the same time.

These hard constraints are almost similar for every case. However the soft constraints can be vary according to the needs of the institutions. The reason for this is that different institutions will have different protocols for maintaining their timetable and there are dynamic scenario of constraints and datasets available for the experiments [8].

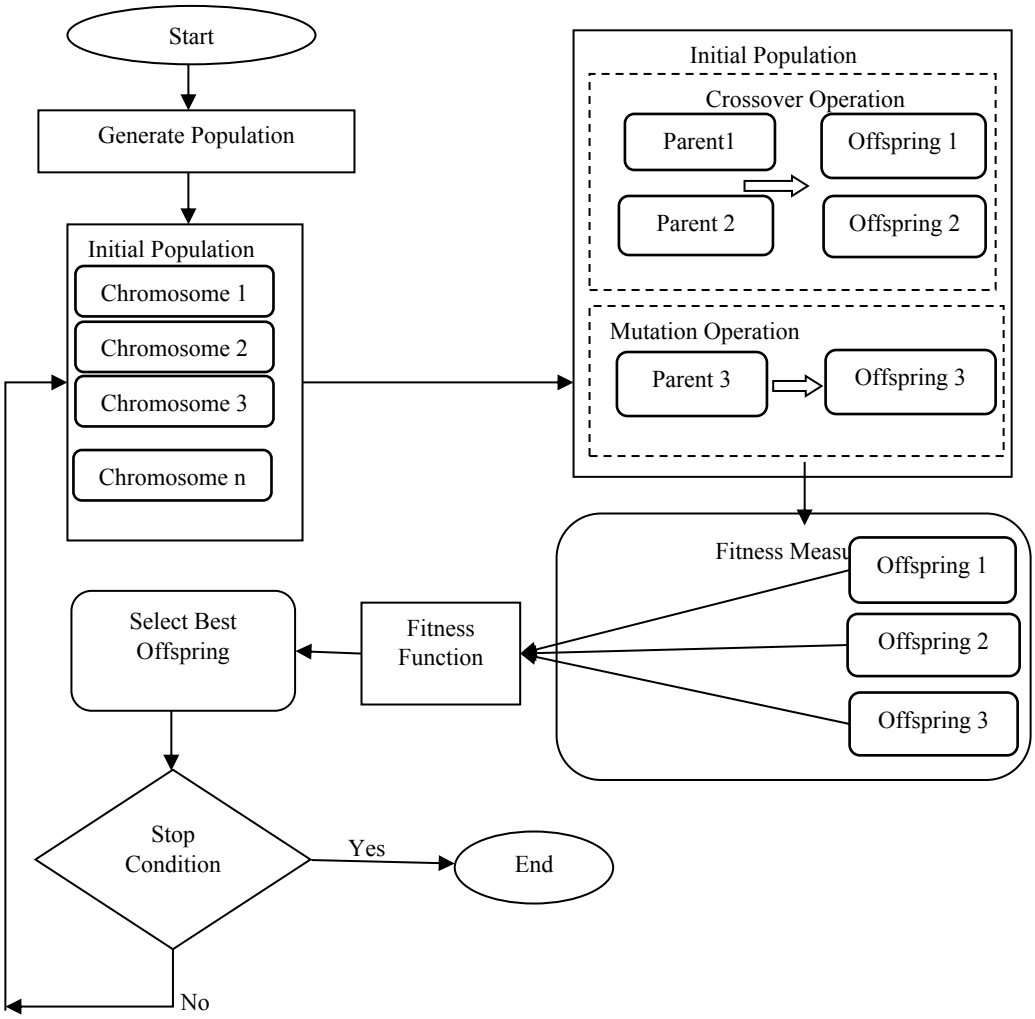

Figure 5: Flow chart of timetable generation [16].

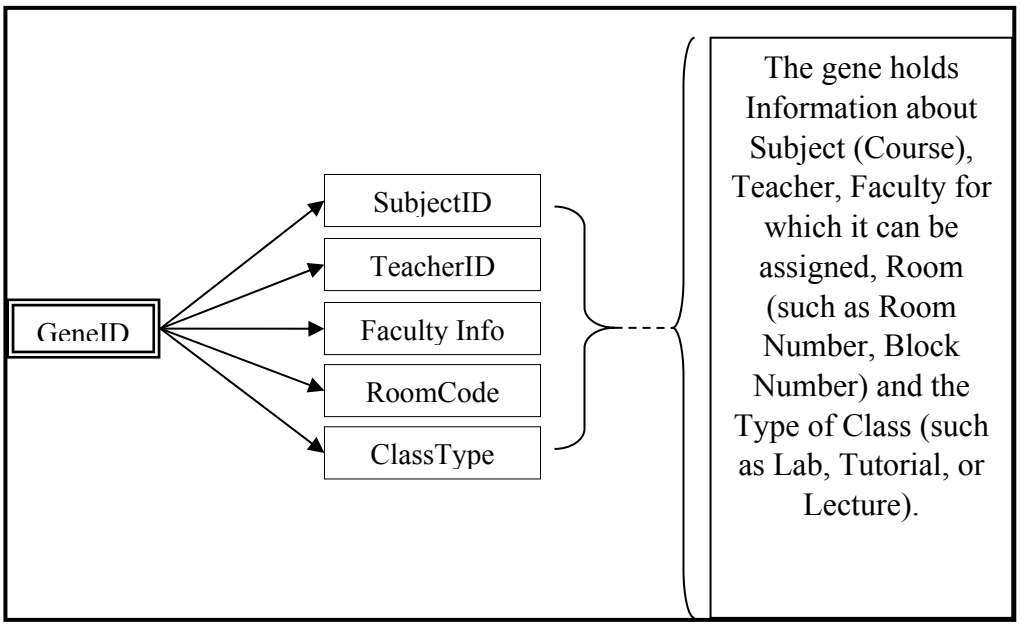

Figure 6: Creation of gene with its characteristics [17]

The first thing is the representation of timetable solution into an encoded form of chromosome [15]. For this gene samples need to be created. The gene is created by giving an ID (identity) and the attributes in such a way that each gene contains unique characteristics.

After, the creation of gene, the chromosome is defined in the form of 2-Dimensional Matrix with the fixed dimension. The dimension is defined according to the design of the timetable.

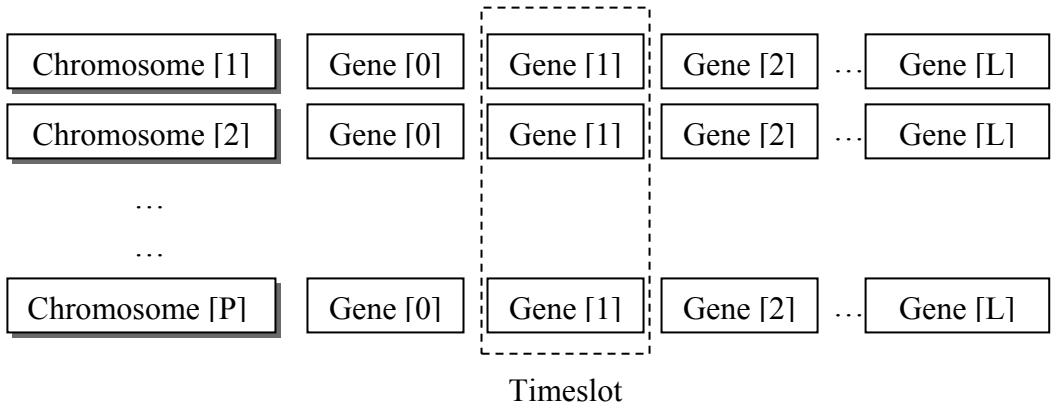

Figure 7: Genetic Representation of Timetable [16]

In the research work, 5×35 matrix is considered in which each row is assigned for 5 faculties (for e.g. consider the engineering department consisting of faculty like civil engineering, electrical engineering, computer engineering, mechanical engineering and architecture) and column represents the period in a week considering 35 periods per week and 5 working days i.e. 7 periods per day. Below is the illustration of format of timetable.

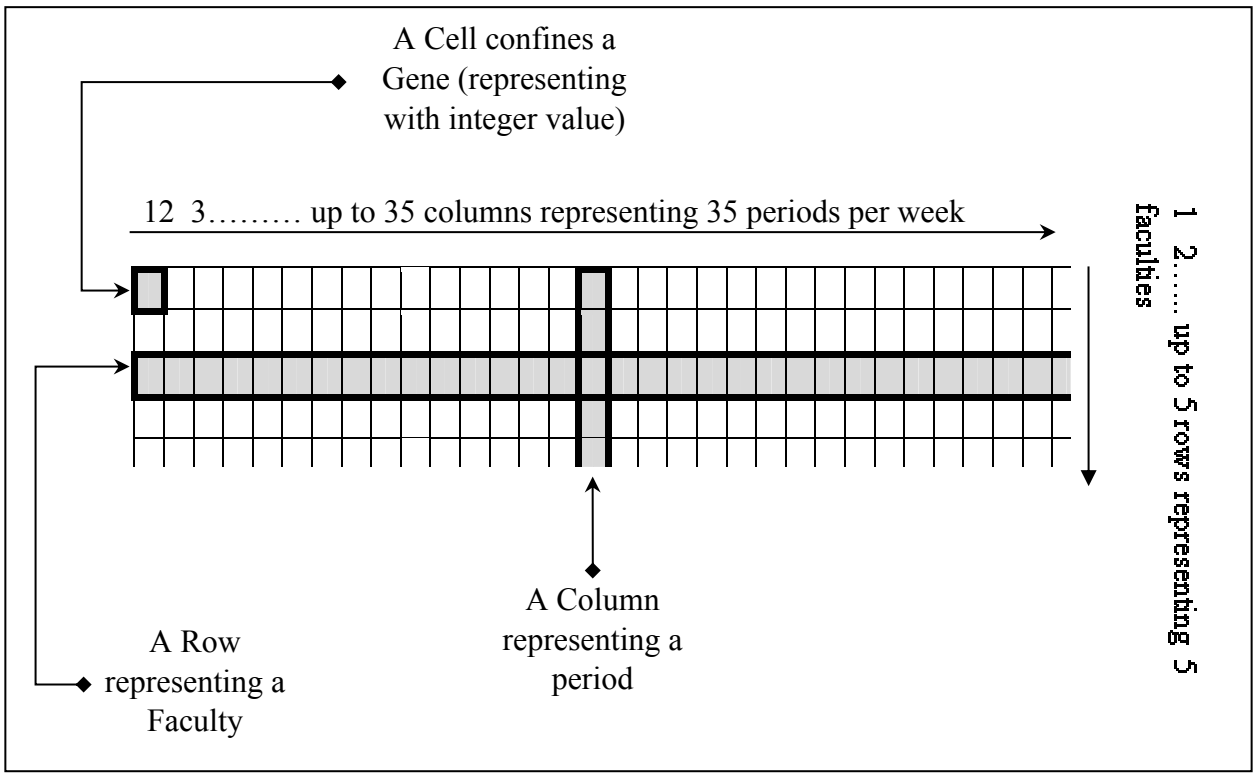

Figure 8: Chromosome representation in 5 x 35 matrix form.

The chromosome is created by the random generation of gene sequence in the gene slot. The chromosome may become infeasible or remain outside the search space. So, to deal with the infeasible chromosomes we applied Fitness Function. For calculation of total fitness value, first calculate the total cost of each violation.

Total Cost = Penalty for violation (Pi) X Number of violations (C)

Total Fitness value of the chromosome $f(T)_i = \sum_{i=1}^{n}(Total\ Cost)$

For each defined constraints penalty value or cost is marked. The cost is marked according to the necessity of the fulfillment of the constraints. The constraint which needs to be satisfied is given high penalty value whereas the constraint which satisfaction is not so important is given with less penalty value. For example: "Lecturer having four theory subjects has no lab assignments" then the cost was assigned as 100 cost value. As like this, in case of violation of the constraint "Subjects which are difficult for students or have more credit hour can be placed in the first hour" then the cost assigned was 50 cost values. For each constraint violated, the module counts the number of violation of each constraints and that count is multiplied by the cost assigned for that violation. After that all the costs were summed to get the total fitness value.

The calculated fitness values are normalized so that it ranges from 0 to 1. To Normalize the Fitness Value, first calculate the Reverse Fitness Value so it can be rank according to the greatest fitness value and as Roulette Wheel Selection procedure gives priority to the highest fitness. For this procedure, below customized equation is applied.

$$Reversed\ f(T)_i = \frac{\sum_{i=1}^{n} f(T)_i}{f(T)_i}$$

Normalization Fitness Value for a Chromosome.

$$Normalized\ f(T)_i = \frac{Reversed\ f(T)_i}{\sum_{i=1}^{n} Reversed\ f(T)_i}$$

The chromosome which has lower cost (total fitness value) will have greater Reversed fitness value and Normalized fitness value. In the research, the chromosome which has less penalty of violation of constraints and less number of violation of constraints are consider as better i.e. greater the normalized fitness value, better the quality of chromosome.

While selecting through Roulette Wheel Selection method, selects the chromosome which have the highest Normalized fitness value. The fitness of the chromosome are selecting for generating the next generation of time table which apply the uses of genetic operators such as crossover and mutation [5]. Here, single point crossover is used and applied 0.8 threshold point. For the mutation 0.15 threshold point is applied.

4. Result and Analysis

Figure below shows the graph between Generation and Normalized Fitness Value. From the graph it is clear that as the number of generation of population increases the fitness value (Normalized) also increases. That means more better and feasible timetable is generated as the number of generation increases.

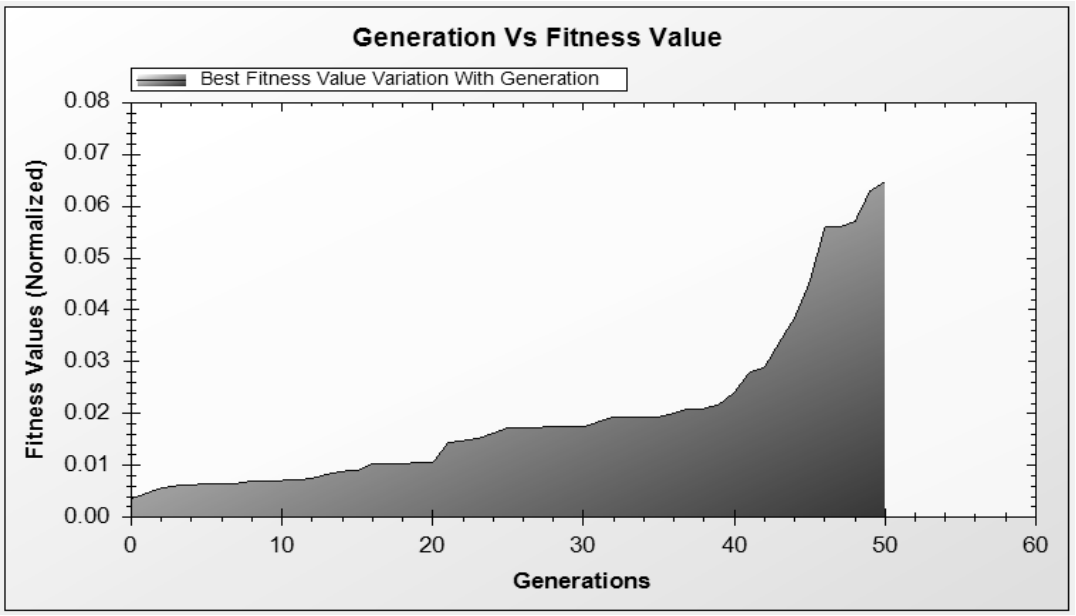

Figure 9: Generation vs. Fitness Value Graph

5. Conclusion

The timetabling problem of academic institution is considered as computationally complex problem. The paper implemented the GA for the effective scheduling of the timetable. GA helps in developing the better timetabling solution which is conflict free, more efficient and utilizing maximum use of resources, thus generating optimized result.

6. Suggestion and Recommendations

The paper focus on some limited hard and soft constraint. In future the timetabling can be made more efficient and powerful by defining more number of constraints and trying to satisfy the entire mentioned constraints. Further enhancement can be the addition and edit features of faculty, lecturer, rooms and subjects.

7. Acknowledgement

I am thankful to Nitu Bharati, Director, Department of Customs, Finance Ministry, Government of Nepal, Hem Bahadur Gurung and Jitendra Kumar Gurung.

References

1. DilipDatta, Kalyanmoy Deb and Carlos M. Fonseca, “Solving Class Timetabling Problem of IIT Kanpur using Multi-Objective Evolutionary Algorithm”.KanGAL2005.
2. Dipesh Mittal, HiralDoshi, Mohammed Sunasra, RenukaNagpure, “Automatic Timetable Generation using Genetic Algorithm”, International Journal of Advanced Reasearch in Computer and Communication Engineering, Vol. 4, Issue 2, February 2015.
3. Edmund Kieran Burke and SanjaPetrovic, “Recent Research Directions in Automated Timetabling”, European Journal of Operational Research – EJOR, 2002, Automated Scheduling, Optimisation and Planning (ASAP) Research Group, School of Computer Science and Information Technology, University of Nottingham, Jubilee Campus Nottingham NG8 1BB UK.
4. LiviuLalescu and CostinBadica, “Timetabling Experiments using Genetic Algotithms” University of Craiova, Faculty of Control, Computers and Electronics, Software Engineering Department, str.Tehnicii, 5, Craiova, RO-1100, Romania.

5. A Kavya Reddy, Nagambika A, Akash J Castelino, Deeksha CS and Mrs. K Panimozhi "Automatic Class Timetable Generation using a Hybrid Genetic and Tabu Algorithm", International Journal on Recent and Innovation Trends in Computing and Communication, Vol: 3 Issue: 5, Dept. of Computer Science and Engineering, BMSCE Bangalore, India.
6. M. Doulaty, M. R. FeiziDerakhshi, and M. Abdi, "Timetabling: A State-of-the-Art Evolutionary Approach", International Journal of Machine Learning and Computing, Vol. 3, No. 3, June 2013.
7. Ahmed Mohammed Ali Qutishat, Universiti Utara Malaysia, "Improving Class Timetabling Using Genetic Algorithm".
8. Sanjay R. SutarRajan and S. Bichkar , "University Timetabling based on Hard Constraints using Genetic Algorithm",International Journal of Computer Applications (0975 – 8887), Vol. 42– No.15, March 2012
9. David Beasley, David R. Bull and Ralph R. Martin,"An Overview of Genetic Algorithm: Part1, Fundamentals", University Computing, 1993.
10. William M. Spears, Vis Anand, "A Study of Crossover Operators in Genetic Programming".
11. NorainiMohdRazali, John Geraghy, "Genetic Algorithm performance with Different Selection Strategies in Solving TSP", Proceedings of the World Congress on Engineering 2011 Vol II WCE 2011, July 6 - 8, 2011, London, U.K.
12. Leon Bambrick and Dr B Lovell, "Lecture Timetabling Using Genetic Algorithms", Department of Electrical and Computer Engineering, The University of Queensland.
13. Melanie Mitchell," An Introduction to Genetic Algorithm", A Bradford Book, The MIT Press, Fifth printing 1999.
14. Brad L. M iller and David E . Goldberg, "Genetic Algorithms, Tournament Selection, and the Effects of Noise, Complex Systems 9, 1995.
15. Alade O. Modupe, Omidiora E. Olusayo and Olabiyisi S. Olatunde, "Development of a University Lecture Timetable using Modified Genetic Algorithms Approach", International Journal of Advanced Research in Computer Science and Software Engineering,Vol 4, Issue 9, September 2014.
16. Salwani Abdullah and Hamza Turabieh, "Generating University Course Timetable Using Genetic Algorithms and Local Search", Third 2008 International Conference on Convergence and Hybrid Information Technology.
17. Nitu Bharati, Ram P. Sapkota, Hem B. Gurung, Jitendra K. Gurung, "Classroom Routine Management System using Genetic Algorithm", December, 2012.
18. http://www.obitko.com/tutorials/genetic-algorithms/operators.php, Introduction to Genetic Algorithms, September 17, 2016.

A REVIEW ON OPEN SOURCE SOLUTION FOR CLOUD COMPUTING

Dr. Gajendra Sharma and Amrita Rai

Department of Computer Science & Engineering

Kathmandu University, Dhulikhel

amrita.rai@student.ku.edu.np

Abstract

Cloud Computing is the latest evolution of internet based computing which assures to provide more flexibility, less expense, and more efficiency in IT services to end users. It is believed that governments, businesses and researchers all can benefit from the adoption of cloud computing services. The aim of this paper is to study four main open source cloud computing platforms available in the market. This paper also highlights their features and limitations which will definitely help service providers and enterprises for selecting best open source cloud computing solutions for their organization according to their needs.

Keywords: Cloud computing, open source, information technology, organization

1. Introduction

1.1 Background and Motivation

In the recent times, "Cloud Computing" has been one of the most discussed terms in the world of Information Technology. The standard definition from the National Institute of Standards and Technology (NIST) is: "Cloud Computing is a model for enabling convenient, on-demand network access to a shared pool of configurable computing resources (e.g. networks, servers, storage, applications, and services) that can be rapidly provisioned and released with minimal management effort or service provider interaction". This model is composed of five essential features, three service models and four deployment models [1].

According to US NIST, five essential characteristics, three service models and four deployment models are as follows:

- Five characteristics: on-demand self-service, broad network access, resource pooling, rapid elasticity, and measured service.
- Three service models: Software as a Service (SaaS), Platform as a Service (PaaS), and Infrastructure as a Service (IaaS).
- Four deployment models: private clouds, community clouds, public clouds, and hybrid clouds.

Cloud computing has been enabled by the developments in virtualization, distributed computing, utility computing, web and software services technologies. It is considered as the next natural step in the evolution of on-demand information technology services and products. Because of its various advantages like: lower cost, high scalability, fast processing, and convenience (i.e. anytime and anywhere), cloud computing is gaining its popularity in business and academic environment. [2]

While big companies such as Amazon, Google and Microsoft are offering public cloud infrastructures like Amazon Elastic Compute Cloud (EC2), Google AppEngine, Microsoft Azure, etc commercially in the market. Many other organizations are trying to set up "private clouds". Private clouds are

internal to the organization providing more security, privacy, and better control on data usage and cost.

There are number of cloud platforms available in the market both commercial and open source softwares. Nowadays, an open source solutions for cloud computing are becoming more popular for organizations willing not to use commercially provided cloud. However, there are many open cloud platforms having their own characteristics and advantages making difficult for service providers and enterprises to choose between these platforms. And this difficulty in choosing appropriate cloud platform motivated me to do the study of open source cloud computing solutions available in the market.

1.2 Problem Statement

With the advancement in Information Technology, numbers of open source solutions are being developed with several features and purposes. However, for the successful utilization of cloud services it is very important to select appropriate cloud computing solutions according to one's needs and business requirements. There are various options for open source cloud computing platforms but the real problem lies in the selection of best open source cloud computing solutions which differ from individual to individual and organizations to organizations. Thus, this study is a step towards understanding several aspects of open source cloud computing platform which will help users to make a correct decision.

1.3 Objective of Study

The main objective of this study is to give a brief introduction of open source cloud computing platforms available in the market. The most popular open source platforms available in the market are: Eucalyptus, OpenStack, CloudStack and OpenNebula. The study also aims to highlight its features and limitaions which will definitely help users for selecting best open source cloud solutions according to their requirement.

2. Research Methodology

To fulfill the above objectives of study, this research is based upon the secondary data. The paper is written based on data collected from:

- Open source cloud computing websites
- Research articles
- Online journal papers

3. Literature Review

3.1 Open Source Cloud Platforms

Open source solutions provide flexibility to users not only to choose the product but also allow users to change source code for their own need. This ability of freedom and openness is encouraging more programmers to migrate towards the work on open source cloud packages as do not need to pay and look over proprietary issues. An open source cloud is growing and becoming more effective for the IT Industries and organizations who wanted to use the cloud facilities for hosting and other services. There are several open source cloud computing platforms available in the market. Among them the most popular are: Eucalyptus, OpenStack, CloudStack and OpenNebula. [3]

3.2 Eucalyptus:

EUCALYPTUS [4] is the full form for Elastic Utility Computing Architecture for Linking Your Program to Useful System, which is an open source private cloud software for building private or

hybrid cloud resources for compute, network, and storage that are compatible with Amazon Web Service (AWS) APIs**.** It was developed by University of California-Santa Barbara for Cloud Computing to implement Infrastructure as a Service (IaaS). Eucalyptus provides an Elastic Compute Cloud (EC2) -compatible cloud Computing Platform and Simple Storage Service (S3)-compatible Cloud Storage. Eucalyptus incorporates high-level components such as Cloud Controller (CLC), Cluster Controller (CC), Storage Controller (SC), and Node Controller (NC). The main benefit to use this open source software is for private clouds as it provides highly efficient scalability and organization agility. Main features [6] are:

- Images-Image is a group of software modules.
- Instances- If an image is using then it is called instance.
- IP addressing- Instances will get both public and private IP addresses when it is created.
- Security is provided by firewall.
- Networking- Three network modes: Managed mode, System mode and Static mode. In Managed mode, local network of instances are controlled where as physical LAN and cloud connection is established in System mode and in static mode DHCP server management and assigning IP addresses to the instances are possible.

3.3 OpenStack:

OpenStack [3, 5] was announced in July 2010 and its initial contributors were NASA and Rackspace. It is one of the fastest growing free open source software available in the market. In the beginning, Rackspace contributed their "Cloud Files" platform (code) while NASA contributed their "Nebula" platform (code). OpenStack open source software is a collection of open source software project that any organization can use to setup and run their cloud compute and storage infrastructure. An OpenStack consist of several components- Compute (Nova), Object storage (Swift), Block storage (Cinder), Networking (Neutron), Dashboard (Horizon), Identity service (Keystone), Image service (Glance), Telemetry (Ceilometer), Orchestration (Heat), Database (Trove). Main properties of OpenStack are [6]:

- Component based architecture- One can easily add new components
- High availability
- Fault Tolerant
- Recoverable- Failures can be easily removed
- Open Standards
- API Compatibility
- Nova follows shared nothing architecture and message passing for communication. Nova is a good interface with hypervisor.
- VM management and caching are the two functions of Nova.

3.4 CloudStack:

CloudStack [7] was initially developed by Cloud.com and purchased by Citrix then later on released into the Apache Incubator program. The first stable version of CloudStack was released in 2013 and this time governed by the Apache Software Foundation and supported by Citrix. CloudStack have commendable features such as:

- Storage independent compute
- New security features
- Smooth Deployment
- Scalability
- Multi Hypervisor support
- Detailed Documentation
- Interactive Web UI i.e. users can manage their cloud with an easy to use Web interface, command line tools, and/or a full-featured RESTful API.
- Access Control –Eucalyptus has an identity. This identity is grouped together for access control

3.5 OpenNebula:

OpenNebula [4] was first established as a research project back in 2005 by Ignacio M. Liorente and Ruben S. Montero. It is used by many enterprises as an open, flexible alternative to vCloud on their VMware-based data center. OpenNebula is primarily used as a virtualization tool to manage virtualized infrastructure in the data center, which is usually referred as private cloud and also supports hybrid cloud to combine local infrastructure with public cloud-based infrastructure, enabling highly scalable hosting environments. OpenNebula cloud infrastructure provides users with an elastic platform for fast delivery and scalability of services to meet the dynamic demand of service end-users. OpenNebula cloud computing toolkit is used by- hosting providers, telecom operators, IT services providers, supercomputing centers, research labs, and international research projects.

3.6 Comparative Study of Cloud Solutions

The following table [8] shows a comparative study of four main open source cloud computing platform based on their characteristics.

Table 1: Comparison of Open Cloud Platform Characteristics

Characteristics	Eucalyptus	OpenStack	CloudStack	OpenNebula
License	Proprietary, GPL v3	Apache license	Apache license	Apache license
Cloud Implementation	Private & Hybrid	Private & Hybrid	Public & Private	Public, Private & Hybrid
Service Type	Compute, Storage	Compute (Nova), Storage (Swift)	Service, Disk, Network Offerings and Templates	Compute, Storage
Compatibility	Support EC2,S3	Supports multiple platforms	Support Amazon EC2 and S3 APIs	Open, multiplatform
	Xen, KVM (VM	Open	VMware, KVM, XenServer, Xen	Xen, KVM,

Hypervisors	Ware in nonopen source)	Virtualization Format (OVF)	Cloud Platform (XCP) and Hyper-V	VMware
Programming Framework	C, Java	Python	Java, Python	C++, C, Ruby, Java, Shell script, lex, yacc
Disk Image Options	Options set by admin	Glance has RESTful API	Users can manage their cloud with Web interface, command line tools, RESTful API	In private cloud, most libvirt options left open
Disk Image Storage	Walrus, which Imitates Amazons S3	Nova	iSCSI or NFS	A shared file system, by default NFS, or SCP
Characteristics	**Eucalyptus**	**OpenStack**	**CloudStack**	**OpenNebula**
Unique Features	User management web interface	Unified Authentication System	Clustered LVM, NetScaler Support & LDAP Integration	VM migration supported

4. Conclusion

Cloud Computing is the latest evolution of technology that has transformed the way hardware and software is now designed and delivered in the IT industry. Open source cloud platform provides an alternative to end-users for improved flexibility, scalability, portability and on demand services. The main advantage of open source solution is that they are customizable according to one's need and desire. This paper gave a brief introduction of four most popular and commonly used open source cloud solutions: Eucalyptus, OpenStack, CloudStack and OpenNebula. The paper also shows a comparative study which would help the users to understand the characteristics and limitations of above popular open source solutions making them able to choose better services according to their requirements.

Since cloud computing is an evolving technology and many features are being added day-to-day, here the comparison is based on the current features and technology available in these open source

platform. However, there is need for incorporating many more features to improve the framework of available open source cloud solutions.

References

1. P. Mell and T. Grance, "The NIST Definition of Cloud Computing." 07-Oct-2009.
2. M. A. Vouk, "Cloud Computing – Issues, Research and Implementations," Journal of Computing and Information Technology, vol. 4, pp. 235–246, 2008.
3. S. Sachdev and A. Mahajan, "Deployment of Private Cloud using Open Stack: An Open Source Cloud Computing Solution for Small and Mid-sized Organizations," International Journal of Advanced Research in Computer Science and Software Engineering, vol. 3, no. 10, pp. 292–304, Oct. 2013.
4. S. Yadav, "Comparative Study on Open Source Software for Cloud Computing Platform: Eucalyptus, Openstack and Opennebula," Research Inventy: International Journal Of Engineering And Science, vol. 3, no. 10, pp. 51-54, Oct. 2013
5. O. SEFRAOUI, M. AISSAOUI, M. ELEULDJ, "OpenStack: Toward an Open-Source Solution for Cloud Computing", International Journal of Computer Applications, vol. 55, no. 03, Oct. 2012 J. S., Manjaly, and J. S., "A COMPARATIVE STUDY ON OPEN SOURCE CLOUD COMPUTING FRAMEWORKS," International Journal Of Engineering And Computer Science, vol. 2, no. 6, pp. 2026–2029, 2013.
6. "Apache Cloudstack," Apache Cloudstack. [Online]. Available:http://cloudstack.apache.org/. [Accessed: 20-Apr-2015]. "Cloud computing comparison," Wikipedia, the free encyclopedia. 16-Apr-2015.

Transfer System for Portable Electronic Devices

Ajay Kumar Sah

Department of Electronics & Communication Engineering

PU School of Engineering & Technology, Biratnagar, Nepal

Email: ajayshah2005@yahoo.com

Abstract

Wireless power transmission is useful in cases where instantaneous or continuous energy transfer is needed, but interconnecting wires are inconvenient, hazardous, or impossible. In this paper, a simple design method of a wireless power transfer system for portable electronic devices using 13.56 MHz ISM band is proposed. The proposed wireless power transfer system consists of rectifier, oscillator, power amplifier, power coil, load coil and two intermediate coils as transmitter antenna and receiver antenna inserted between power coil and load coil.

Keywords: Wireless Power Transfer, Resonant coupling, Oscillator, Intermediate coils, Power transfer efficiency.

1. INTRODUCTION

Wireless power transmission is useful in cases where instantaneous or continuous energy transfer is needed for portable electronic devices, but interconnecting wires are inconvenient, hazardous, or sometimes impossible [1].

The history of wireless power transmission dates back to the late 19th century with the prediction that power could be transmitted from one point to another in free space by Maxwell in his "Treatise on Electricity and Magnetism". Heinrich Rudolf Hertz performed experimental validation of Maxwell's equation which was a monumental step in the direction. However, Nikola Tesla's experiments are often considered as being some of the most serious demonstrations of the capability of transferring power wirelessly even with his failed attempts to send power to space [2].

There are three types of Wireless Power Transfer (WPT): radiative transfer, inductive transfer, and resonant coupling. Radiative transfer, although suitable for exchanging information, can transfer only small power (several milliwatts), because a majority of energy is wasted into free space. Directive radiative transfer using highly directional antennas can be efficiently used for power transfer, even for long distances, but require existence of an uninterruptible line-of-sight and have harmful influences on human body. On the other hand, inductive coupling can transfer power with very high efficiency but in a very short range (just in several centimetres) [2].

The last type of WPT, resonant coupling, can transfer high power at the medium range (several meters). Recently, Massachusetts Institute of Technology proposed a new scheme based on strongly coupled magnetic resonances, thus presenting a potential breakthrough for a mid-range wireless energy transfer. The fundamental principle is that resonant objects exchange energy efficiently, while non-resonant objects do not. The scheme is carried with a power transfer of 60 W and has RF-to-RF coupling efficiency of 40% for a distance of 2 m, which is more than three times the coil diameter. I expect that coupled magnetic resonances will make possible the commercialization of a midrange wireless power transfer [3].

2. WPT SYSTEM DESIGN CALCULATIONS

A. Block Diagram of Proposed System

This paper will be based on the principle of resonant inductive coupling. Magnetic coupling is an old and well understood method in the field of wireless power transfer. But as the magnetic field decay very quickly, magnetic field is effective only at a very short distance. By applying resonance with in magnetic coupling, the power transfer at a greater distance can be obtained. For near field wireless power transfer, Magnetic resonant coupling can be the most effective method than any other method available. The structure of the whole system is shown in Fig. 1 below.

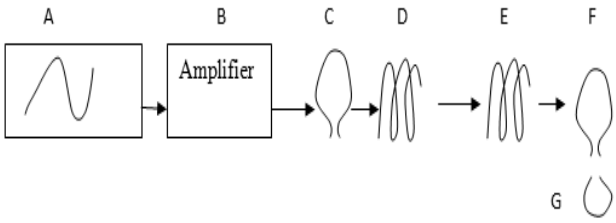

Fig. 1 Structure of the WPT System

Here,

Object A represents high frequency oscillator.

Object B is representative of signal amplifier.

Object C is a source coil.

Object F is a load coil.

Object G is a resistive load (Portable electronic device).

Object D and E are transmitter and receiver antenna respectively.

By including a signal amplifier in the system, it will be able to amplify the amount of power that is transmitted. From the amplifier the signal is then dumped into object C. This is located at the top of the object D. This allows for the resonate frequency to pass from the object C to the D. When the transmitting antenna begins to resonate, it generates the evanescent resonate waves. Object E will pick-up these waves. From the receiving antenna, the signal is then passed to the object F. The load coil will then pass the signal on to the load (Portable electronic device) G.

The intermediate coils D and E are placed between object C and F, which is tuned at the same frequency as C and F. The coil D being in the area of the magnetic field generated by coil C, receives power. Similarly, the coil E being in the area of the magnetic field generated by coil D, receives power. Not having any resistive load, the coil in turn generates its own oscillating magnetic field. The advantage of using these intermediate coils is that these coils are completely separated from the source internal resistance. This increases the Q-factor, allowing greater power to be transmitted.

The block diagram of the whole system is shown in Fig. 2 below:

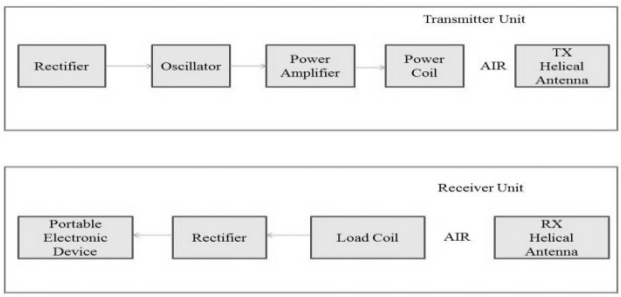

Fig. 2 Block Diagram of the whole system

For the dc source, the simple full wave bridge model is used just for the simplicity of the design. At the same time the capacitor is used for smoothing the output curve. The PSPICE circuit diagram is given in Fig. 3 below.

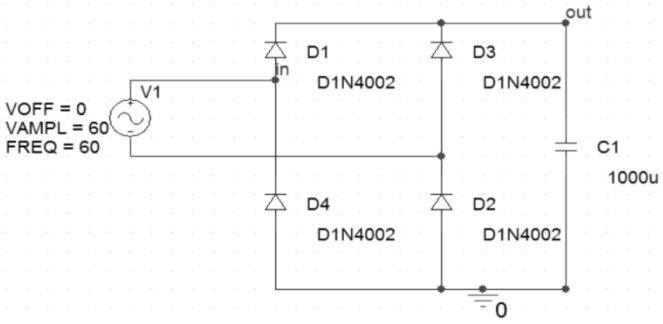

Fig. 3 Rectifier

The main advantages of a full-wave bridge rectifier is that it has a smaller AC ripple value for a given load and a smaller reservoir or smoothing capacitor than an equivalent half-wave rectifier. The full-wave bridge rectifier is designed on the Cadence, PSPICE Simulator as shown in Fig. 3 and the result is shown in Fig. 4.

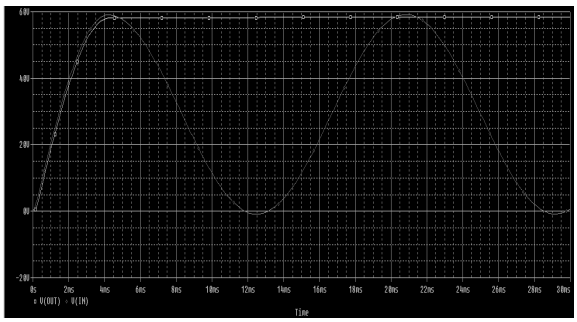

Fig. 4 Input and Output curves of Rectifier

The following oscillator circuit shown in Fig. 5 is used. This oscillator uses PSPICE VPULSE that generates square wave in combination with H bridge amplifier.

When MOSFET M1 and M4 are turned on, there is a positive voltage, when all 4 MOSFETs are off, there's 0 voltage, and when MOSFETs M2 and M3 are turned on, the result is what appears to be a negative voltage because of the direction the current flows. For this reason, an h-bridge amplifier creates a more efficient amplifier because there are both positive and negative voltage from a single power supply. The designed h-bridge amplifier is shown in Fig. 5.

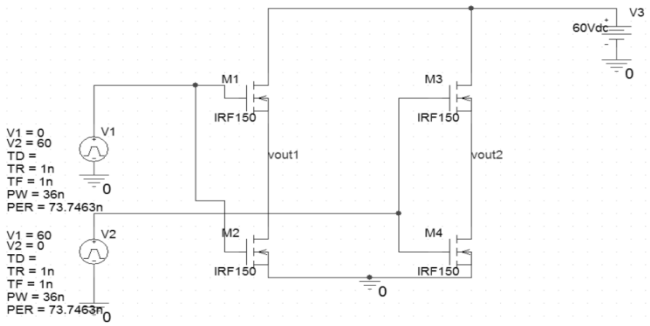

Fig. 5 H-Bridge Amplifier

The transient analysis of the designed h-bridge amplifier through PSPICE simulation is done. The oscillator generates 13.56MHz frequency and can be verified with simulation result given below in Fig. 6.

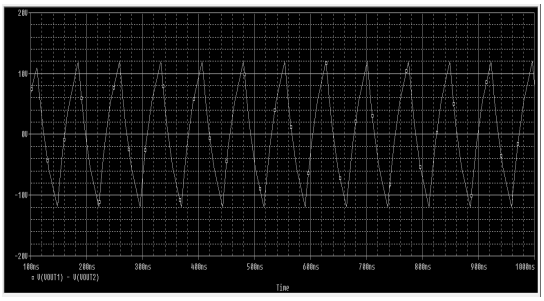

Fig. 6 Output of H Bridge Amplifier

For the rectifying purpose at the receiver, the simple full wave bridge model is used.

B. Parameter Identification of Proposed System

From [1],

$$L = \frac{N^2R^2}{2.54(9R + 10H)}$$

Where,

L = inductance in micro-Henries

N = number of turns of wire

R = radius of coil in cm

H = height of coil in cm

For Power Coil,

N = 2, R = 5 cm, H = 3.3 cm, Then, L ≈ 0.5 uH

Also we have from (1),

$$f_r = \frac{1}{2\pi\sqrt{LC}} = 13.56\ MHz$$

C = 275.518 Pf

The design parameters for all the antenna are listed in Table I below:

TABLE I: PARAMETERS OF COIL ANTENNAS

Coil(antenna)	N(turns)	R(cm)	H(cm)	L(uH)	F(MHz)	C(Pf)
Power	2	5	3.3	0.5	13.56	275.518
Transmitter	3	6	4.4	1.3	13.56	105.968
Receiver	1.67	6	4.4	0.4	13.56	344.398
Load	1	3.7	2	0.1	13.56	1.377nf

With the value given in Table I, quality factors, coupling coefficient and the maximum value of magnitude of S21 parameter is calculated as follows [1],

$$\omega_0 = \omega_1 = \frac{1}{\sqrt{L_1 C_1}} \approx 85.2 \times 10^6 [\text{rad/ s}]$$

Assuming RS=RL=50 Ohm and R1=R2=R3=R4 =0.015 Ohm,

$$Q_1 = \frac{\omega_0 L_1}{R_s + R_1} \approx 1.7 \quad Q_2 = \frac{\omega_0 L_2}{R_2} = 7384 \quad Q_3 = \frac{\omega_0 L_3}{R_3} = 2272 \quad Q_4 = \frac{\omega_0 L_4}{R_L + R_4} \approx 0.17$$

It is assumed that the distance between power coil and transmitter coil antenna is fixed, so the coupling coefficient (k12) is fixed and assumed k12= 0.1. Also it is assumed that the distance between load coil and receiver antenna is fixed, so the coupling coefficient (k34) is also fixed and assumed k34= 0.01.The varying distance is between transmitter coil antenna and receiver coil antenna, so the coupling coefficient (k23) is a varying parameter. When the distance between Tx and Rx increases, the coupling between them decreases.

The coupling coefficient is calculated as [1],

$$k_{23}^* = \sqrt{\frac{(1 + k_{12}^2 Q_1 Q_2)(1 + k_{34}^2 Q_3 Q_4)}{Q_2 Q_3}} = 4.29 \times 10^{-3}$$

The maximum value of magnitude of S21 parameter is calculated as follows [1],

$$|S_{21}|_{max} = \frac{k_{12} k_{34} Q_1 Q_4 R_L}{k_{23}^* \sqrt{L_1 L_4} \omega_0} \approx 0.884$$

Power Transfer Efficiency of the WPT system is calculated as [1],

$$n_{21} = S_{21}^2 \times 100\ \% = 78.20\%$$

3. DESIGN VERIFICATION THROUGH SIMULATION

The equivalent circuit model of whole WPT system is simulated by using an advanced design system (ADS), a popular electric automation tool in RF engineering of Agilent Technologies with the circuit setup illustrated in Fig. 7.

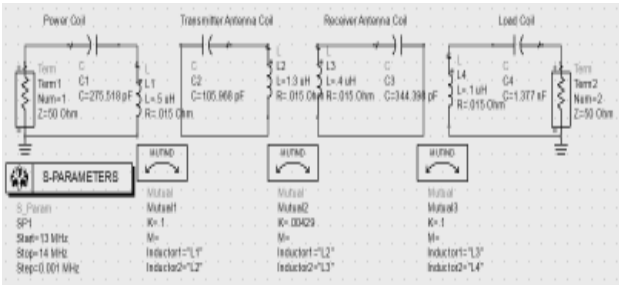

Fig. 7 Equivalent circuit of WPT system on ADS

The parameters values are taken from the Table I. The radius of power coil is 5 cm, the radius of load coil is 3.7 cm, radius of transmitter and receiver coil is 6cm. The power coil has two turns, load coil has one turn, transmitter coil has three turns and receiver coil has 1.67 turns.

The parameter S11 is the power reflection, which is the ratio of the receiving power at the transmitter divided by the transmitting power at the same transmitter and the S21 is the power transfer, which is the ratio of the receiving power at the receiver divided by the transmitting power at the transmitter. The result of the magnitude of S21 and S11 can be obtained as shown in Fig. 8.

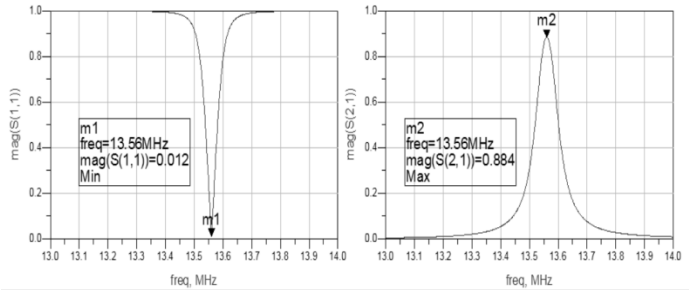

Fig. 8 Simulation result showing $|S11|$ and $|S21|$

It can be seen from the above plot in Fig. 8, the parameter $|S21|$ has maximum value 0.884 which is very much close to theoretically calculated value 0.882 at operating frequency of 13.56 MHz at a distance that corresponds to the coupling coefficient k23=0.00429.

The smith chart plot of Input Reflection Coefficient (S11) and Output Reflection Coefficient (S22) is shown in Fig. 9.

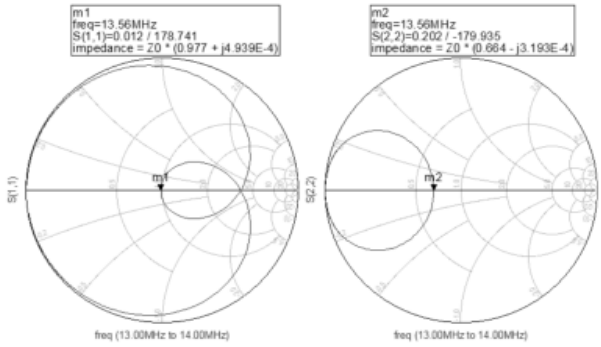

Fig. 9 Input and Output Reflection Coefficient

It can be seen from the above plot in Fig. 9 that the S11 and S22 lie on the real axis at operating frequency 13.56 MHz. The value of input port source impedance is Zo*(0.977 – j 4.939E-4) ohms and the value of output port load impedance is Zo*(0.664 – j 3.193E-4) where Z0 =ZL=50 Ohm.

The result of power transfer efficiency of the designed WPT system is shown in Fig. 10.

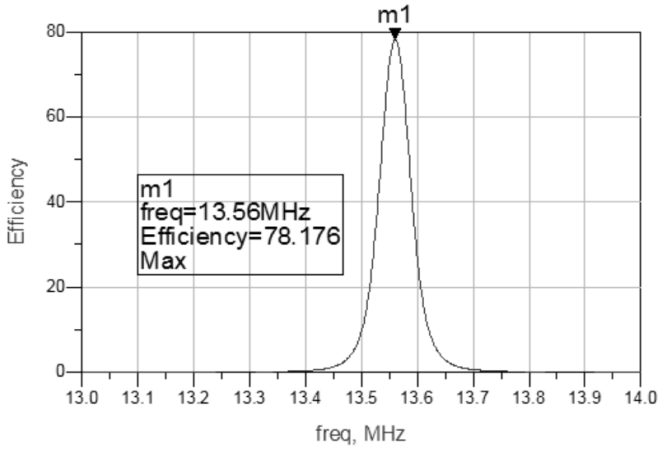

Fig. 10 Power transfer efficiency of WPT system

The maximum power transfer efficiency of the WPT system as seen from the above result is equal to 78.176% which is very close to the theoretically calculated maximum power transfer efficiency 78.20%.The above results can be tabulated as shown in Table II.

TABLE II: THEORETICAL AND SIMULATED EFFICIENCY OF WPT SYSTEM

Parameter	Theoretical	Simulation
Maximum Power Transfer	0.884	0.884
Power transfer efficiency	78.20%	78.176%

4. CONCLUSION

The goal of this paper was to present a method to design a wireless power transfer system for powering portable electronic devices. The designed WPT system has power transfer efficiency 78.176% at a coupling coefficient 0.00429. Simulated results are in good agreement with the theoretical models. It is described that magnetic resonant coupling can be used to deliver power wirelessly from a source coil to a load coil with two intermediate coils placed between the power (source) and load coil and with capacitors at the coil terminals providing a simple means to match resonant frequencies for the coils. This mechanism is a potentially robust means for delivering wireless power to a portable electronic device from a power (source) coil at a fixed distance.

The distance at which the system has coupling coefficient 0.00429 and maximum efficiency of 78.176% can be found by designing the prototype of the system and using Vector Network Analyzer (VNA).

REFERENCES

1. Sah, Ajay Kumar and Timalsina, Arun. “Design of Simple Wireless Power Transfer System via Magnetic Resonant Coupling at 13.56MHz.” Proceedings of IOE Graduate Conference, Vol. 1, pp. 206-210, November 2013

2. William C. Brown, "The history of wireless power transmission," Solar Energy, vol.56, no.1, pp. 3-21, Jan. 1996
3. Sanghoon Cheon, Yong-Hae Kim, Seung-Youl Kang, Myung Lae Lee, and Taehyoung Zyung "Wireless Energy Transfer System with Multiple Coils via Coupled Magnetic Resonances" ETRI Journal, Volume 34, Number 4, August 2012
4. Mandip Jung Sibakoti, Professor Derin Sherman and Joey Hambleton "Wireless Power Transmission Using Magnetic Resonance" Cornell College PHY312, December 2011.
5. Kurs, A. Karalis, R. Moffatt, J. D. Joannopoulos, P. Fisher, M. Soijacic, "Wireless Power Transfer via Strongly Coupled Magnetic Resonances", Massachusetts Institute of Technology, 2007 Science, Vol. 317. no. 5834, pp. 83— 86, 2007.
6. Kawamura, Atsuo, and Tae-Woong Kim. "Proposed Equivalent Circuit and Parameter Identification Method for Electro-Magnetic Resonance Based Wireless Power Transfer." April 2013.
7. Hoang, Huy, and Franklin Bien. "Maximizing Efficiency of Electromagnetic Resonance Wireless Power Transmission Systems with Adaptive Circuits."Wireless Power Transfer– Principles and Engineering Explorations: K. Y. Kim, ed., InTech, 2012. Print.
8. Jordan, Edward C., and K. G. Balmain. Electromagnetic Waves and Radiating Systems. Second ed. New Dehli: Prentice-Hall of India, 2006. Print.
9. Nilsson, James William., and Susan A. Riedel. Electric Circuits. Boston: Prentice Hall, 2011. Print.

Proceedings
of
1st National Conference
on
Science, Engineering and Technology
(SET Conference 2016 – A Conference on Knowledge, Electronics and Information Technology)

Vol: 1

November 19, 2016

Editors:

Purushottam Bagale

Vijit Atreya

Ajaya Shrestha

Amit Kumar Rauniyar

Prerana Khwaunju

Committee Members of Set Conference -2016

Advisory Board

Prof. Dr. Subarna Shakya

Prof. Shashidhar Ram Joshi, PhD

Assoc. Prof. Dr. Vinod Parajuli

Er. Santosh Kumar Shrestha

Assoc. Prof. Laxmi Bhakta Maharjan

Executive Committee

President

Assoc. Prof. Dhaneshwar Sah

Vice President

Er. Purushottam Bagale

Secretary

Er. Amit Kumar Rauniyar

Finance Coordinator

Er. Prerana Khwaunju

Media Coordinator

Er. Vijit Atreya

Technical Coordinator

Er. Ajaya Shrestha

Members

Er. Krishna Kumar Jha

Er. Prajwol Suwal

Er. Prem Chandra Roy

Er. Santosh Panjiyar

Er. Arun Kunwar

Er. Dinesh Gothe

Er. Narayan KC

Er. Ram Prasad Sapkota

Er. Pradip Khanal

Er. Subed Lamichhane

Er. Pratik Shrestha

Event Management Team

Er. Anku Jaiswal

Er. Pratik Adhikari

Er. Surendra Khadka

Er. Neha Karn

Er. Prakash Upadhyaya

Er. Prathana Khakurel

Er. Roji Kayastha

Er. Jamuna Maharjan

Er. Pratikshya Pokharel

Mr. Shyam Mani Acharya

Mr. Prakash Gautam

Mr. Satish Ghimire

Mr. Ukesh Lal Shrestha

Mr. Pushpa Raj Basnet

Mr. Kiran Maharjan

Mr. Shiva Hari Aryal

Mr. Amar Pariya

Table of Contents